2

RE-ENTRY SYSTEMS
DEPARTMENT

[redacted]

GPO PRICE $ ________

CFSTI PRICE(S) $ ________

Ha' .copy (HC) $3.00

Microfiche (MF) ________

ff 653 July 65

FACILITY FORM 602

N68-13047 (ACCESSION NUMBER)	(THRU)
132 (PAGES)	1 (CODE)
CR-91372 (NASA CR OR TMX OR AD NUMBER)	18 (CATEGORY)

GENERAL ELECTRIC

RSD Prop. No. N30122
5 February 1963

Study of ELASTOMERIC SHIELD MATERIALS (ESM) for APOLLO

Prepared for

National Aeronautics and Space Administration
Manned Spacecraft Center
Houston, Texas

GENERAL ELECTRIC

RE-ENTRY SYSTEMS DEPARTMENT
A Department Of The Missile and Space Division
3198 Chestnut Street, Philadelphia 4, Penna.

PROPRIETARY NOTICE

TABLE OF CONTENTS

TABLE OF CONTENTS (Continued)

DEFINITIONS

Hard Bond	Phenolic bond, HT-424 or equivalent.
Soft Bond	RTV-60 Silicone Adhesive or equivalent.
Honeycomb	Unless otherwise specified, refers to Hexcel HRP-1/4-GF-12-5.5.
ESM 1000	General family of Elastomeric Shield Materials produced by GE-RSD.
ESM 1001	53 lb/ft^3 blend of ESM 1000 in Honeycomb, Hexcel HRP-1/4-GF-12-5.5.
ESM 1002	45 lb/ft^3 blend of ESM 1000 in Honeycomb, Hexcel HRP-1/4-GF-12-5.5. (Formerly designated ESM 1001A)
ESM 1020	20 lb/ft^3 blend of ESM 1000 in Honeycomb, Hexcel HRP-1/4-GF-12-5.5, formulated to permit antenna transmission before and after exposure to heat flux.

I. INTRODUCTION

Rapidly developing interest and experimentation on the General Electric ESM 1000 Series of ablation materials has led to a considerable amount of test data. This document was prepared by General Electric Re-entry Systems Department (GE-RSD) to accumulate this data for evaluation and use. It summarizes the testing and evaluation activities conducted over the last six months. Most of the work has been performed in connection with manned space flight applications and the Apollo Command Module in particular

Subjects which are discussed herein are as follows:

(1) Data from in-house work with ESM
(2) Data from Flight tests of ESM
(3) Data from the October-November 1962 NASA/MSC evaluation of ESM
(4) Data from the December 1962-January 1963 NAA evaluation of ESM
(5) Other related developments involving ESM
(6) Advanced ESM concepts
(7) Planned and funded work with ESM within GE
(8) Present Apollo/GE/ESM design concept
(9) Suggested program for further Apollo shield development

The results of the current study on the design of an ESM 1000 thermal shield for the Apollo Command Module are included to illustrate the tremendous potential of this material. The ESM material can be fabricated into a simple monolithic shield having outstanding thermal characteristics and mechanical properties that are both superior and unique.

Among the advantages that accrue to a thermal shield fabricated of ESM are the following:

(1) Excellent mechanical compatibility over a wide temperature range.

(2) Simplicity of manufacture, leading to low cost of development and fabrication.

(3) Resistance to service damage that might occur during flight or prior to launch.

(4) Resistance to micrometeorite damage.

(5) Ease of repair.

(6) Resistance to ground environmental factors including humidity, thermal cycling, erosion, fungus, vibration, shock, and aging.

(7) Excellent resistance to radiation and other factors of space environment.

(8) Density variability over a wide range permitting tailoring to a specific requirement.

(9) High backface temperature permissible allowing full use of high temperature properties of substructure.

(10) High heat of degradation, leading to an efficient low weight shield.

There is a firm conviction within GE-RSD that a unique material is at hand and should be carefully evaluated because of its vastly superior mechanical properties and resultant high reliability.

Thus, the purpose of this report is to accumulate for our own information, the data available from these many varied material evaluations. Based on this information, we can recommend specific design and development steps. We respectfully offer this information to the Manned Spacecraft Center and its contractors who have a need to know. The help from both NASA and NAA in "feeding back" ESM test results for accumulation into this report is gratefully acknowledged.

II. HISTORY

Late in 1961, General Electric interest in ablation materials exhibiting elastic characteristics of large magnitude prompted investigation into various silicone rubbers for such material bases. Subsequent development and testing evolved blends that offered exceptional heat of ablation at relatively low fluxes (10-100 Btu/ft^2-sec). Char strength additives and other improvements were incorporated, and by mid 1962, this material was suggested as a thermal shield possibility for the Apollo re-entry vehicle. A presentation at NASA Houston on August 24, 1962, suggested this in the light of desirable characteristics such as large monolithic construction and lessened shield weight.

The concept in August 1962 was necessarily based on the limited material design characteristics obtained to date. Consequently, a more comprehensive assessment program of the GE Elastomer (1000 Series) and several other materials was undertaken by NASA Houston. Laboratory evaluations were conducted at Langley and Plasmadyne; materials were flown on the MA-8 vehicle for recovery, and General Electric flew patches of ESM 1001 on a ballistic re-entry vehicle recovered in the Pacific. At a higher flux level (about 900 Btu/ft^2-sec), these various materials were tested in the General Electric Space Sciences Laboratory; micrometeorite tests were conducted by Ames and, at higher velocities, were attempted by GE. These last-mentioned GE micrometeorite impact tests did not meet desired specifications, leading to further development of this facility which is discussed later in this report.

As a result of the above October-November 1962 assessment by NASA, North American was asked to undertake a program to obtain more complete material design information on a few of the screened materials; ESM 1000 and others. Samples of ESM 1002 (a specific blend at 45 lb/ft^3 density) were supplied to NAA. General Electric was able to participate with NAA via engineering consultation and test recommendation with respect to our material. A section of this document is devoted to the results of the NAA work with ESM, but data is not available at submittal time and will be provided later.

During the October 1962 to January 1963 period, General Electric has also continued an in-house program with the ESM series, and the continuing first-quarter 1963 effort is funded and underway.

III. GE IN-HOUSE ESM INFORMATION

During the latter half of 1962, considerable data was obtained by the General Electric Re-entry Systems Department pertaining to the characteristics of ESM 1000 Series materials. The data is of three basic types:

(1) Thermal

(2) Mechanical

(3) Environmental

Most of this information is for ESM 1001, a particular blend in 1/4-inch honeycomb at 53 lb/ft^3 density. Some information at densities as high as 77 lb/ft^3 is on hand. Due to the interest in lower densities for afterbody protection, a small amount of data is already available at 26 lb/ft^3 and, as discussed in Section IX, a first-step basic program for the characteristics of 20 lb/ft^3 material is funded and underway.

A. THERMODYNAMIC DATA

1. SUMMARY OF ESM ABLATIVE CHARACTERISTICS

A significant amount of screening data on the ablative characteristics of the ESM Series of heat protection system materials has been obtained in recent months by GE-RSD. This data has been obtained in arc-driven test facilities and in the Malta Rocket Exhaust Test Facility. Performance characteristics of these facilities are described in Section VII. The primary objective of these tests was the qualitative assessment of the ablative characteristics of the ESM Series of materials over a sufficiently wide range of heating rate, shear, and enthalpy environmental conditions to insure its adequate performance for the Apollo mission. It is recognized that further ablative testing is required to provide quantitative and statistical information to comprehensively evaluate the Apollo heat protection system and margin requirements.

A summary of the ablative performance of the ESM Series of materials is presented in Figure III-1. The index of performance shown in the figure is that of heat of degradation. The definition of this index is shown on the figure. This index has been utilized by GE-RSD for several years for preliminary design purposes. Its use for preliminary design stems from its definition of where the plastic decomposition boundary is located, since this location, as a function of time (as well as the related Thermogravimetric Analysis results discussed later), is necessary to realistically determine the shield insulation requirements. Further, the movement of the decomposing interface is required by the structural engineer, since the strength of the decomposed material is never used for structural purposes.

When establishing such an overall index of performance for application over the wide variation in environment to which the Apollo Command Module is exposed, it is necessary to obtain the variation of the value of the index parameter (heat of degradation) with the key environmental parameters. For Apollo these are heat rate, air enthalpy, aerodynamic shear, and exposure time.

It can be seen from Figure III-1 that the index parameter, heat of degradation, is relatively invariant within the Apollo mission shear environment.* It would also appear that the heat of degradation may be a function of material density; for example, the heat of degradation shown in Figure III-1 is somewhat higher for the class of density approaching 75-77 lbs/ft^3 than for the density of 45-53 lbs/ft^3. Certain quality control advantages may be gained by limiting the extent of foaming for certain portions of the vehicle, particularly the forward face. Since the increased density material may have increased ablative performance, this increase may offset the increase in insulation requirements in the face area. This choice may be made after additional, controlled testing has been completed and weight tradeoffs made.

In order to obtain information on the performance of the ESM materials in extremely severe environments, such as may arise from a localized heating perturbation such

*For the major portion of the Apollo Command Module.

as an undershoot trajectory, several tests were conducted in the GE Malta Rocket Exhaust Test Facility located at Ballston Spa, New York. In these series of tests, flat plates of ESM and phenolic nylon material were mounted side by side on a blunted wedge (see Figure III-2).

The phenolic-nylon half of the face of the wedge serves as a reference ablation surface. A static pressure tap and copper calorimeter slug are provided on the phenolic-nylon side of each wedge face to measure the environmental conditions. The test condition of the rocket exhaust facility are given in Section VII.

On each test run, the following procedure was employed. Each model was installed so that the centerline of model and engine are aligned such that the nose of the model is located approximately two inches downstream of the nozzle exit. The model is then adjusted so as to give the proper angle of attack of each face (to obtain different heating and shear condition). Since the nozzle is designed to give a smooth flow, considerable latitude exists in placing the model in the facility. The motor is then started and brought to a stabilized condition before the motor is gimballed onto the model. The models were then exposed for 4 - 5 seconds.

2. ABLATION CHARACTERISTICS — ROCKET EXHAUST FACILITY

Photographs of typical pre- and post-test samples of ESM materials tested in the GE Malta rocket exhaust are shown in Figures III-3 to III-10. Salient features are noted on the figures. Note that in Figure III-3 an instrumentation array of a surface and subsurface calorimeter are shown, together with a pressure tap. This instrumentation was used to check the state of flow (laminar or turbulent) and to evaluate local heat rates and flow properties, i.e., pressure. In general, these tests indicated material performance similar to that of phenolic-nylon material, particularly at the higher densities and heat rates. Although the surface appears quite rough, it is nonetheless of uniform roughness. Further, the more realistic specimen size provides a better example of a potential re-entry mission surface.

3. AIR-ARC TEST RESULTS

The primary portion of air-arc test data shown in Figure III-1 has already been reported to NASA personnel and is available within General Electric in PIR form. Figures III-11 to III-13 show typical results from these tests.

a. Supersonic Arc Tunnel

Figure III-11 shows the backface temperature response of ESM material exposed to low-level heating rate, long-time thermal environment. The material was shaped into a trapezoidal plate configuration to fit the wall of the facility nozzle. This flux level is representative of that on the Apollo aft section.

b. Hypersonic Arc Tunnel

Figure III-12 shows the backface temperature rise of ESM 1000. The specimen was tested in the hypersonic arc tunnel at a cold wall calorimetric heat rate of 80 Btu/ft^2-sec. and an approximate enthalpy ratio, hs/RT_0, of 400. The specimen was 3/4-inch in diameter and fitted into a truncated conical holder to protect from side heating. The ESM 1000 material was 0.577-inch thick corresponding to 2.25 lb/ft^2.

The results reported in Figure III-13 were obtained in the hypersonic arc tunnel subjected to air at an enthalpy of approximately 13,600 Btu/lb with an enthalpy ratio of 400. The air mass flow was 1.2×10^{-3} lb/sec, expanded from a stagnation pressure of approximately 1040 mm Hg. The heat transfer to a cold wall averaged 120 Btu/ft^2-sec, determined by calorimetric measurements. Models were made in the form of 1-inch diameter cylinders with a 1/2-inch spherical radius on the end. Each was bored with a 1/4-inch diameter hole which was filled with plugs of the same material. Each insert was made to a length corresponding to a weight of 4.7 lb/ft^2. A thermocouple was attached to the back of each insert. The surface temperature reported in Figure III-13 was obtained using the two-color pyrometer. The temperature shown on the figure is color temperature. Inasmuch as the chars on the test specimens are essentially black, the values of the temperatures are very nearly true.

4. THERMAL CONDUCTIVITY

Material thermal insulation characteristics are critical to the design of the heat protection system, particularly in the regimes of low aerodynamic heating. The conductivity information obtained to date is shown in Figure III-14, together with values used for design purposes, see Section X. The test results indicate a significant decrease in the thermal conductivity with decrease in density. The lowest density specimen of ESM material available for conductivity evaluation was 26 lb/ft^3. Tests are continuing on the lower density (20 lb/ft^3) formulation, but results are not available for this report.

As shown in Section X, a significant weight saving exists by using the 20 lb/ft^3 formulation. Further, it allows the fabrication of a somewhat thicker, though lighter, section, with subsequently improved handling and damage-resistant characteristics.

5. THERMOGRAVIMETRIC ANALYSIS

Figure III-15 presents typical thermogravimetric (TGA) data for elastomeric materials. From this data, the temperature of decomposition which controls the conduction of heat towards the interior may be obtained. Experience has shown that this temperature should be obtained at a W/w_o value of 0.95. These values are also used in GE-REKAP analyses.

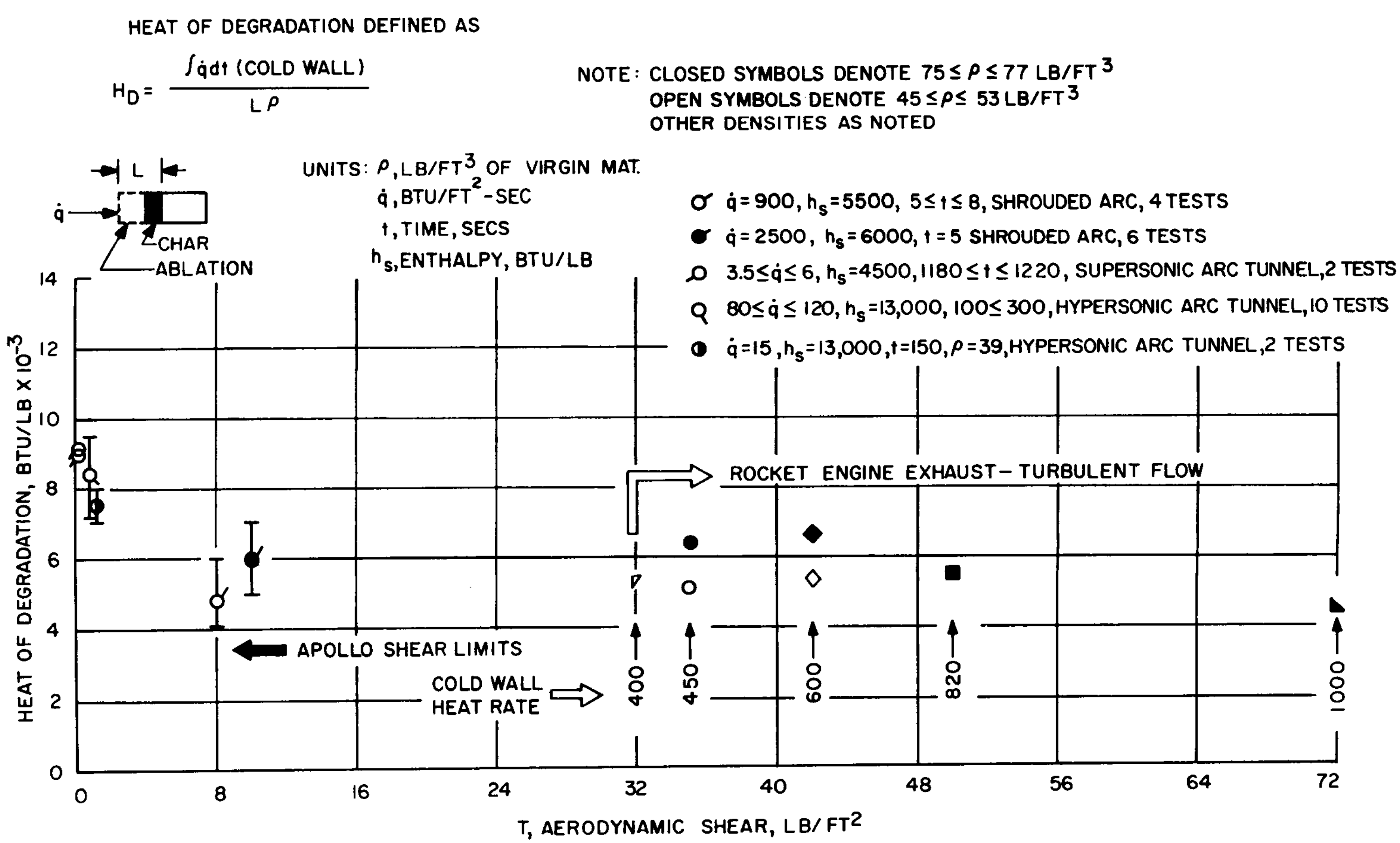

Figure III-1. Summary of Key GE ESM Ablation Performance Data

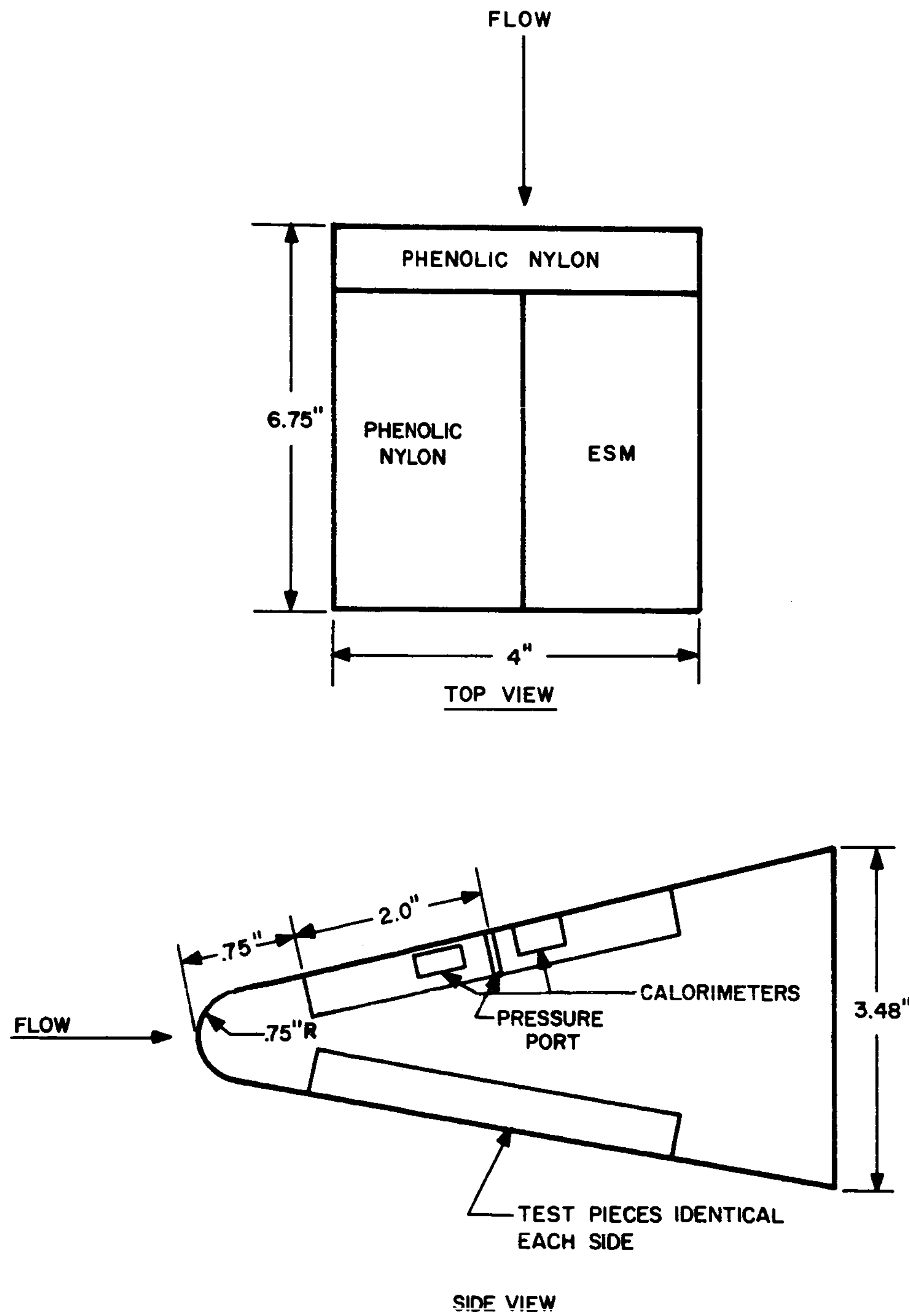

Figure III-2. Test Geometry for ESM Evaluation, Malta Test Facility

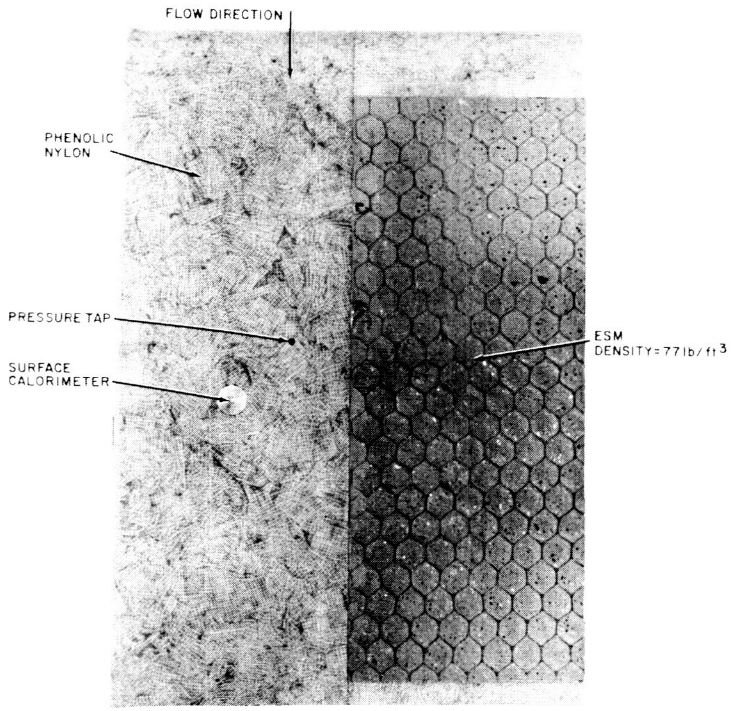

Figure III-3. ESM Material on Test Wedge Prior to Test, Density = 53 lb/ft^3

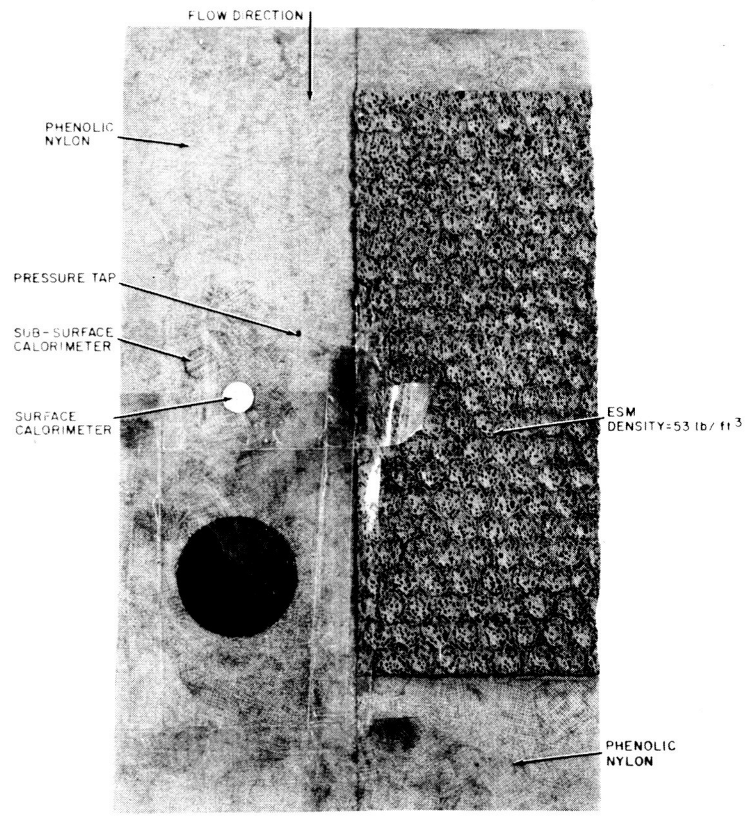

Figure III-4. ESM Material on Test Wedge Prior to Test, Density = 77 lb/ft^3

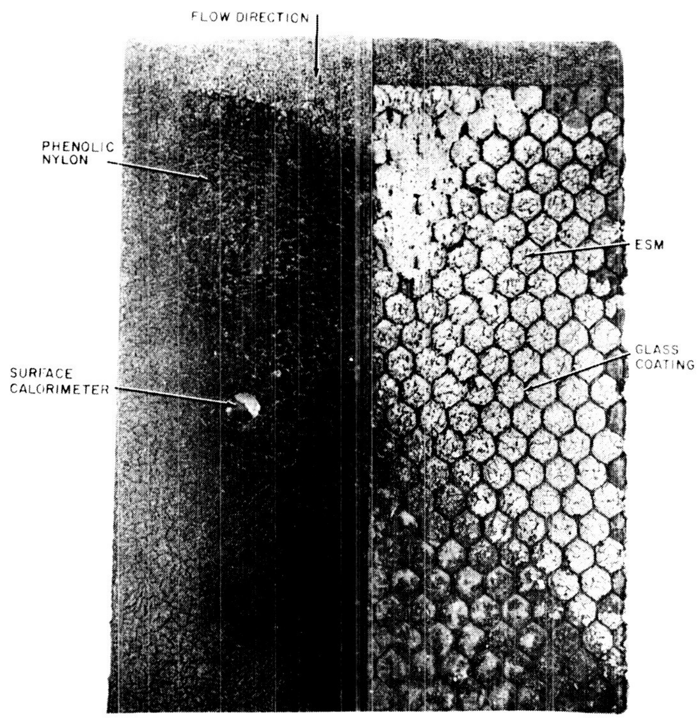

Figure III-5. ESM Material, Post Test, Density = 53 lb/ft^3

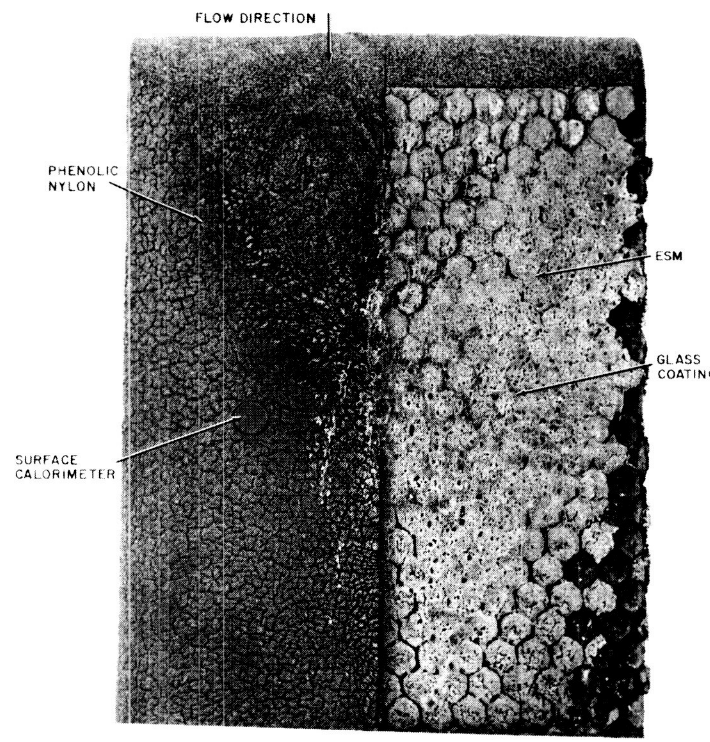

Figure III-6. ESM Material, Post Test, Density = 53 lb/ft^3

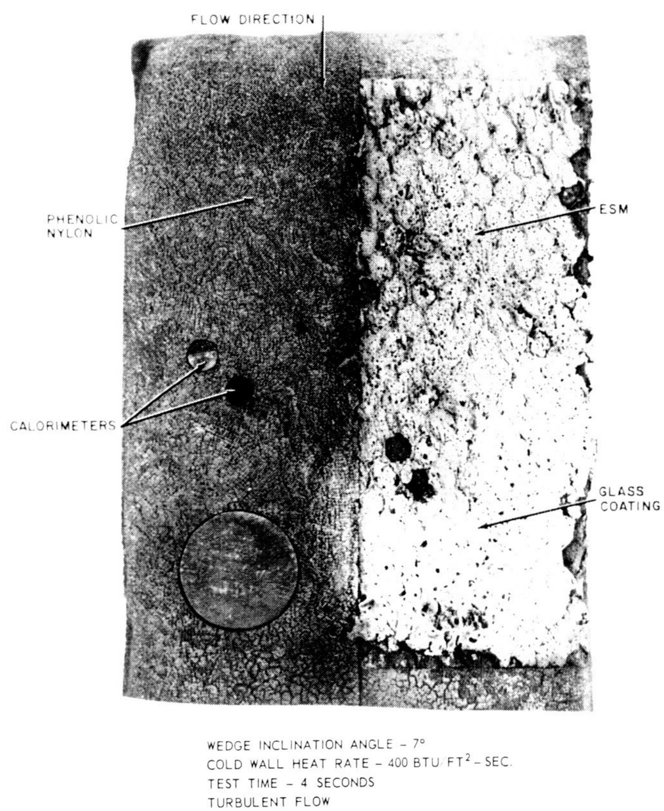

Figure III-7. ESM Material, Post Test, Density = 53 lb/ft^3

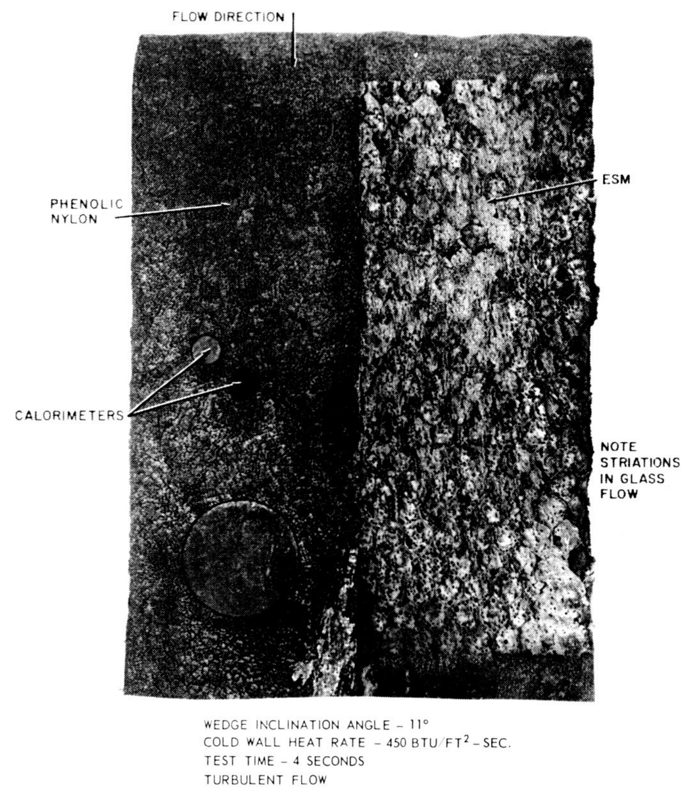

Figure III-8. ESM Material, Post Test, Density = 53 lb/ft^3

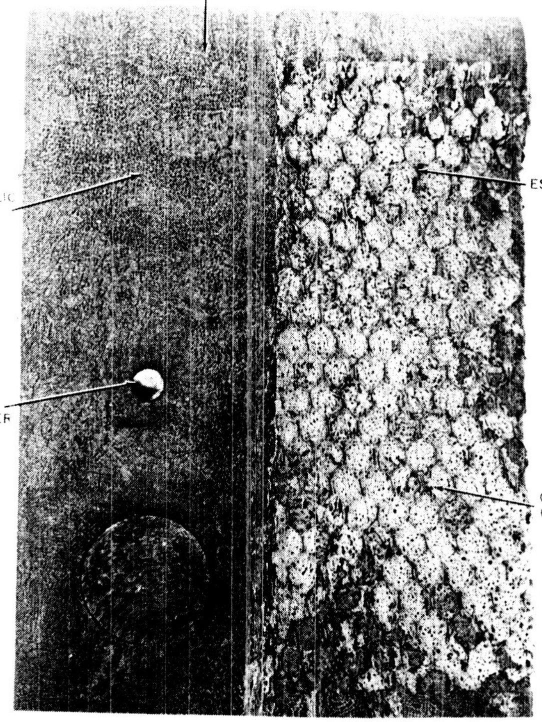

WEDGE INCLINATION ANGLE – 18°
COLD WALL HEAT RATE – 600 BTU/FT^2 – SEC.
TEST TIME – 4 SECONDS
TURBULENT FLOW

Figure III-9. ESM Material, Post Test, Density = 53 lb/ft^3

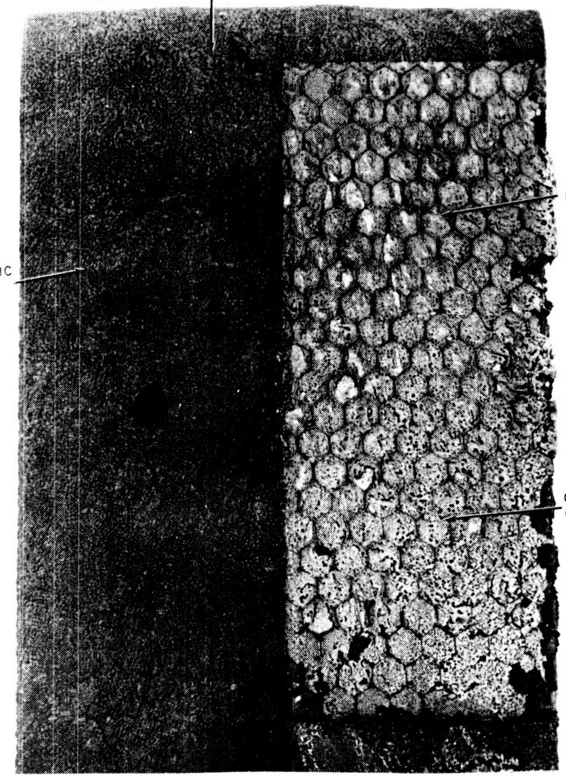

WEDGE INCLINATION ANGLE – 18°
COLD WALL HEAT RATE – 820 BTU/FT^2 – SEC.
TEST TIME – 4 SECONDS
TURBULENT FLOW

Figure III-10. ESM Material, Post Test, Density = 77 lb/ft^3

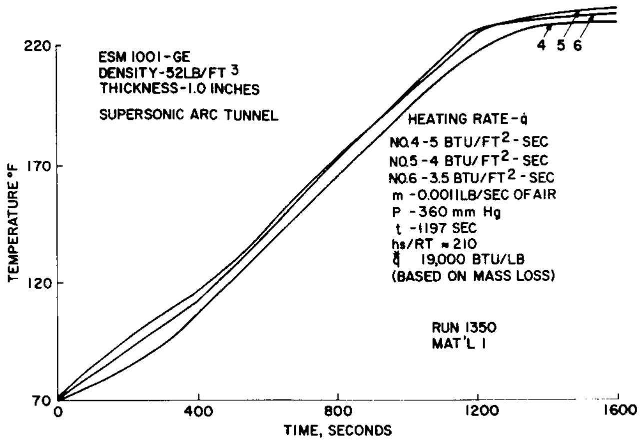

Figure III-11. Backface Temperature

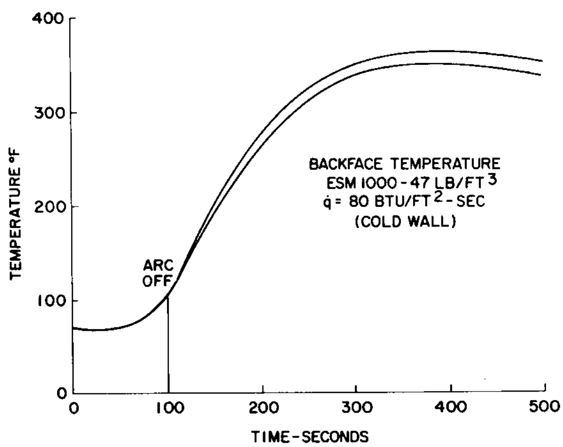

Figure III-12. ESM Backface Temperature Response

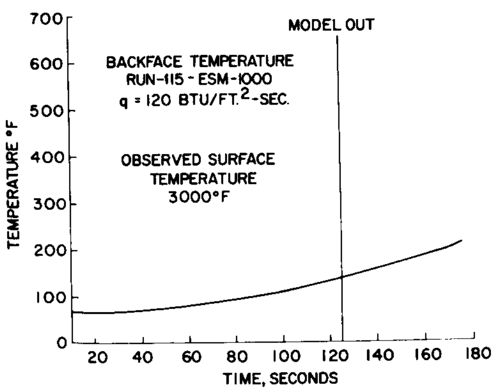

Figure III-13. ESM Backface Temperature Response

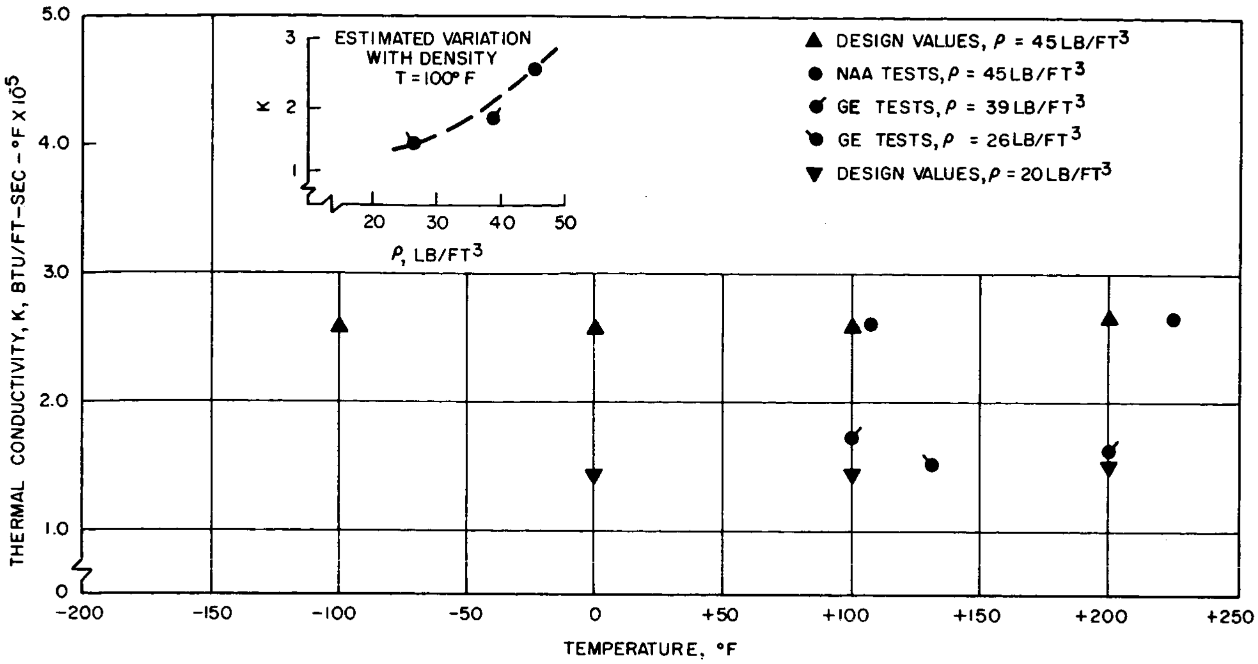

Figure III-14. Thermal Conductivity of GE ESM Material

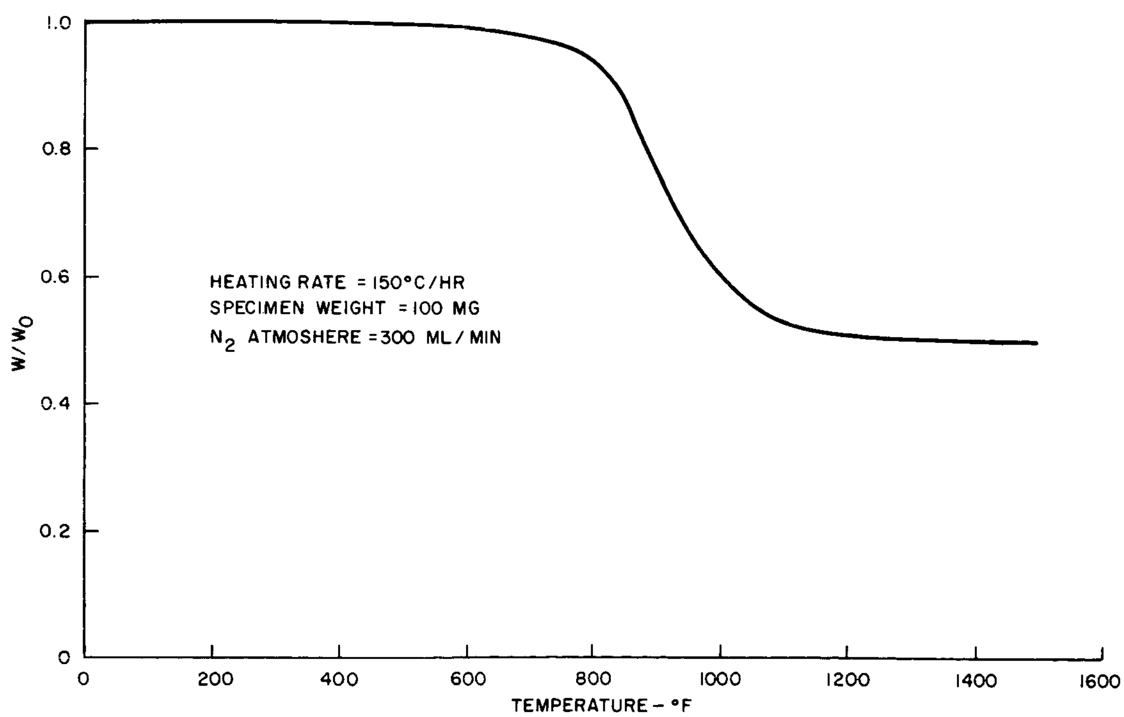

Figure III-15. Typical TGA Data for ESM Materials
Residual Weight Fraction vs Temperature

B. MECHANICAL PROPERTIES

1. TENSILE PROPERTIES

a. Sample Preparation

Tensile specimens were cut from an 0.5-inch thickness of ESM 1001 using a specially fabricated cutting die. The dumbbell-type specimens had a cross-section of 1 inch by 1/2 inch and gauge length of 1-1/4 inch. They were fabricated with two orientations, with-tape (WT) and across-tape (AT), as determined by the characteristics of the phenolic-glass honeycomb matrix.

b. Test Procedures

Specimens with both orientations were tested in tension at +75°F, -150°F, and -250°F at 0.02-in./min crosshead travel. An Instron testing machine and a Missimers air-circulating, liquid N_2-coolant temperature chamber were employed, with recordings made on an Offner oscillograph. Strain measurements were made with extensometers in both the axial and transverse directions at +75° and -50°F. Only axial strain measurements could be obtained at -150°F, and strain measurements at -250°F could only be obtained on one specimen. Specimens were brought to the test temperature and then soaked for a minimum of twenty minutes to ensure constant temperature throughout the specimen.

c. Test Results

Figures III-16 through III-21 show the stress-strain curves resulting from the testing of three specimens in each of two directions at +75°, -50°, and -150°F. At -250°F, the following ultimate stress values were obtained:

With Tape Direction	Across Tape Direction
950 psi	700 psi
580 psi	580 psi
730 psi	830 psi
	470 psi
	*380 psi

*(0.2% elongation at failure)

Failure was defined as the first sudden drop-off of load due to partial or complete separation at an interface or within either component of the honeycomb-elastomer composite.

d. Discussion of Results

The pronounced anisotropic behavior of ESM 1001 due to the inherent characteristics of the honeycomb matrix is probably a primary consideration in evaluating the significance of reported properties. Because the honeycomb thickness does not strain to a significant degree, we have a plane strain condition (on a macroscopic scale). In this situation, we must consider the simultaneous changes in both directions. The importance of this behavior due to thermal loads is exemplified by the thermal expansion data which shows contraction with increasing temperature in the WT direction while the AT direction expands. Although no attempt is made here to develop behavior mechanisms, it may be pointed out that the across tape (AT) direction is the direction of least resistance to change as demonstrated by the tensile behavior. In general, the elastomeric filler tends to expand with increasing temperature at a greater rate than phenolic-glass. Therefore, the elastomer exerts a force on the cell walls which tends to expand the area (equivalent to volume) of the given cell. The geometry of a "theoretical" cell (assuming a six-sided irregular polygon with its rigid sides hinged at their ends) is such that an initial increase in the AT dimension (with corresponding decrease in the WT direction) will actually increase the cell area up to approximately one percent. Figure III-22 shows the general effect on cell area of a change in either direction. Further evidence of complex anisotropy is obtainable by considering the ratio of transverse-to-axial strain at a given stress level in uniaxial tension. This ratio appears to vary from the WT direction to the AT direction and within a single direction as temperature changes.

No attempt to average the replicate test results has been attempted since the cause of variation of data has not yet been determined to be either experimental variation or behavioral variation due to possible nonhomogeneity of the composite material.

2. THERMAL EXPANSION PROPERTIES

a. Sample Preparation

Specimens of ESM 1001 were cut and machined to a 3" x 3" x 1-1/8" configuration with square corners and parallel faces. The with-tape and across-tape dimensions were equal (3 inches). One specimen of honeycomb without filler was tested.

b. Test Method

Changes in length with temperature were measured simultaneously in three directions. The relative motion of flat plates bearing against surfaces of the specimen were monitored with motion transducers and extension rod systems. The temperature of the specimens was lowered to $-260^{\circ}F$; then changes in lengths were measured while increasing the temperature at approximately $1^{\circ}F/min$ to $+600^{\circ}F$.

c. Test Results

Figures III-23, 24, and 25 show the results obtained for three specimens of ESM 1001. Figure III-26 shows the behavior of one specimen of unfilled phenolic-glass honeycomb (Hexcel HRP-1/4 inch-G. F.-12-5.5). The results are expressed as curves of change in length/initial length versus temperature for each dimension with a reference temperature of $+70^{\circ}F$.

d. Discussion

The sudden break in the thermal expansion curve which occurs between -50° and $0^{\circ}F$ requires discussion. This inflection in the curve is most probably due to crystallization of the silicone-elastomer filler. The same phenomenon has been noted previously in testing materials with the same base polymer. The previous data shows this crystallization to occur at -50° to $-40^{\circ}F$, a smaller temperature range than shown in testing ESM 1001. Increasing the rate of temperature change causes a transition zone to occur over an apparently broader temperature range;

however, it may be assumed that this volumetric change of ESM 1001 (shrinkage with decreasing temperature) occurs at -40° to -50°F. The crystallization of a polymer does not necessarily cause a large variation in mechanical behavior. In fact, the tensile behavior of ESM 1001 as reported here at -50°F is not significantly different from behavior at +75°F. The transition of ESM 1001 to glassy behavior (actually the transition of the silicone-elastomer filler) occurs well below -50°F, most probably at about -100°F.

3. COMPRESSION PROPERTIES

This section describes the sample preparation, test, and results of the compression properties of ESM 1001. This data is intended for preliminary design and proposal purposes only. ESM 1001 has a density of 53 lb/ft^3. The ESM 1001A (45 lb/ft^3) fabricated for NAA differs primarily in density. ESM 1001A was redesignated as ESM 1002.

a. Test Conditions (Compression of 53 lb/ft^3 ESM 1001 formulation)

Specimen size: 1" x 1" x 1".

Temperatures: 75°, 150°, 250°, 600°F.

Directions: Two - With tape (also called "ribbon direction"), and Across tape (also called "transverse direction").

Number of Specimens: Three per temperature per direction.

Test Equipment: Instron Testing Machine with circulating-air temperature chamber.

Initial Strain Rate: 0.02 in/in/min (0.02 in/min crosshead speed).

Strain Measurement: Crosshead travel motion synchronized with time axis of X-Y recorder. (At loads up to 1000 pounds on the Instron Machine, crosshead travel measurement is equivalent to actual deflection of the test specimen.)

b. Test Results

(1) Figures III-27 through III-34 show individual stress-deflection curves obtained for ESM 1001 specimens in compression for each temperature and test direction.

(2) Figures III-35 and III-36 summarize the variations of ultimate stress, stress at 25 percent deflection, and strain to failure (ultimate compressive strain) with temperature and two orientations of honeycomb matrix.

(3) Table III-1 lists the individual and average data calculated from the stress-strain curves.

c. Discussion

From the compression results, ESM 1001 exhibits no major transition properties over the temperature range of 75° to $600^{\circ}F$. A consistent decrease in stress at both failure and 25 percent deflection is noted with increasing temperature for both directions investigated (Figure III-35).

The most significant finding is the characterization of degree of anisotropy between the two directions which is due to the inherent structure of the honeycomb matrix.

In comparing the general shapes of the stress-strain curves for any single temperature, it can be observed that the across-tape (AT) curve is smooth and characteristic of rubber-like compression (approaching a finite volumetric compressibility). The with-tape (WT) curve deviates from this behavior in that the shape is not smooth. The initial portion of the WT curve exhibits a rigid or "still" behavior up to 5 to 15 percent deflection. The stress at 25 percent deflection is higher for the WT direction, but ultimate compressive stress and strain are greater for the AT direction. Not yet completely understood are the mechanisms of strain and failure of the composite material and the contribution of the elastomer to overall stress-strain behavior. Terminal fracture appears to be initiated by failure of the honeycomb matrix in bending or in tension perpendicular to the direction of loading. Preliminary results in tension indicate that the major load bearing component is the honeycomb,

TABLE III-1. COMPRESSION PROPERTIES OF ESM 1001 (53 LB/FT^3 DENSITY) AT A STRAIN RATE OF 0.02 IN/IN/MIN FOR 1" X 1" X 1" SPECIMENS

Specimen No.	Test Temp. °F	Direction of Loading*	Ult. Comp. Stress, psi		Ult. Deflection, %		Aver. Comp. Stress @ 25 % Deflection, psi
			Indiv. Tests	Aver.	Indiv. Tests	Aver.	
1	75	WT	171	184	36	40	108
2	75	WT	155		33		
3	75	WT	227		50		
4	75	AT	370	381	47	48	92
5	75	AT	389		48		
6	75	AT	384		49		
7	150	WT	153	162	40	39	103
8	150	WT	179		46		
9	150	WT	154		31		
16	150	AT	319	296	53	52	73
17	150	AT	268		54		
18	150	AT	300		48		
10	250	WT	114	107	36	30	78
11	250	WT	104		24		
12	250	WT	102		30		
19	250	AT	227	259	52	49	76
20	250	AT	247		46		
21	250	AT	302		49		
13	600	WT	44	48	33	36	32
14	600	WT	50		38		
15	600	WT	48		35		
22	600	AT	178	163	56	55	27
23	600	AT	151		54		
24	600	AT	159		54		

* WT = with-tape direction (also called "ribbon direction")

AT = across-tape direction (also called "transverse direction" or "direction perpendicular to ribbons") with only minor contribution of the filler. The same general behavior may be expected to hold under compressive loads.

For specific design purposes, future investigations should further clarify the compression mechanisms questioned above and should include evaluating the significance of specimen size and shape characteristics with respect to heat shield design applications.

4. BOND-SHIELD MECHANICAL CHARACTERISTICS

Bond-shield preliminary mechanical properties are listed below. Although density can be controlled over a wide range, these properties were determined on a 45 lb/ft^3 material in honeycomb, ESM 1001. In most cases, the reported values are minimum-maximum results from three test samples.

Bond Line (Bond-Shield System)

Shear Strength

	Ult Stress (PSI)	Ult Strain (%)	H/C Direction	Temp (^oF)	Substrate Material
1.	26 - 33	15 - 30	P	75^o F	Al
2.	31 - 49	16 - 20	T	75^o F	Al
3.	14 - 25	12 - 15	P	180^o F	Al
4.	14 - 26	12 - 16	T	180^o F	Al
5.	225 - 287	22 - 35	P	-80^o F	Al
6.	50 - 105	25 - 38	T	-80^o F	Al
7.	330 - 500+	—	—	-200^o F	Al
8.	6.5 - 10.0	34 - 38	—	+600^o F	Al
9.	94.5 - 105	13 - 19	—	74^o F	Be
10.	68 - 86	26 - 37	—	200^o F	Be
11.	26 - 32	7 - 32	—	400^o F	Be

Tensile Strength

	Ult Stress (PSI)	Temp (^oF)	Substrate Material
1.	35 - 58	74^o F	Be
2.	63 - 104	200^o F	Be
3.	26 - 32	400^o F	Be

5. SURFACE COATINGS

Emissivity control of the shield by application of coatings to give values of absorptivity, α_s, from 0.2 to 0.95 and emissivity, ϵ_n from 0.6 to 0.9, depending upon requirements:

Surface Emissivity

Absorptivity, α_s = 0.75

Emissivity, ϵ_n = 0.94

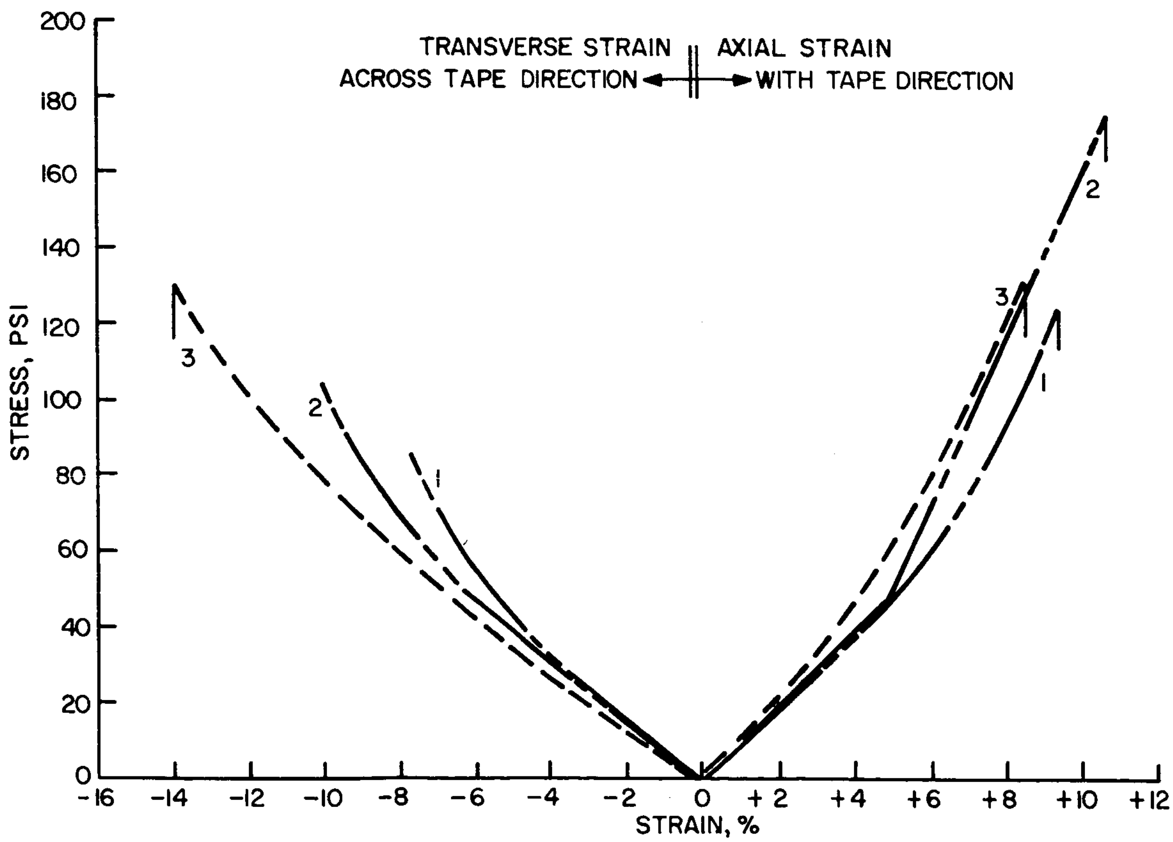

Figure III-16. ESM 1001 (53 lb/ft^3 Density) Tension — with Tape Direction +75^{o}F.

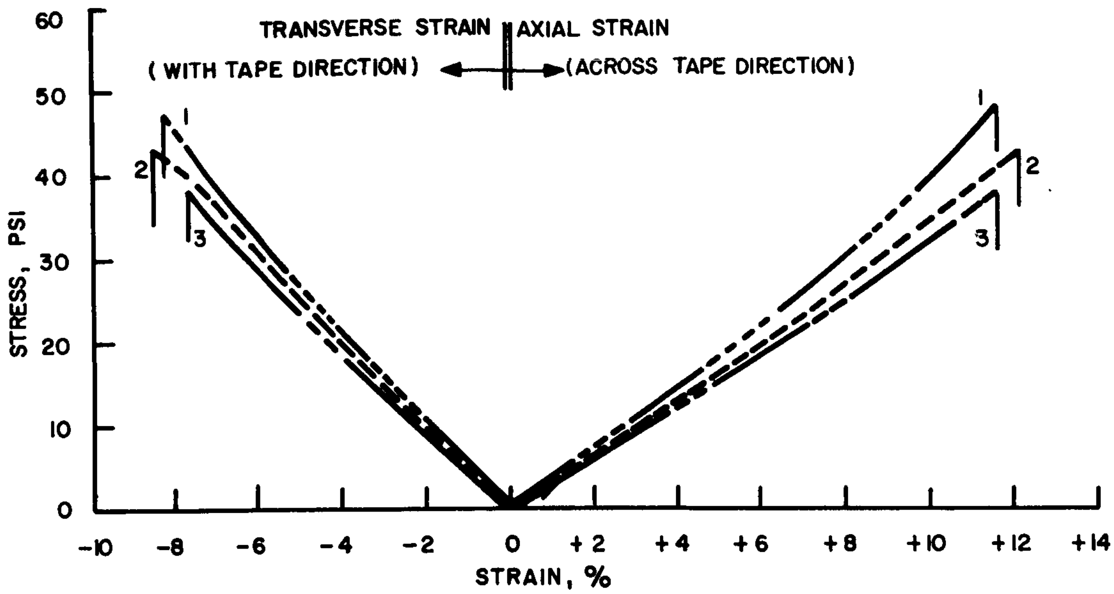

Figure III-17. ESM 1001 (53 lb/ft^3 Density) Tension — Across Tape Direction +75°F.

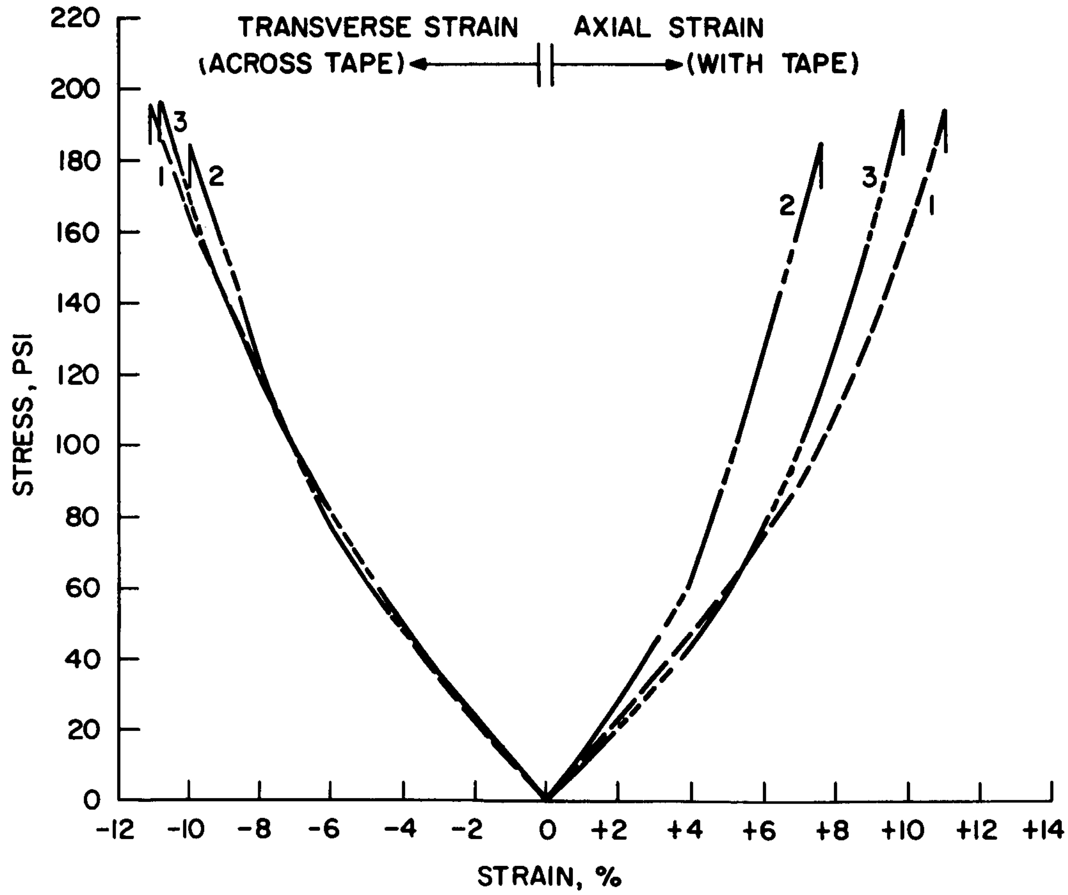

Figure III-18. ESM 1001 (53 lb/ft^3 Density) Tension — With Tape Direction -50°F.

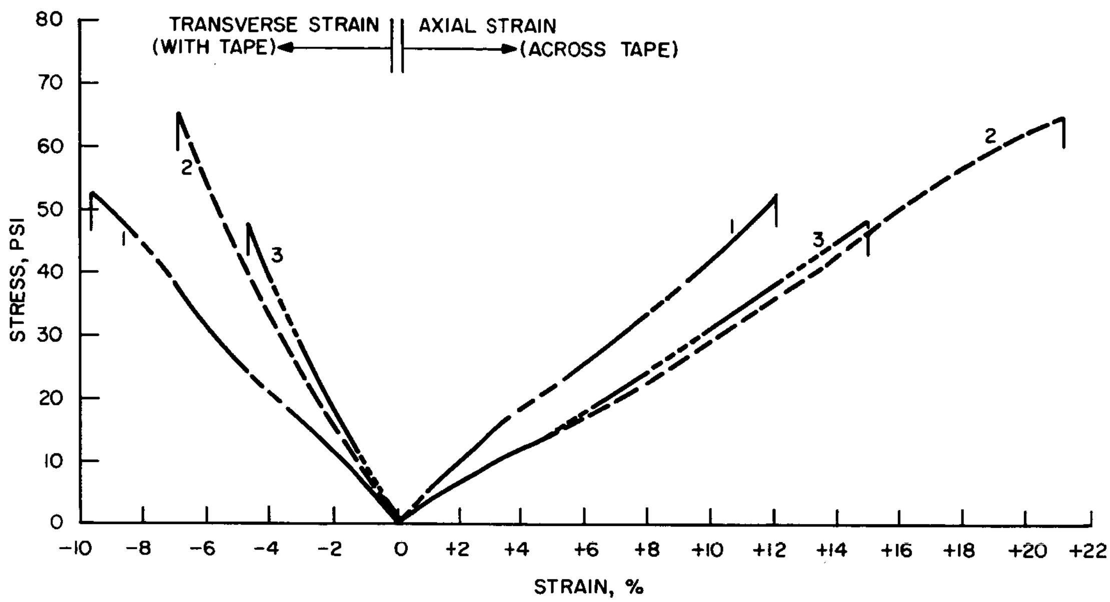

Figure III-19. ESM 1001 (53 lb/ft^3 Density) Tension — Across Tape Direction -50°F.

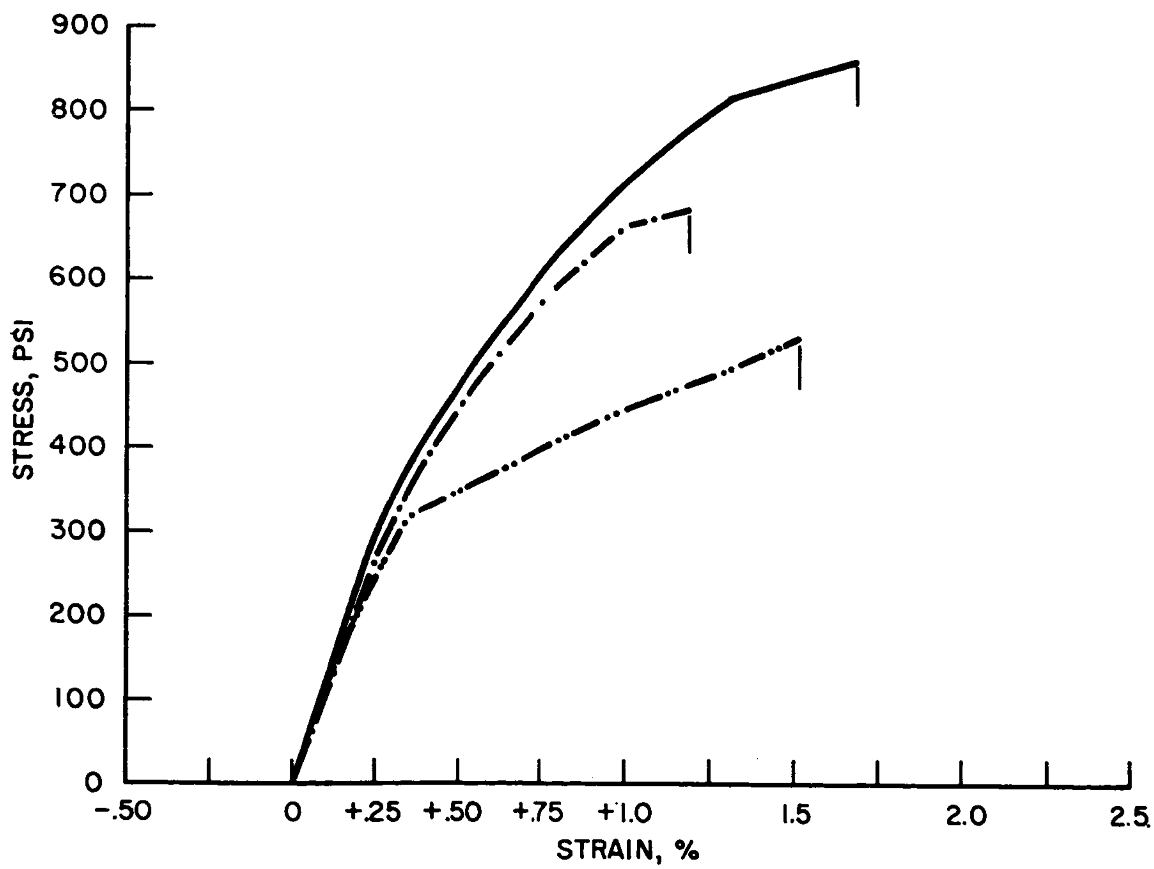

Figure III-20. ESM 1001 (53 lb/ft^3 Density) Tension — With Tape Direction -150°F.

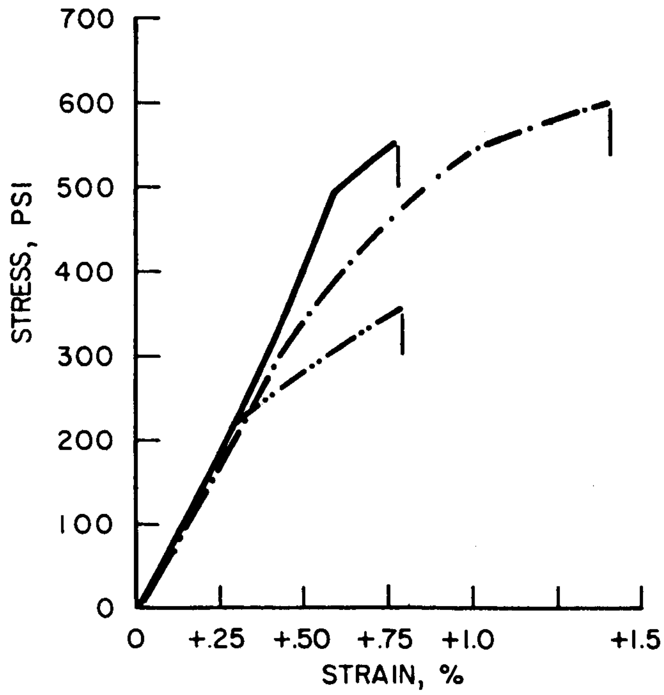

Figure III-21. ESM 1001 (53 lb/ft^3 Density) Tension — Across Tape Direction -150°F.

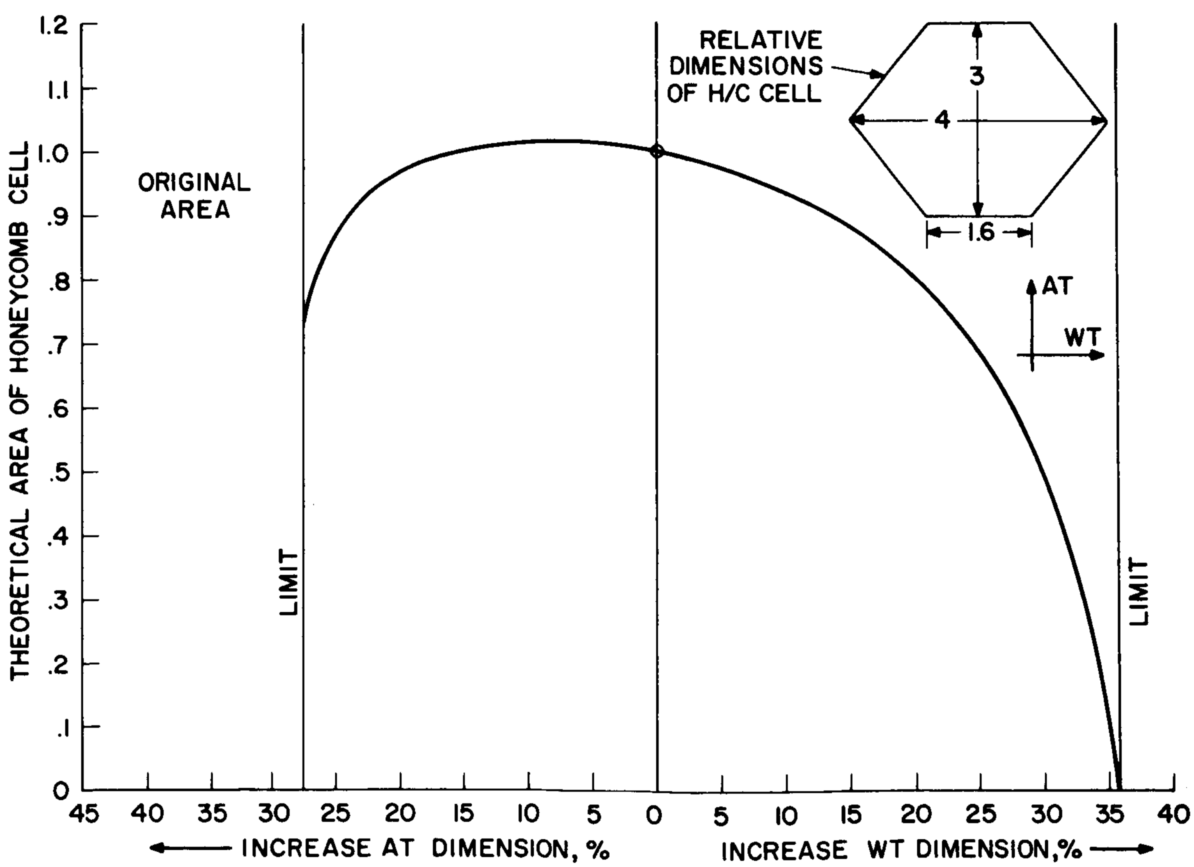

Figure III-22. Area of a "Theoretical" Honeycomb Cell.

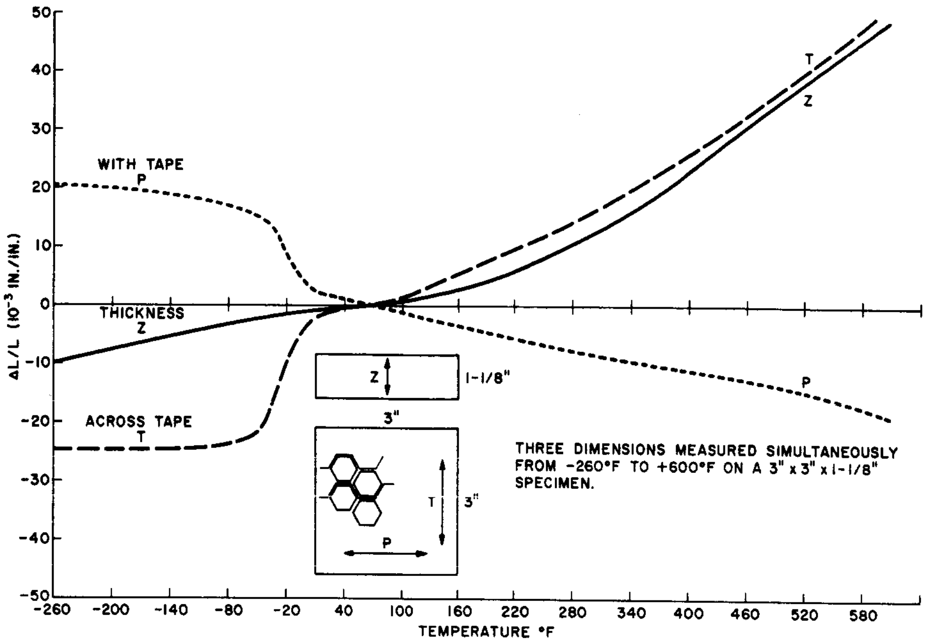

Figure III-23. Linear Thermal Expansion Behavior of ESM 1001 Specimen 1 (53 lb/ft^2 Density).

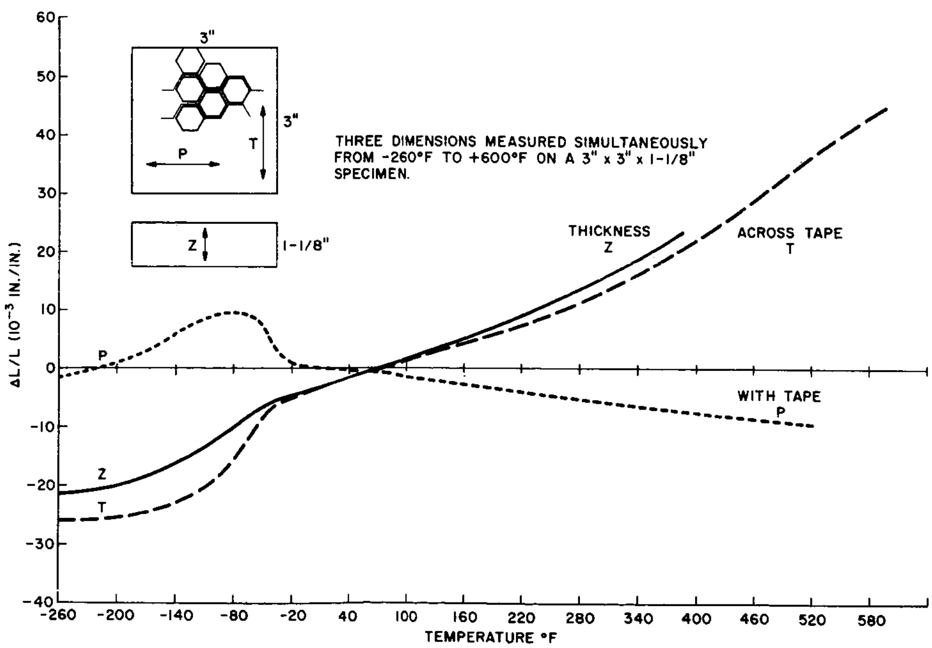

Figure III-24. Linear Thermal Expansion Behavior of ESM 1001 Specimen 2 (53 lb/ft^2 Density).

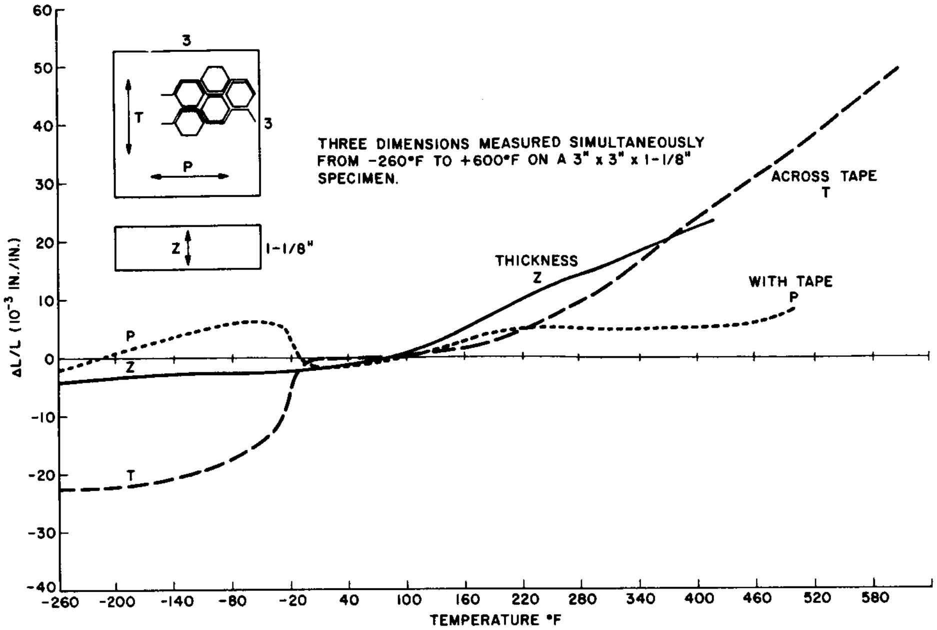

Figure III-25. Linear Thermal Expansion Behavior of ESM 1001 Specimen 3 (53 lb/ft^2 Density).

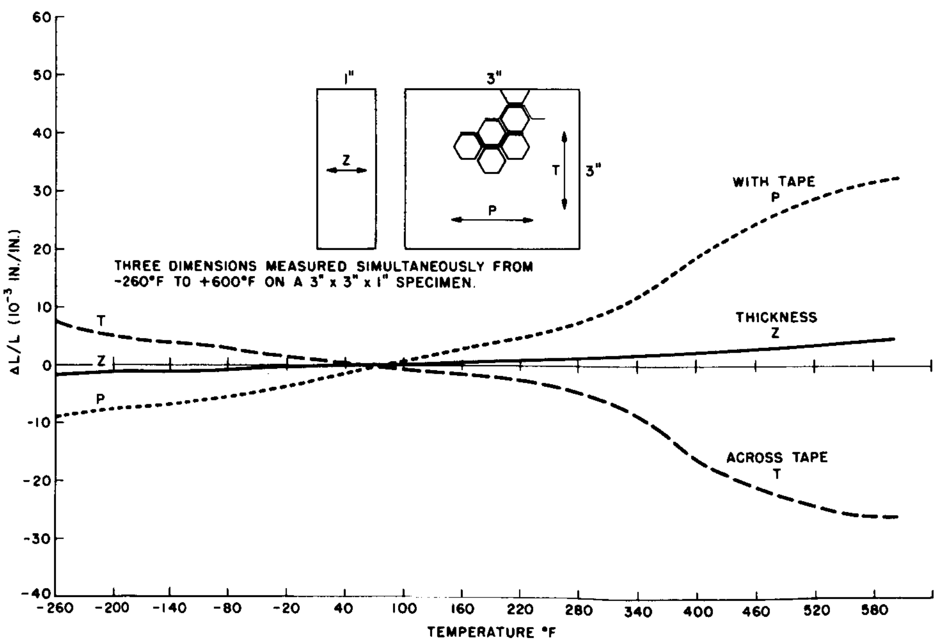

Figure III-26. Linear Thermal Expansion Behavior of Phenolic-Glass Honeycomb (HRP-1/4-G. F. -12-5. 5) Without Elastomeric Filler.

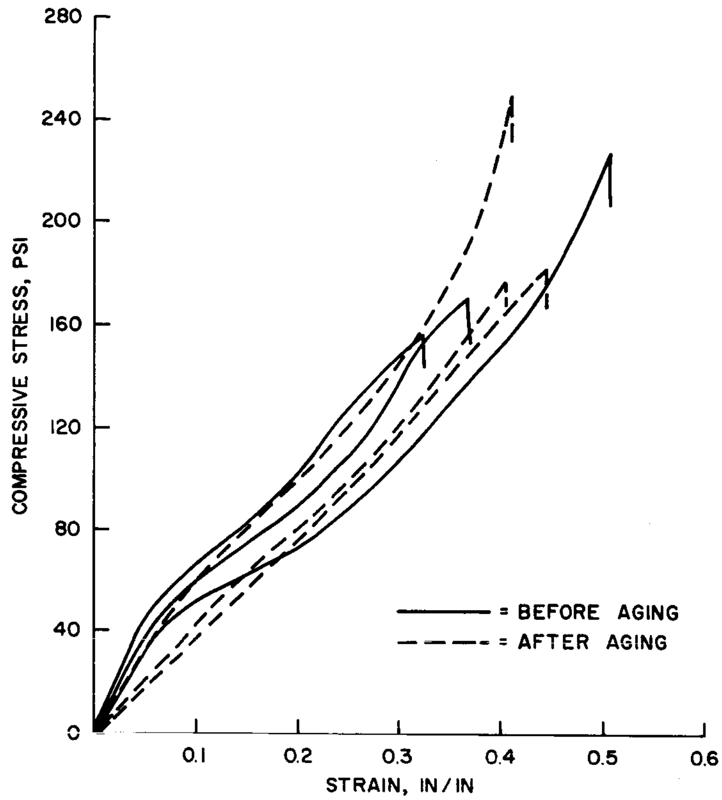

Figure III-27. ESM 1001 +75°F With Tape

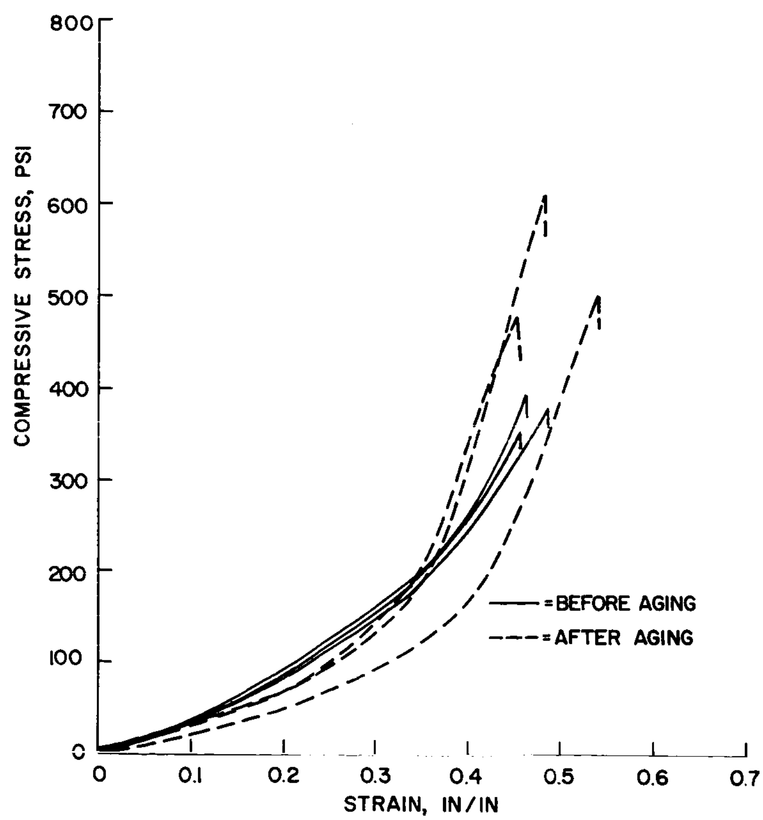

Figure III-28. ESM 1001 +75°F Across Tape

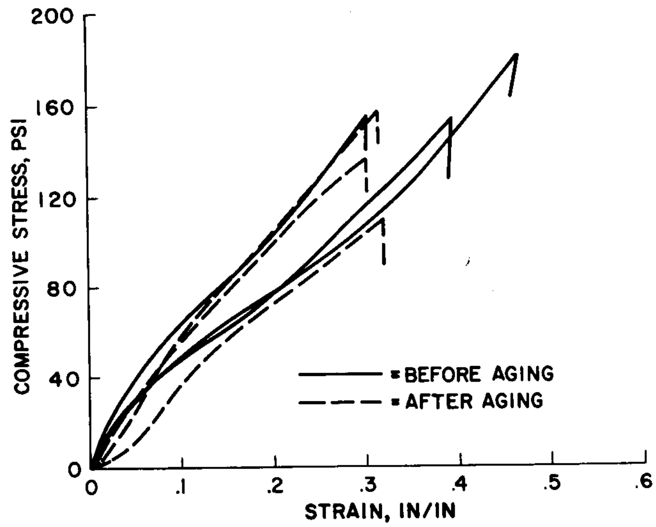

Figure III-29. ESM 1001 +150°F With Tape

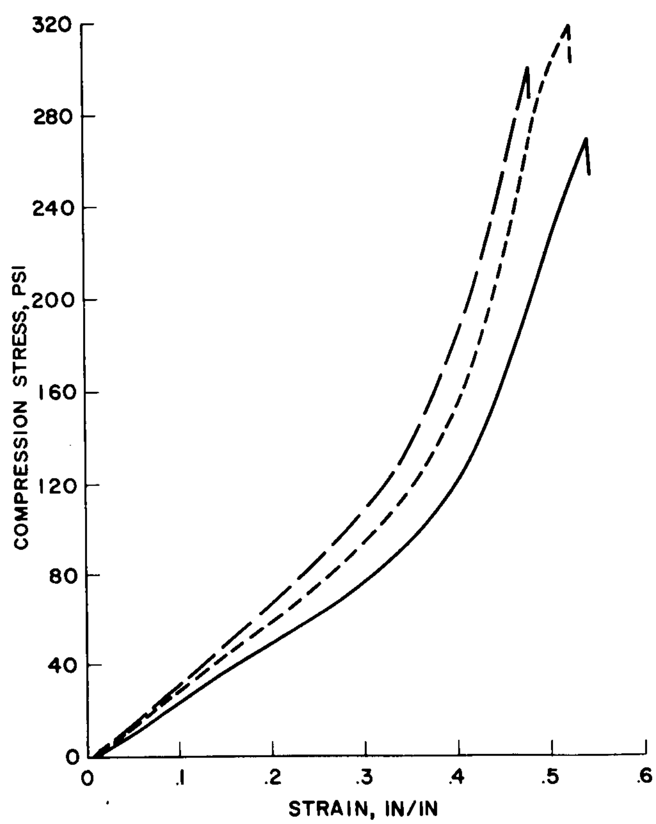

Figure III-30. ESM 1001 +150°F Across Tape

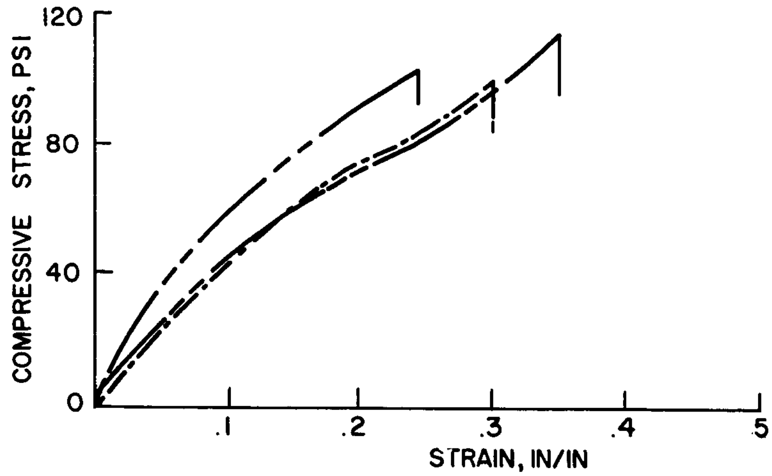

Figure III-31. ESM 1001 +250°F With Tape

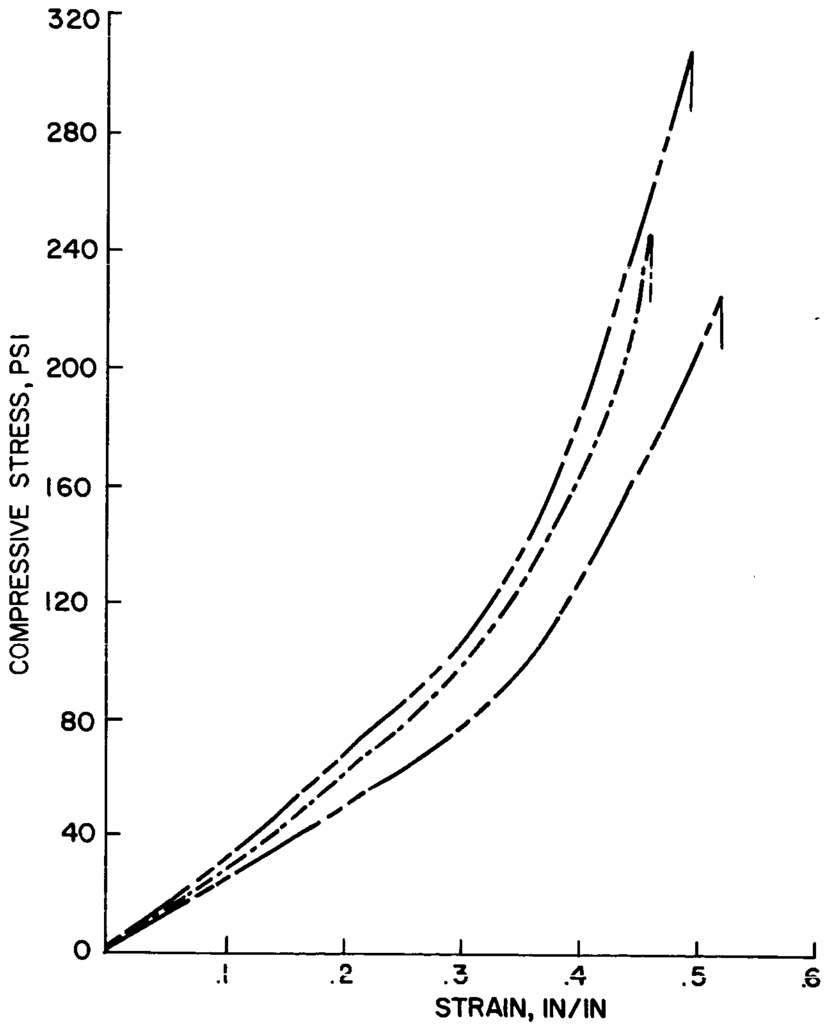

Figure III-32. ESM 1001 +250°F Across Tape

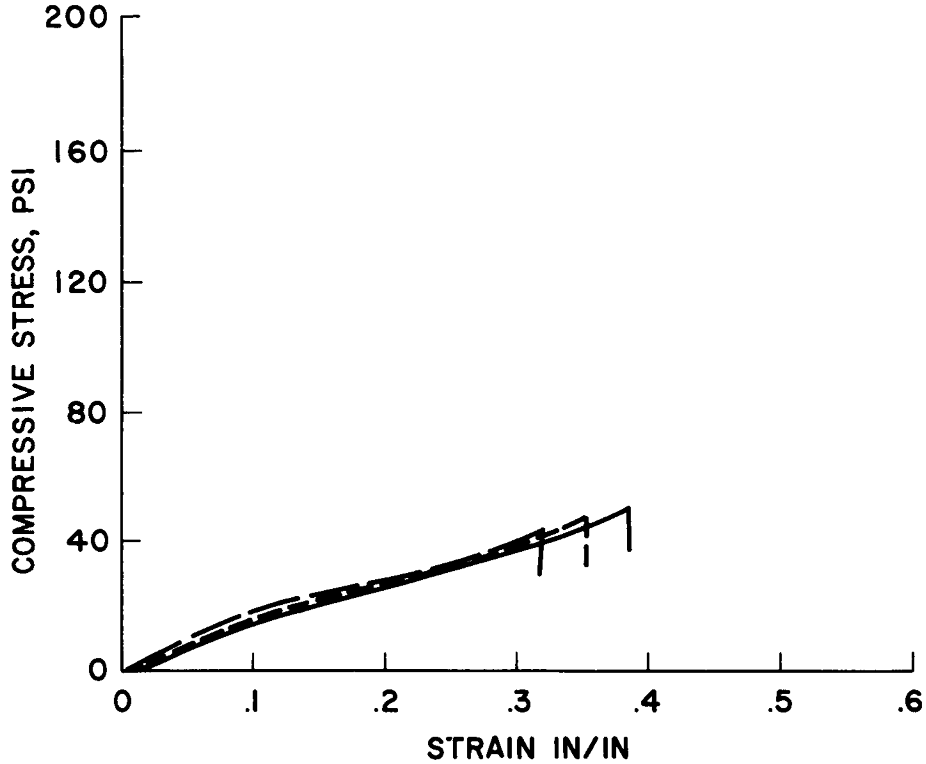

Figure III-33. ESM 1001 +600°F With Tape

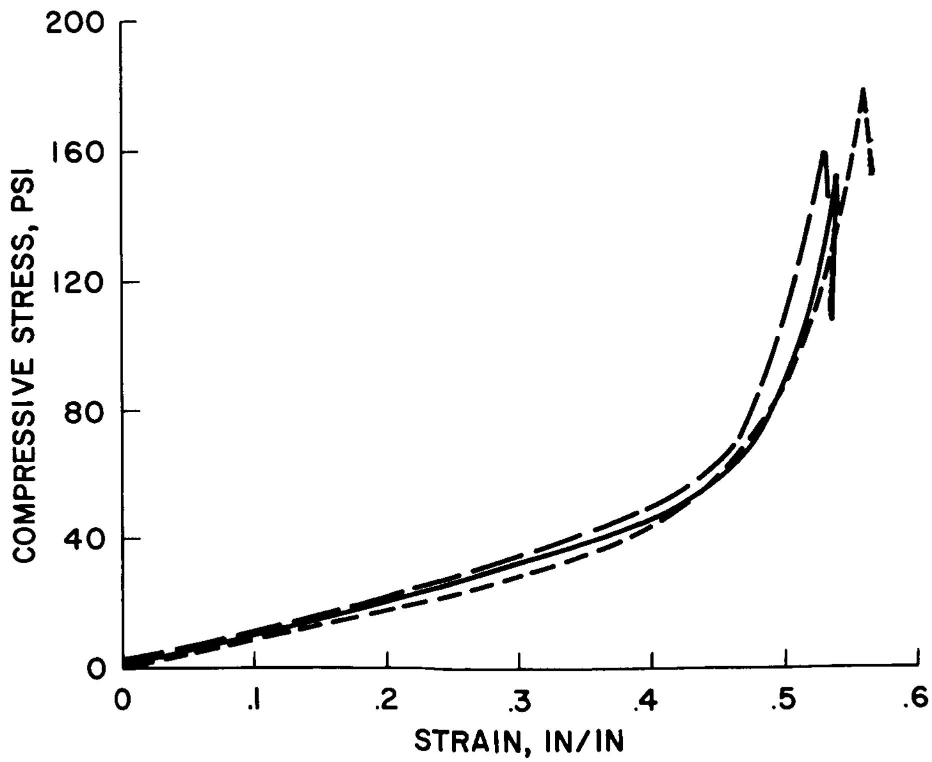

Figure III-34. ESM 1001 +600°F Across Tape

C. VACUUM/THERMAL BEHAVIOR OF ESM 1001

1. WEIGHT AND DIMENSIONAL CHANGES

Ten specimens each of free foam and honeycomb composite ESM 1001 were aged in vacuum at elevated temperature. Five specimens in the form of one inch cubes were included in each cell. The final pressure attained was 5×10^{-5} torr. This pressure was maintained for fourteen days while heating at 250°F.

Following the exposure, the cells were immediately cut open and the following measurements made: (1) weight loss, (2) dimensional change, (3) density change. These results are reported in the accompanying Table III-2.

The dimensional changes were rechecked seven days after the first measurement. These values remained essentially unchanged. We therefore feel that the change is permanent and recovery will not occur in a reasonable time.

Preliminary conclusions based on this study are that properly post-cured honeycomb ESM-1001 undergoes only minor chemical and physical changes under the conditions used for aging.

TABLE III-2

EFFECT OF HEAT AND VACUUM ON ESM 1001

Sample	Weight Loss %	% Change in Length	% Change in Width	% Change in Height	% Gain in Density
ESM-1001 Honeycomb #1	0.83	-0.22	+0.49	-2.74	1.77
Honeycomb #2	0.95	-1.61	-0.29	-0.58	1.53
Honeycomb #3	0.81	-1.98	-1.47	-0.10	2.00
Honeycomb #4	0.90	+0.54	-2.10	-0.78	1.30
Honeycomb #5	0.88	-2.93	-0.99	-1.75	4.93
Honeycomb #6	0.93	-3.14	-0.49	-0.09	2.94
Honeycomb #7	0.78	-0.22	-0.00	-1.77	1.20
Honeycomb #8	1.10	-1.31	-1.22	-4.17	5.95
Honeycomb #9	1.00	-2.68	-0.60	-0.09	2.42
Honeycomb #10	0.72	-0.55	+0.92	-3.26	2.18

2. MECHANICAL PROPERTIES

Specimens of ESM 1001 honeycomb composite and specimens of ESM 1001 elastomer foam without honeycomb core were vacuum aged at elevated temperature. The specimens were packaged with desiccant material and subsequently tested for compressive behavior. Comparison with previously reported control specimen results showed no significant deviations for the composite material from preaged behavior. Figures III-35 and III-36 summarize this comparison of data. Results are tabulated in Table III-3 and stress-strain curves are presented in Figures III-37 and III-38.

TABLE III-3

COMPRESSION PROPERTIES OF ESM 1001 (53 lb/ft^3) AFTER VACUUM AGING (14 DAYS AT 5 x 10^{-5} MM HG. AND 250°F)

Direction* of Loading	Temp of Test, °F	Ult Stress psi		Ult Strain, %		Compressive Stress at 25% Deflection, psi	
		Indiv Samples	Aver	Indiv Samples	Aver	Indiv	Aver
WT	75	235	198	41	42	120	105
WT	75	182		44		96	
WT	75	177		40		100	
WT	150	132	132	30	31	117	108
WT	150	108		32		85	
WT	150	156		32		122	
AT	75	500	545	54	50	98	88
AT	75	610		49		95	
AT	75	528		46		70	
ESM 1001 Without Honeycomb Core Material (Elastomer Foam):							
-	75	284	-	66	72	51	45
-	75	445		70		44	
-	75	965		82		40	
-	150	218	226	63	64	46	48
-	150	234		64		51	

Weight Loss due to aging: ESM 1001 0.89%
Density Change (lb/ft^3): ESM 1001 from 52.5 to 53.9 (2.7% increase)

Test Conditions: 1" x 1" x 1" specimens compressed at 0.02 "/"/min. (0.02 "/min crosshead travel

(* WT = With Tape Direction: AT = Across Tape Direction)

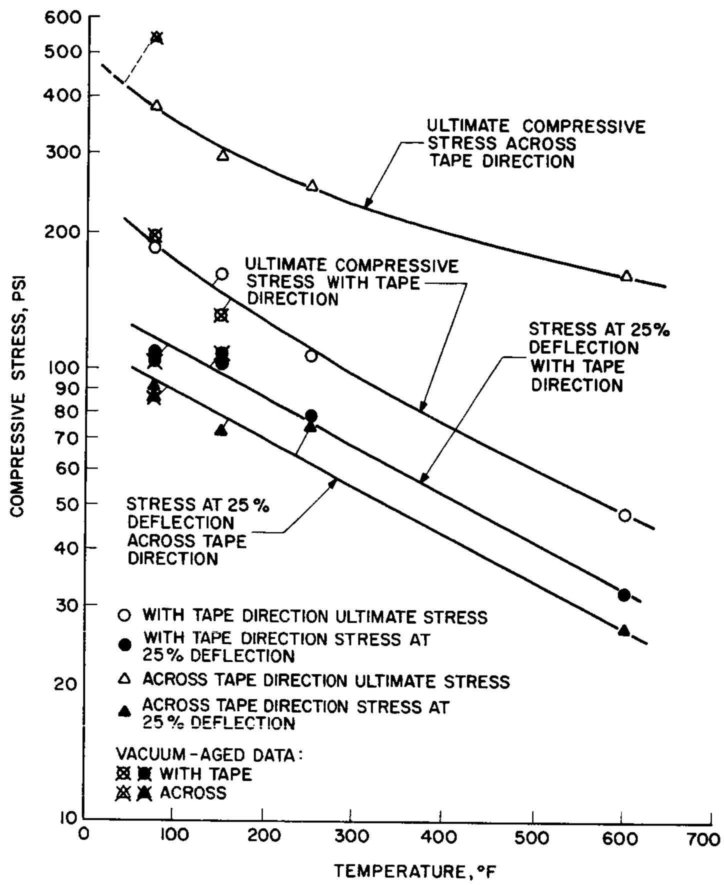

Figure III-35. Compressive Stress Variation with Temperature and Orientation of ESM 1001 (53 lb/ft^3 Density); Strain Rate 0.02 in/in/min.

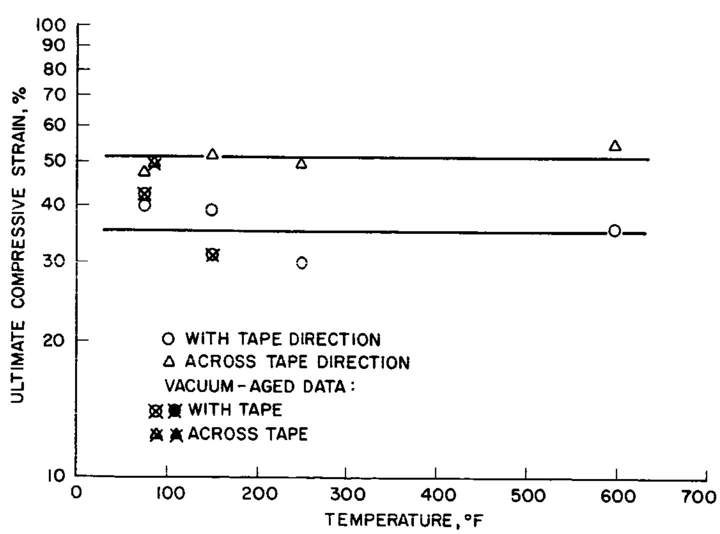

Figure III-36. Ultimate Compressive Strain Variation with Temperature and Orientation of ESM 1001 (53 lb/ft^3 Density); Strain Rate 0.02 in/in/min.

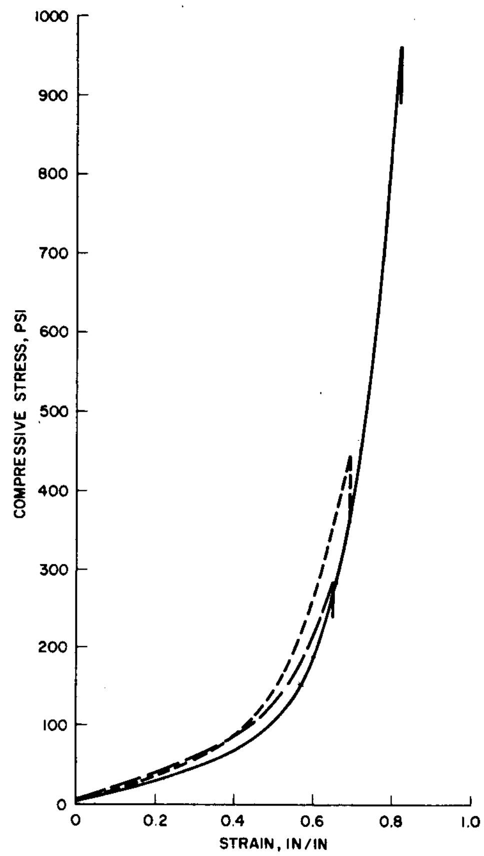

Figure III-37. ESM 1001 Elastomer Foam without Core Material Test Temperature +75°F. Vacuum-Aged (Density: before 42.5; after 45.3 lb/ft^3).

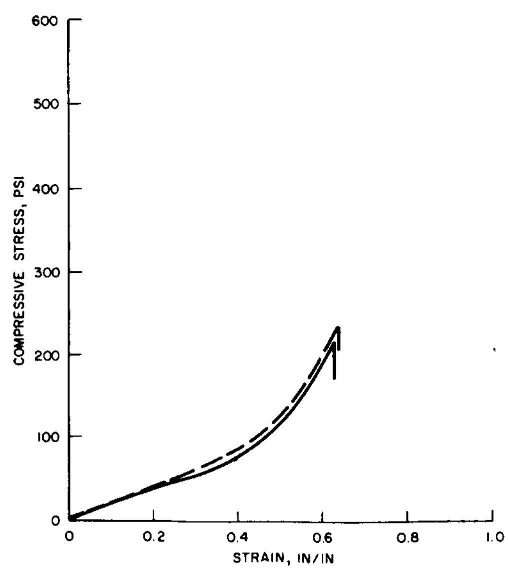

Figure III-38. ESM 1001 Elastomer Foam without Honeycomb Core Material Test Temperature +150°F. Vacuum-Aged (Density: before 42.5; after 45.3 lb/ft^3).

IV. ESM FLIGHT TEST DATA

Two ESM data sources other than laboratory tests are available:

(1) Flight on the MA-8 Recovery Vehicle.

(2) Flight on a ballistic re-entry vehicle, with recovery.

Both of these flights have provided confidence in the ESM material. These flight tests were not instrumented except that the Mercury ESM test installation had temperature-sensitive paints on the mounting panel.

A. ESM 1001 SAMPLE TEST ON MERCURY MA-8

An excellent opportunity was afforded for flight testing ESM 1001 on the Mercury MA-8 flight. On this flight, a group of materials were tested by attachment to the exterior of the beryllium shingles as shown in Figure IV-1. The prepared shingle before flight is shown in Figure IV-2 and the recovered shingle in Figure IV-3. The sample of ESM 1001 was 0.090-inch thick as installed. Note the small square patches of material at the corners of the sample. These were "intentional damage" where the cracks were patched with ESM material to demonstrate the repair capabilities of ESM. NASA-Houston reported the performance of the ESM 1001 material as follows:

"There was no discernible thickness change, no char, and no weight loss. The peak heating rate was 4.8-5.2 Btu/ft^2-sec reached approximately 100 seconds after the beginning of the 300-second re-entry heating cycle. The backface temperatures at three locations on the beryllium shingle were (a) greater than 149^{o}F but less than 293^{o}F, (b) less than 365^{o}F, and (c) less than 428^{o}F. (These qualitative values were determined by temperature-sensitive paints.)"

This sample test of the ESM 1001 is of great use in evaluating the material performance for space flight missions. Although re-entry fluxes as noted were lower and shorter than for the Apollo re-entry, the space environment to which the material was exposed is very similar and is an excellent test, particularly for the cold-soak conditions. Since the MA-8 vehicle was in the dark for periods of about 40 minutes, the thin ESM 1001 and the highly conductive beryllium shingle must have had sufficient time to cool to the minimum temperature possible. Based on this test, as well as analysis, confidence is generated in the capability of ESM material to withstand the environmental conditions of the Apollo flight.

B. TEST OF ESM MATERIAL ON BALLISTIC RE-ENTRY VEHICLE

GE Elastomeric Shield Material (ESM 1001) was flown on an ICBM re-entry vehicle. The test specimen, a 2" x 2" x 1/2" slab, was affixed to the aft area of the R/V where it was exposed to a maximum flux rate of 60 Btu/ft^2-sec, integrated to 600 Btu/ft^2 (cold wall basis). No active instrumentation was mounted in the specimen; water recovery was required for post-flight examination and analysis. The specimen was recovered in two pieces which could be joined together to provide a nearly complete section. The breakup of the specimen was a result of high loads resulting from high velocity water impact. Examination of the specimen indicated no adverse effects of re-entry or impact upon the integrity of the honeycomb and filler. Analysis of the ablative performance was qualitative only; however, no deleterious effects were observed, with no major degradation of the material as a result of the thermal environment. Aerodynamic shear loads were less than 1 lb/ft^2.

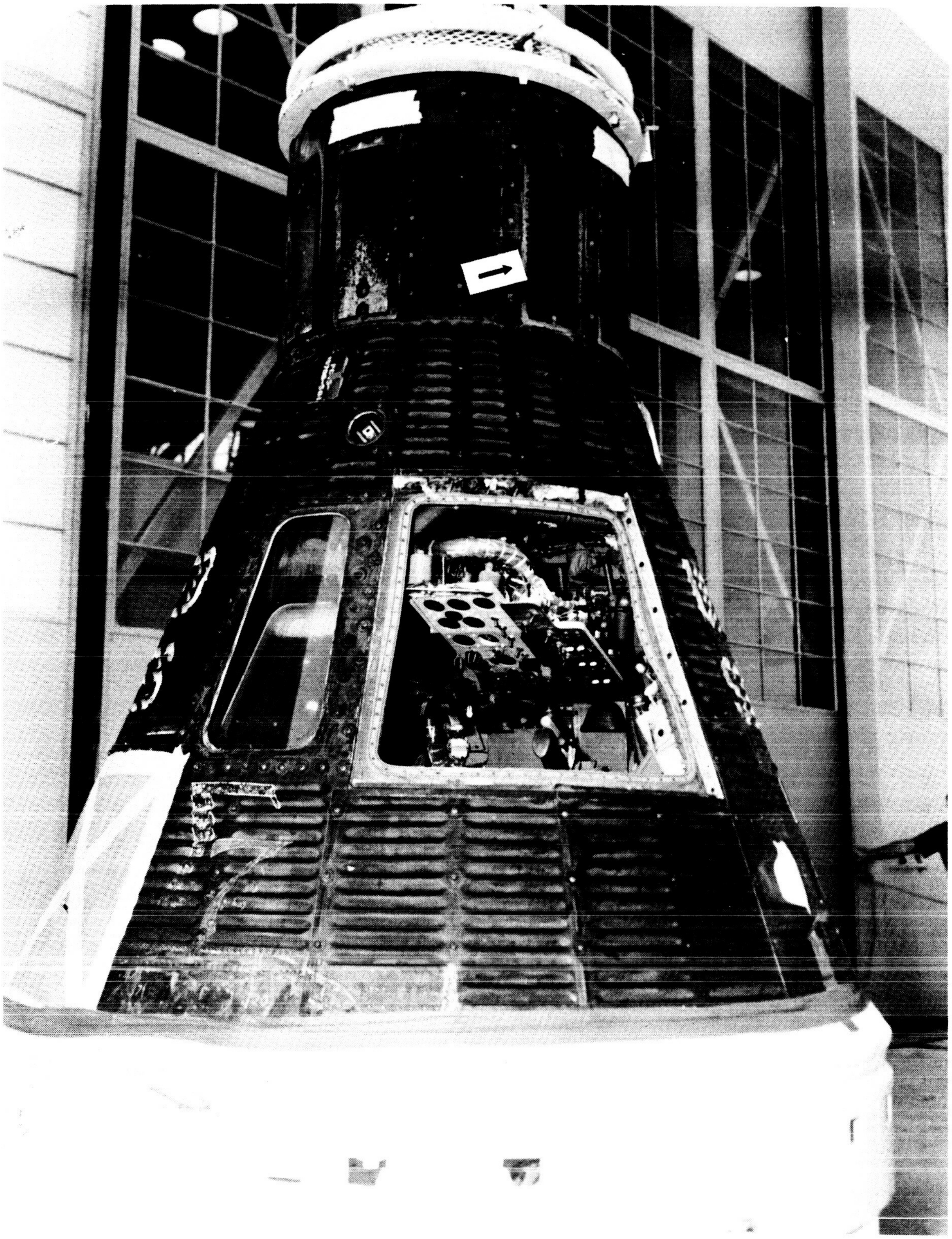

Figure IV-1. View of the Mercury MA-8 Spacecraft After Recovery. The arrow indicates the GE materials.

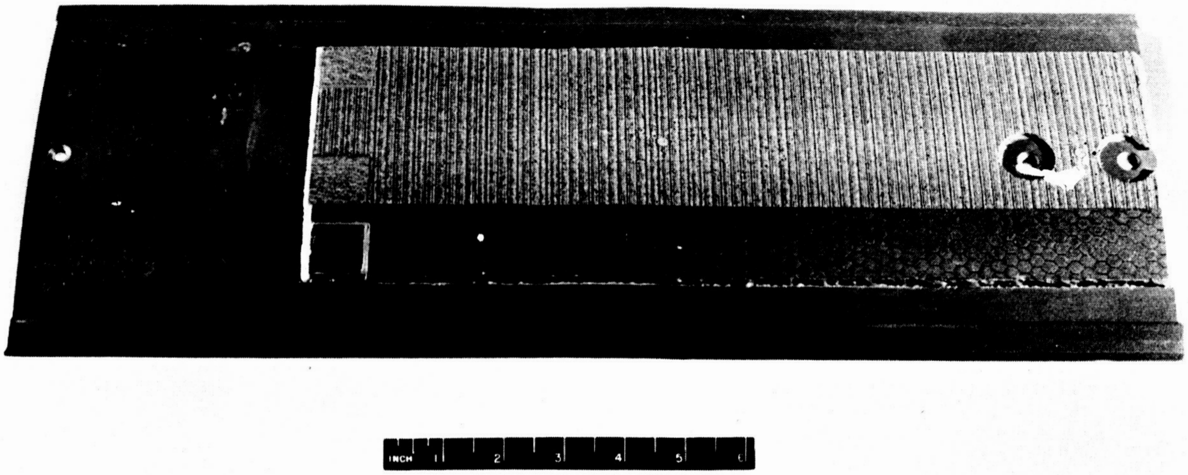

Figure IV-2. The Beryllium Shingle Flown on the Mercury MA-8 Spacecraft with the Two Thermal Shield Materials Attached. The Wider Specimen is ESM 1001. (The Narrow Specimen is GE Series 500, also in the Phenolic-Fiberglass Honeycomb.)

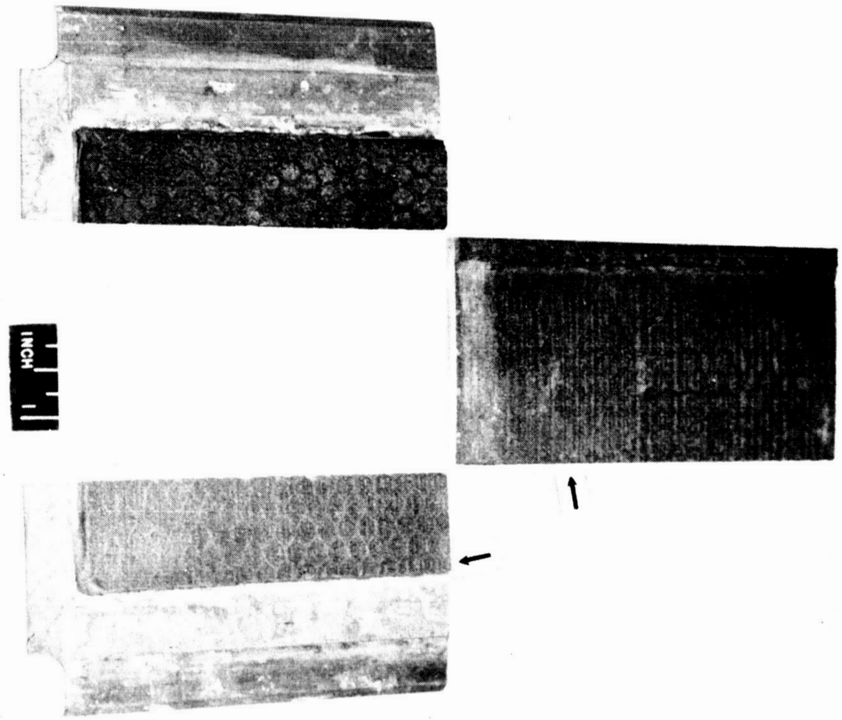

Figure IV-3. Close-up View of the Upper End of the Recovered Mercury MA-8 Shingle. The Center and Lower Sections Contain the ESM 1001 Material (Arrows).

V. NASA EVALUATION PROGRAM (OCTOBER–NOVEMBER 1962)

A. INTRODUCTION

This section has been prepared primarily to accumulate in one source for General Electric's consideration the data available from the initial material screening tests conducted by NASA in October-November 1962. NASA has cooperatively supplied most of this data and is perhaps more aware of interpretations than GE; only the data concerning GE ESM 1001 is, of course, presented.

B. PLASMADYNE DATA

Mass loss and temperature response of ESM material obtained at Plasmadyne were forwarded by NASA to GE. Test conditions and mass losses are shown in Table V-1.

TABLE V-1. PLASMADYNE TEST CONDITIONS

Model No.	h_s (Btu/lb)	P_T (atm)	P_o[1] (atm)	P (atm)	q_s model (Btu/ft^2-sec)	time (min)	change in wt. (grams)
10	10,400	.227	.043	.00414	232	0.75	5.4
11	10,348	.229	.042	.00414	231	1.0	7.05
106*	13,350	.069	.0123	.00122	101	3.0	23.7
115	13,330	.069	.0123	.0012	101	3.0	17.9
112	10,190	.029	.0056	.00052	52	3.0	12.3
113	10,005	.0286	.0054	.00052	51	4.2	18.4

* Phenolic nylon

Evaluation of the heat of degradation of Model No. 115, relative to the known performance of phenolic nylon for these conditions, was 9000 Btu/lb, similar to values observed in GE facilities for similar test conditions.

C. LANGLEY TESTS OF MA-8 MATERIAL

Prior to flying test panels on the MA-8 Mercury vehicle, tests were conducted at Langley Field on each of the various materials. Figures V-1 and V-2 show the backface temperature data available to GE, namely, the Langley Reference PNM (specimens 2, 3, and 4), the GE Low-Density 500, and the GE ESM 1001 elastomer. All specimens were 5" x 5" bonded to beryllium, with thickness sized to 1/2 lb/ft^2 (ESM thickness was 0.092 inch including bond).

Test condition was 2 Btu/ft^2-sec followed by 6 Btu/ft^2-sec intended to approximate the expected MA-8 thermal pulse. There were two general criteria in this assessment: (1) backface temperature rise characteristic and (2) physical erosion, cracking, etc., to be judged from post-test visual inspection.

Discussion with NASA of the results led to the following conclusions:

(1) Of all materials (other manufacturers not specifically known), four seemed satisfactory from a visual inspection point of view. Criteria were erosion, cracks, loose material, "mud-cracking", etc. The Langley PNM, the ESM, and the Series 500 were three of the four materials judged satisfactory.

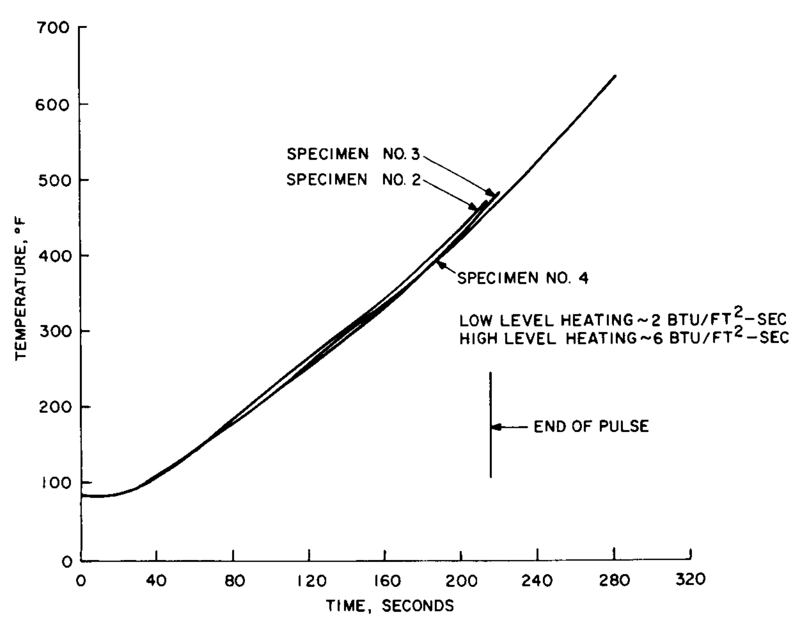

Figure V-1. Langley Research Center — MA-8 Flight Material

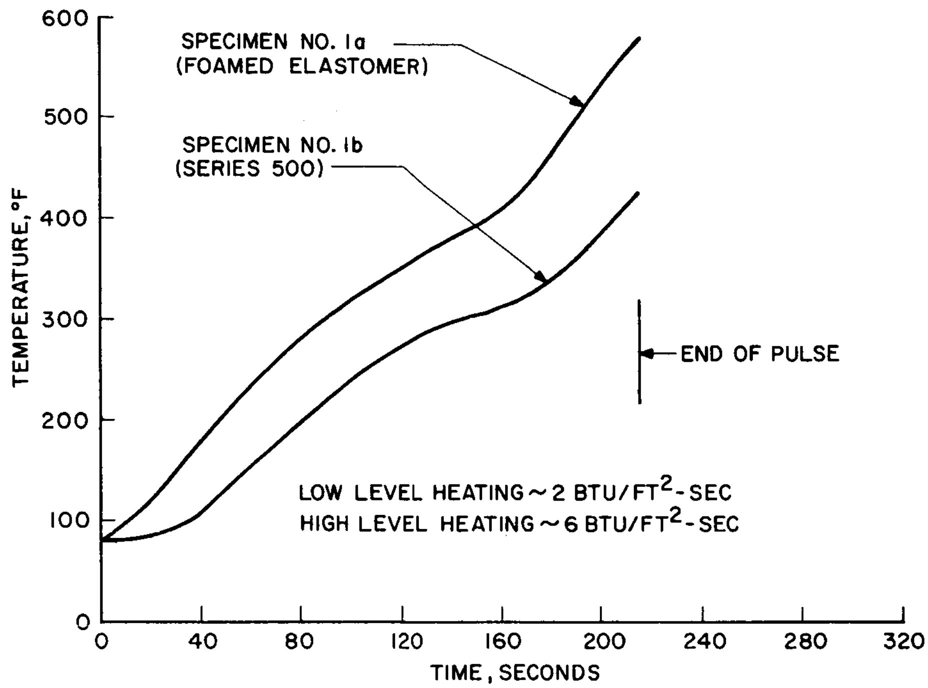

Figure V-2. General Electric — Foamed Elastomer and Series 500

	2 Btu/ft^2-sec	6 Btu/ft^2-sec
G.E. Series 500–27	Material gradually turned darker in color. No burning observed but temperature of beryllium sheet showed continuous rise.	Material burned on surface causing some removal of honeycomb walls. There was no blistering, separation or loss of material from honeycomb. Surface after test was rough but regular.
G.E. Foamed Elastomer	Material gradually turned darker in color. No burning observed but temperature of beryllium sheet showed continuous rise.	Material burned on surface and gradually turned white in color. There was no blistering, separation, or loss of material from honeycomb.

(2) Backface temperature rise was least of all for the GE Low-Density 500 (385° F after 200 seconds). The PNM was considered satisfactory (430° after 200 seconds). The GE-ESM was also considered satisfactory (520° after 200 seconds). The fourth material judged satisfactory from a post-test inspection point of view was, of course, another manufacturer's and the backface temperature for this material is not known by GE.

It should be noted that it has been reported that none of the materials flown on the MA-8 appeared to be as seriously eroded, cracked, etc., after the actual MA-8 flight as they were after the Langley test. This difference was attributed to oxygen content or other characteristics of the laboratory test.

D. MICROMETERORITE IMPACT TESTS AT AMES

Several thermal shield materials which were being considered by NASA in October 1962 were programmed for impact tests at the Ames Research Center. The results on samples of ESM 1001 were qualitatively reviewed by NASA with General Electric. ESM samples were 6" x 6" x 3/4" and weighed 3.75 lb/ft^2. They were bonded to 0.15 stainless with a soft bond, RTV 60.

It was reported that even at the low temperature (-150°F), no "shattering" occurred. A rather outstanding result seemed to be the retention of bond about the penetrating hole. Generally, no bond separation other than that from the "petals" of backface material occurred.

Actual firing information is as follows:

Firing	Particle (Grams)	Impact Speed (fps)	Impact Angle (Degrees)	T ($^{\circ}$F)	Penetration Diameter Particle Diameter	Remarks
A	.036	20,940	$\cong 90^{\circ}$	72°	5	Best of lot, good adhesion to honeycomb; penetration localized to cells; back plate hollowed out, not penetrated.
B	.036	20,300	$\cong 90^{\circ}$	-75°	N.A.	Example of classical diag. failure, 4 petal. Good adhesion of elastomer to honeycomb and backplate up to point of petaling out.
C	.036	18,670	$\cong 90^{\circ}$	-150°	2	Similar to B but petal penetration.
D	.036	18,471	$\cong 45^{\circ}$	-127° F	N.A.	Particle impacted target at an angle of 45°, penetrated about 1/2 thickness of target.

The significance of these tests was (1) the ability of the ESM 1001 to retain non-shattering elastic properties at very low temperatures and (2) the ability of the soft bond to retain adhesion except at the actual penetration damage locale.

E. 900 BTU THERMAL TESTS AT GE

As part of the October-November assessment of possible materials for an alternate Apollo shield, NASA had several materials tested at the General Electric Space Sciences Laboratory. Tests were to be nominally at a flux of 900 Btu/ft^2. Complete test results were submitted to NASA in the final report for this contract (NAS 9-976) on November 16, 1962. Excerpted herein is the test data for the ESM 1001 samples. The test facility was a water-cooled shroud which received heated air from a vortex-stabilized graphite electric arc. The test specimen was inserted concentrically within the shroud with only a few mils clearance.

Test specimens were of nominal one-inch diameter and a thickness defined by a nominal one lb/ft^2. Each specimen was photographed after exposure. Backface temperatures were measured. Specimens selected by NASA were weighed and measured after exposure. Table V-2 presents the test conditions for the three ESM 1001 specimen; Figures V-3, 4, and 5 present the backface temperature time histories, each showing sharp temperature rises at about four seconds. This data shows the almost-negligible backface temperature rise up to the time that the char interface reaches the temperature-monitored slug.

TABLE V-2. TEST CONDITIONS — ESM 1001

Run No.	NASA Model No.	Stagnation Press. (Psia)	Heat Transfer (Btu/ft^2-sec)	Gas Enthalpy (Btu/lb/RT_o)	Model Test Time (sec)	Length Change (inches)	Wt. Change (Grams)
2308	F2	33	805	149	8	—	—
2313	F4	43	940	173	5	—	—
2318	F3	42	960	172	5	—	—

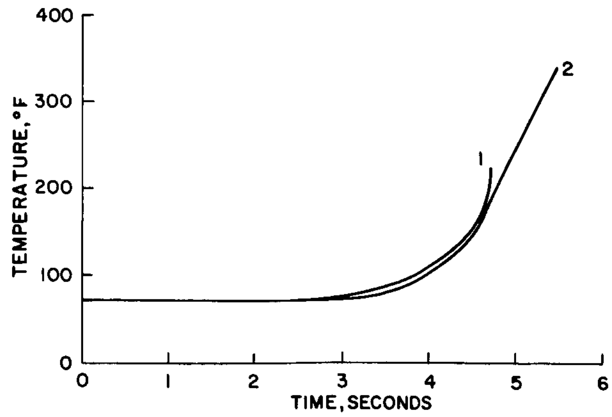

Figure V-3. Backface Temperature — NASA - F2

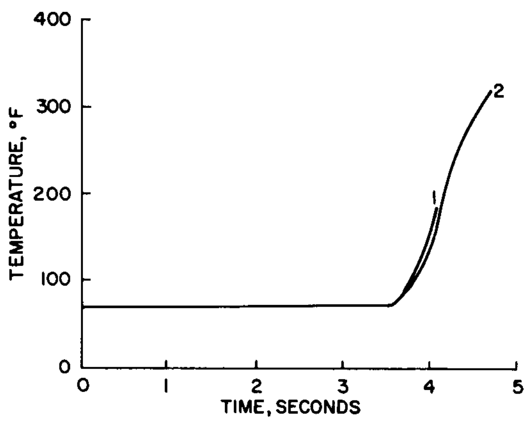

Figure V-4. Backface Temperature — NASA - F3

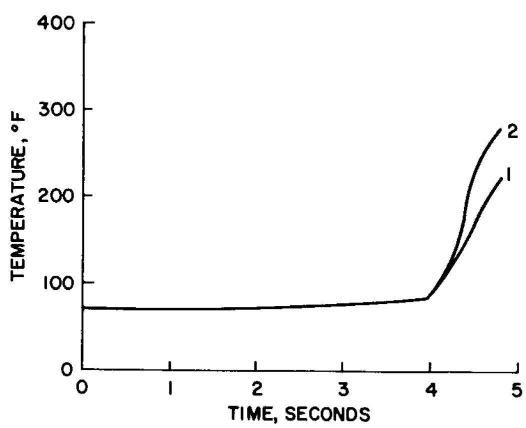

Figure V-5. Backface Temperature — NASA - F3

F. GE-MICROMETEORITE PROGRAM

A fixed price contract was awarded GE-RSD on 9 October 1962 to perform fifteen tests on samples to be provided by NASA - Manned Space Center. A single particle of 0.075 grams ±50 percent was to strike each sample with a velocity of 40,000 fps ±15 percent at sample temperature varying from -80° F to -200° F. The samples were 6" x 6" x 3/4" with three each of five materials supplied by the following:

(1) Avco

(2) McDonnell

(3) Emerson

(4) NASA - Langley

(5) GE-RSD

All work was to be completed by 30 October 1962. Between 24 September and 9 October, twelve firings of the high-explosive shaped-charge projector were conducted to check out and calibrate the range. Velocity measurements obtained on 8 out of these 12 firings varied from 8,400 to 35,000 fps and particle mass obtained on 2 of the 12 firings varied from 0.6 to 2.3 grams. Three of these firings were against GE-ESM 1001 targets at -80° F and -200° F.

From 11 October through 16 October, a total of 7 firings were made against the thermal shield targets provided and were witnessed by a NASA-MSC observer. Velocity measurements obtained on 6 of 7 firings varied from 6,300 to 28,000 fps and particle mass obtained 3 of 7 firings varied from 0.02 to 0.8 grams. The temperatures of the thermal shield targets were between -75° F and -258° F. Since these velocities and particle sizes were outside specifications, it was decided to stop firing against thermal shield targets and use steel targets until the specified conditions could be met.

From 17 October through 3 November, a total of 22 firings were made. Velocity measurements obtained on 21 of these firings varied from 9,900 to 35,800 fps and particle mass obtained on only 2 out of 22 firings varied from 0.3 to 3.2 grams. The reason for obtaining measurements of particle size on only 2 of these firings was due to the failure of three x-ray tubes used in measuring particle size.

In summary, then, out of 41 firings, 5 were within velocity requirements and none within particle mass specifications. This information was presented to NASA-MSC on 4 November 1962.

Considering the development state-of-the-art of the shaped-charge projector, and the instrumentation required, NASA decided not to do any further tests until RSD could assure repeatability in velocity and greater assurance of controlling and measuring particle size. RSD could not give any reasonable time estimate as to when the above requirements could be met. RSD then recommended to NASA that the contract be terminated at no cost to NASA. RSD agreed to absorb all costs to date and to continue development of the facility. When RSD considers that it can meet the contract requirements, negotiations could be reopened for further tests. This was agreed to by NASA-MSC.

Although some valuable qualitative information was obtained from the firings which had been made (total shattering of some materials and penetration only of others), development of the projector <u>is</u> required and <u>is</u> proceeding. This is reported in Section VII.

VI. NAA PROGRAM (DECEMBER 1962—JANUARY 1963)

A. INTRODUCTION

Following the NASA-MSC evaluation of several materials in October-November, 62, North American entered a program to more fully evaluate recommended materials. The General Electric ESM 1001 material was out of these.

On November 7, 1962, a meeting was held with NAA, at their request, wherein RSD was asked to supply ESM samples in support of a material screening program for the Apollo Command Module Alternate Shield. ESM-1002 with a density of 45 ± 2 lbs/ft^3 was supplied in the following sizes and quantities:

Qty	Size
29	12" x 12" x 1" thick
40	12" x 12" x 2" thick
12	6" x 6" x 3" thick

The first delivery was made December 7, 1962, and the order was completed on January 24, 1963. All deliveries were timely, based on receipt of the honeycomb supplied by NAA. The 1" and 2" samples were made in a 25" x 25" mold and cut to size after post-cure, providing a start for the scale-up process necessary to build large structures like Apollo.

In addition to the above samples, the following bonded test specimens of ESM-1002 were provided to NAA:

Qty	Size	Purpose
20	3" x 3" x 1"	Tensile adhesion
20	1" x 1" x .05"	Tensile shear
20	1" x 1" x .125"	Tensile shear
20	1" x 1" x .250"	Tensile shear

These initial specimens were shipped on January 14, 1963, and the order was completed by January 24, 1963. All items were shipped in sufficient time to permit test results to be available per the NAA schedule. All the above samples were provided on a fixed-price basis.

B. DATA FROM THE NAA EVALUATION OF ESM 1001

Although some information has been obtained through discussions with NAA, most data was as yet single-point or otherwise preliminary. As this data becomes available early in February 1963, it will be presented directly by NAA to NASA and will also be available to GE-RSD. Therefore, this section will be revised later. It should be noted that the preliminary data from the NAA work, while not contained herein, has confirmed some characteristics (thermal conductivity, etc.) also being obtained by GE.

C. TECHNICAL CONSULTATION WITH NAA

As part of the December-January material assessment program by NAA, General Electric participated by providing engineering liaison in the thermodynamics, materials, and test areas. This was physically done by visits of NAA personnel to GE at Philadelphia, by GE to NAA Downey, and by telephone and letter exchange.

Areas of Investigation in which GE has provided technical assistance to NAA were ablative material test design, instrumentation, and data analysis. A typical problem on which assistance was provided is shown below.

APOLLO ABLATION TESTS*

Objectives

Determine ablation characteristics under the following conditions:

Shear (τ) (lb/ft^2)	Heating Rate ($\dot{q}$) (Btu/ft^2sec)
0 to 1	≈ 1400
3 to 8	≈ 1800

Discussion

Several techniques have been pursued, including several different types of test model and several different facilities. Malta Test Station can provide the high-flux, high-shear conditions, using a flat-faced cylindrical model; in fact, the low-shear conditions also exist on this model, but over a very small area.

An alternate method of obtaining $3<\tau<8$ was studied, using wedge models of various wedge-angles ($0^{o}<\delta<25^{o}$). With this approach, the desired shear levels could be attained, but not simultaneously with the heating rates of interest.

To achieve the low shears ($0<\tau<1$) it was decided that the GE Space Sciences Laboratory Supersonic Arc Tunnel would provide the most satisfactory simulation, of the facilities investigated. This will provide appropriate wall shear stress, but low heating rate. Simultaneous provision of τ and $\dot{q}$ is not known to be feasible in any facility. The test model in the Supersonic Arc Tunnel would be a flat plate substituted for a portion of the wall in the diverging section of the nozzle.

The low shears could also be obtained in the GE-SSL Hypersonic Arc Tunnel, but this facility is not presently adapted for accepting a test material as a portion of the nozzle wall. It would, however, provide approximately the heating rate of the Supersonic Arc Tunnel.

The use of negative angles of attack of wedge models in the Malta rocket exhaust was also checked (for low shear). Such large negative angles were found to be required to get sufficiently low shear that separated flow was likely to result.

*Details of instrumentation and data analysis were included in these discussions, but are not included in this document.

D. GE-NAA VISITS AND CORRESPONDENCE

1. VISITS

   a. W. Mertz (GE Thermodynamics) to NAA — January 10, 11, 1963.

   b. S. Allen and L. Laciny, NAA to GE on 18 Dec. 1962, to W. Mertz, J. Glancey.

2. TECHNICAL CORRESPONDENCE

J. Bueche to L. Laciny on December 28, 1962, Recommended facilities and instrumentation for low-shear, high-heat-flux environment.

VII. RELATED DEVELOPMENTS

Thus far, this study has reviewed the history of ESM material and discussed the test data accumulated from various sources. General Electric's next planned work with ESM as well as the present concept of an Apollo thermal shield designed to use ESM 1000 will be discussed later in this document. However, before proceeding to these next steps, this Section describes several signficant activities that either have been related to the Apollo shield development to date, or use ESM for other applications. These are as follows:

(1) GE Hypervelocity Projector Facility Developments

(2) GE Thermal Test Facility Developments

(3) Other applications for which ESM series materials are being considered.

A. HYPERVELOCITY PROJECTOR FACILITY DEVELOPMENT

The Superpressure Studies Operation of the General Electric Space Sciences Laboratory has been working for more than five years in various phases of hypervelocity impact with the principal emphasis on the development of hypervelocity projectors. The early work was with a type of gun using high explosive as a propellant. This gun, which was originally developed in the 1957-58 period, was very competitive with light gas guns of the same period when used to fire aluminum projectiles. The upper velocity of this type of projector is limited by the detonation velocity of the explosive and does not appear to be capable of velocity much in excess of 20,000 feet per second. However, it has the advantage, of firing a preformed projectile, is relatively inexpensive, and is useful for a great number of experiments that do not require velocities in excess of its capabilities.

Approximately one year ago, as part of the General Electric Independent Research Program, Superpressure Studies started working on projectors employing the hypervelocity jet principle for achieving extremely high velocity. These projectors are somewhat similar in principle to the hypervelocity jet projectors that were developed by the Ballistics Research Laboratories. These latter projectors have achieved a velocity of approximately 79,000 feet per second and a beryllium projectile approximately 5/8-inch long, 1/8-inch in diameter, and weighing approximately one-quarter gram.

The BRL Hypervelocity Jet Projector achieves its outstanding performance by attempting to match the detonation velocity of the high explosive to the velocity of sound in the jet liner material. Superpressure Studies achieves comparable results by using a matching section between the high explosive and the jet liner material. This matching section seems to act as an impedance-matching device to couple more of the energy of the explosive into the liner, thereby producing a higher velocity.

It should be noted that instrumenting tests on Hypervelocity Jet Projectors presents some extremely difficult problems, some of which have been solved in only a partially satisfactory manner. The seemingly simple problem of measuring velocity, for example, presents some truly formidable problems. Superpressure Studies generally uses three independent means of measuring velocity in order to achieve reasonable confidence in the velocity results obtained. The first (and probably the most precise) velocity measuring system is to allow the projectiles to pass through electrically charged screens spaced at known distances apart, so as to produce electrical pulses that can be recorded on some form of high speed timer. Superpressure Studies uses two raster oscilloscope systems, capable of being read to an accuracy of better than 10^{-7} seconds, for timing transits through the velocity screens. In addition, at least three velocity screens are used for each shot. Unfortunately, a velocity screen is incapable of distinguishing what passed through it. Thus there is always some possibility that the pulse produced by one velocity screen may not have been caused by the same particle that caused the pulse from another velocity screen. For this reason, one cannot fully trust velocity data obtained solely from velocity screens.

In order to resolve the possible ambiguity in velocity screen data, Superpressure Studies normally attempts to observe the projectiles in flight by means of a high-speed camera. Unfortunately, very high-speed particles are usually surrounded by ablation products and/or shock-heated gases and are therefore not visible using visible light photography. However, the gaseous products surrounding the projectile are visible and are relatively stable so measurements of their velocity are reasonably good measurements of the projectile velocity. A rotating-mirror camera is generally used for this work, and the velocity results so obtained generally are in reasonable agreement with the results obtained from velocity screens.

In addition to the velocity measurements previously discussed, it is customary to try to observe the high-speed particles in flight by means of microflash x-ray. This is the only way presently known for determining the mass of the fast particles. Furthermore, if the time of functioning of the x-ray apparatus is precisely known, the picture of the particle on the x-ray screen is a good measure of its velocity. Unfortunately, the x-ray is a single-shot device and yields no information unless triggered at precisely the correct time. Furthermore, the particles of interest are near the limit of resolution of microflash x-ray equipment; therefore, they are extremely difficult to see on the x-ray plate. For this reason, it is extremely difficult to specify the mass of the fast particles to a very high degree of precision.

Many of these state-of-the-art problems became apparent during the micrometeorite testing attempted for NASA in October 1962 as discussed in Section V. Since that date, about 50 firings have been accomplished in a program to attain reproducibility and measurability of these high-speed particles. The specific steps that have been taken are:

(1) Reduction of charge size and length from four inches to about two inches. No significant velocity decrease but less blast and debris are encouraging results.

(2) Aluminum liners have been used rather than steel. This, too, has resulted in improved performance.

(3) Instrumentation via x-ray of the particle has been enhanced by the use of a 4" x 20" film rather than 8" x 10" as previously used.

(4) A further improvement in particle x-ray has been obtained by triggering with an ionization probe at the bottom of the charge, rather than with a velocity screen.

Subject to the complications of measurement discussed in the previous paragraphs, Superpressure Studies has progressed to the point where it can achieve velocities in excess of 40,000 feet per second with aluminum particle masses in the order of 0.1 gram with reasonable consistency. It should be noted that the shot-to-shot reproducibility of this type of projector is not very good at the present time. This is now under intense investigation; some progress has been made, and further improvement is expected in the near future.

In addition to its work on Hypervelocity Jet Projectors, Superpressure Studies has done some work with small cylindrical shaped charges using brittle cast iron liners. These charges yield a small cloud of cast iron particles in the 10 to 100-micron size range moving at a velocity of approximately 50,000 feet per second. This significant development may offer particles which nearly match expected micrometeorites. To date, impact on a sample is typified by a two-inch diameter cloud fired from a point source at a range of eight inches.

B. GE EXPERIMENTAL CAPABILITIES FOR CONDUCTING THERMAL SHIELD HEAT PROTECTION STUDIES

Since the inception of the ballistic missile programs of the United States Air Force, the General Electric Company, and particularly the Space Sciences Laboratory, has been engaged in the experimental evaluation of the performance of ablation materials for thermal shield applications. Numerous types of electric-arc-heated test facilities have been developed and used to provide the various environments in which such materials evaluation can be performed. Current practice in the industry and at SSL uses arc-heated test configurations such as atmospheric free jets, wind tunnels, and other specially designed test stands for specific environmental simulation. While detailed descriptions of all such facilities are not contemplated here, it may be of interest to describe briefly some of the latest simulation techniques and experimental studies that are appropriate for thermal shield materials performance evaluation.

1. COMBINED RADIATIVE-CONVECTIVE THERMAL TEST FACILITY

Currently there is being conducted at the Space Sciences Laboratory an experimental program to study the effect on ablation materials of combined radiative and convective heating pulses. A tandem-Gerdien arc heater (developed at this laboratory) that has been shown to be capable of generating extremely clean (100 ppm), very high stagnation enthalpy air flows ($^{h}s/RT_0 > 400$) was modified to further increase the test gas enthalpy, thereby providing a source of appreciable radiant intensity for model test purposes. To control the convective heat transfer from the high stagnation enthalpy flow, a bleed arrangement is incorporated whereby the radiating gas is diverted prior to its arrival at the model location.

Facility calibration, total calorimetry, and model testing with ablation materials have been conducted at somewhat less than two atmospheres stagnation pressure and radiant intensity values around 200 watts/cm^2. At these conditions, convective heating can be varied from 50 to approximately 2000 Btu/ft^2-sec. Calorimetry measurements to date indicate the total enthalpy ($^{h}s/RT_0$) at the entrance to the test region to be in excess of 700, which represents escape velocity enthalpy simulation. (Theoretical calculations of the energy transfer in this test unit confirms the above figure.) Sufficient data was obtained in the preliminary tests to indicate that the experimental technique is feasible and that meaningful test data can be measured. Currently, calibration is being performed at the five-atm. pressure level prior to the initiation of model testing. At these conditions, radiant intensity is being measured by a laboratory-developed sensor as well as by the use of thermopile techniques. Preliminary measurements indicate increased intensity values.

All-important in the evaluation of ablation materials in experimental facilities is an accurate knowledge of the test flow properties. Although heat transfer, pressure, and enthalpy measurements have always been conducted in any test program, a more detailed understanding of the flow is necessary, especially when attempting to extrapolate test data to free-flight performance or correlate with theory. Presently

GE is engaged in such a study of the test flows in the Space Sciences Laboratory hypersonic arc tunnel. Measurements include the following: stagnation enthalpy from total calorimetry at the throat of the nozzle, stagnation enthalpy profiles at the nozzel exit (5" diameter) with an enthalpy probe, static pressure profiles across the flow and along the nozzle axis, electron concentration and electron temperature, gas species concentrations, total pressure profiles, rotational gas temperature, and velocity determination — all at the nozzle exit. Upon the completion of these studies, the data will be compared with theoretical calculations of the chemically reacting nozzle test flows. The net result of this effort will be to improve the capability to evaluate material performance in well-characterized simulated environments of arc-heated test facilities.

2. MALTA ROCKET EXHAUST TEST FACILITIES

A small rocket engine exhaust facility is available at the GE Malta test Station for screening purposes (designated Pit No. 1 and a complementary larger development-type facility (designated Pit No. 4).

Pit No. 1 employs a rocket motor with a five-inch exit diameter shockless nozzle, designed to produce parallel exhaust flow at a Mach No. of about 2.45. The facility is equipped with all the instrumentation and apparatus required to record the engine and model operating conditions. Nominal operating conditions are as follows:

Oxygen-to-Fuel Ratio	2.10
Total Chamber Pressure	300 psia
Model Stagnation Pressure	110 psia
Total Enthalpy	3000 Btu/lb
Mach No.	2.45
Test Time	60 seconds

By judicious selection of model geometry and variation of engine operating conditions, considerable variation in local test conditions can be obtained. For example, Figure VII-1 shows local environmental conditions obtained on a blunted wedge, for laminar

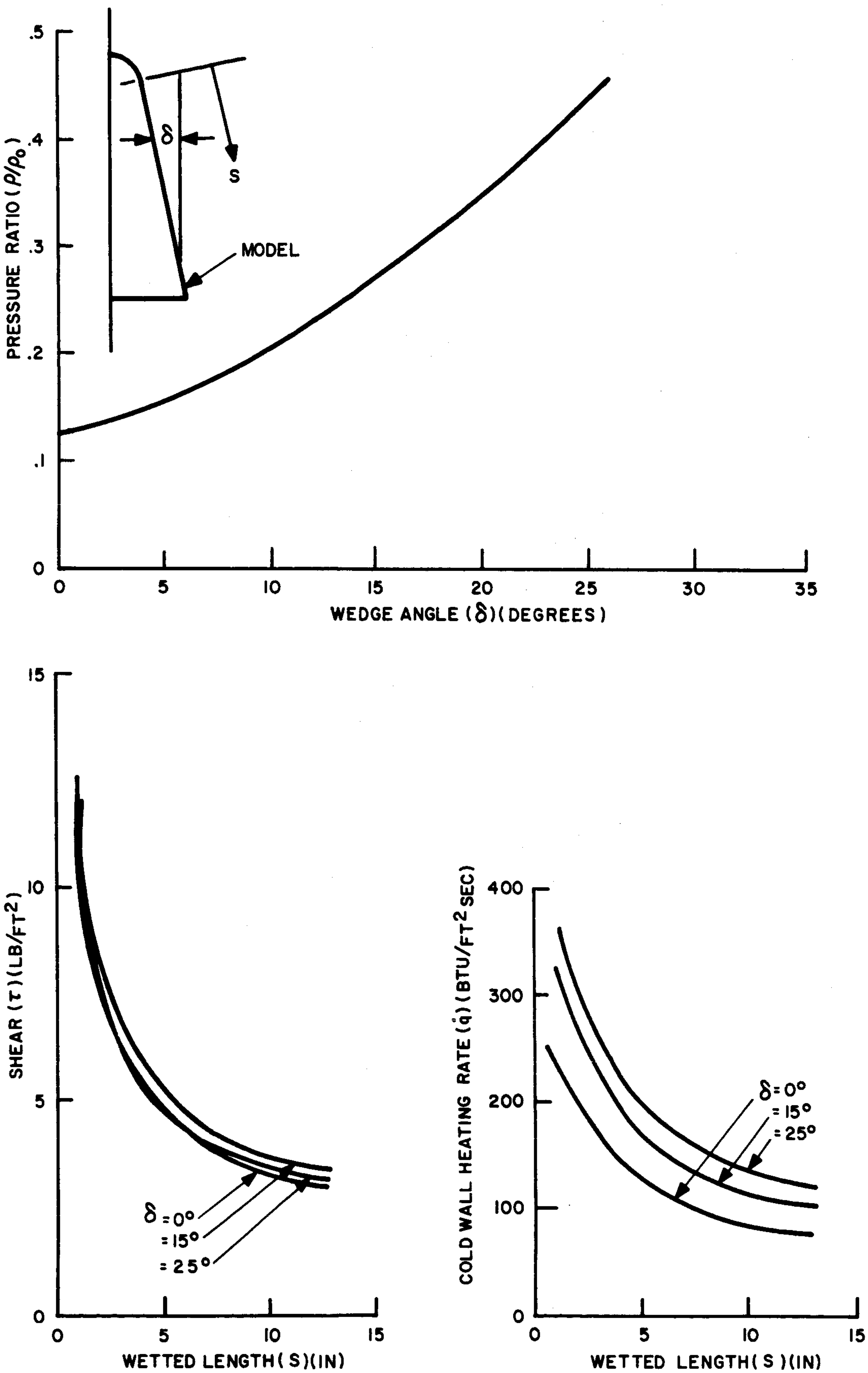

Figure VII-1. Malta Wedge Model Tests (Laminar Flow)

flow. Experience has shown, however, that above local δ's of 9^{o} that the flow becomes turbulent, thus affording evaluation of sizable test sections in this flow environment.

Pit No. 4 is a design similar to Pit No. 1 except that model sizes at least a factor of four larger may be tested. Model stagnation pressure is 150 psia, enthalpy 3500, and Mach No. ~ 3.0.

Such facilities have proven extremely useful for evaluating fabrication techniques, gaps, cut-outs, etc.

3. SPACE SCIENCE ARC-DRIVEN TEST FACILITY

Brief descriptions of the General Electric Space Sciences Laboratory material test facilities are presented below.

a. Hypersonic Arc Tunnel (Operational since 1961)

A moderately high Mach number (to M = 8) low-density wind tunnel which uses superheated air as the test gas. The gas is heated by an electric arc unit of the Tandem-Gerdien or divided-flow type (Figure VII-2), the heat sensitive components of which are water cooled to permit continuous operation over extended test periods. The arc unit is supplied from a 500 kw d-c ballast-stabilized power source.

The test gas is heated in the arc column, collected in a central plenum, and expanded through a sonic throat and conical nozzle to a low pressure test section. From here the gas continues on through a diffuser and a two-stage 5500 cfm mechanical vacuum pumping system. The test section is of the free jet type, the model being lowered into position downstream and just ahead of the diffuser inlet (Figure VII-3).

Two test stations are currently available. The normal station is at the 5" diameter nozzle exit and is fully visible. The secondary station, at the 1.2" diameter nozzle exit, is directly visible for surface temperature instrumentation only. Area ratios are 1000 and 58 respectively.

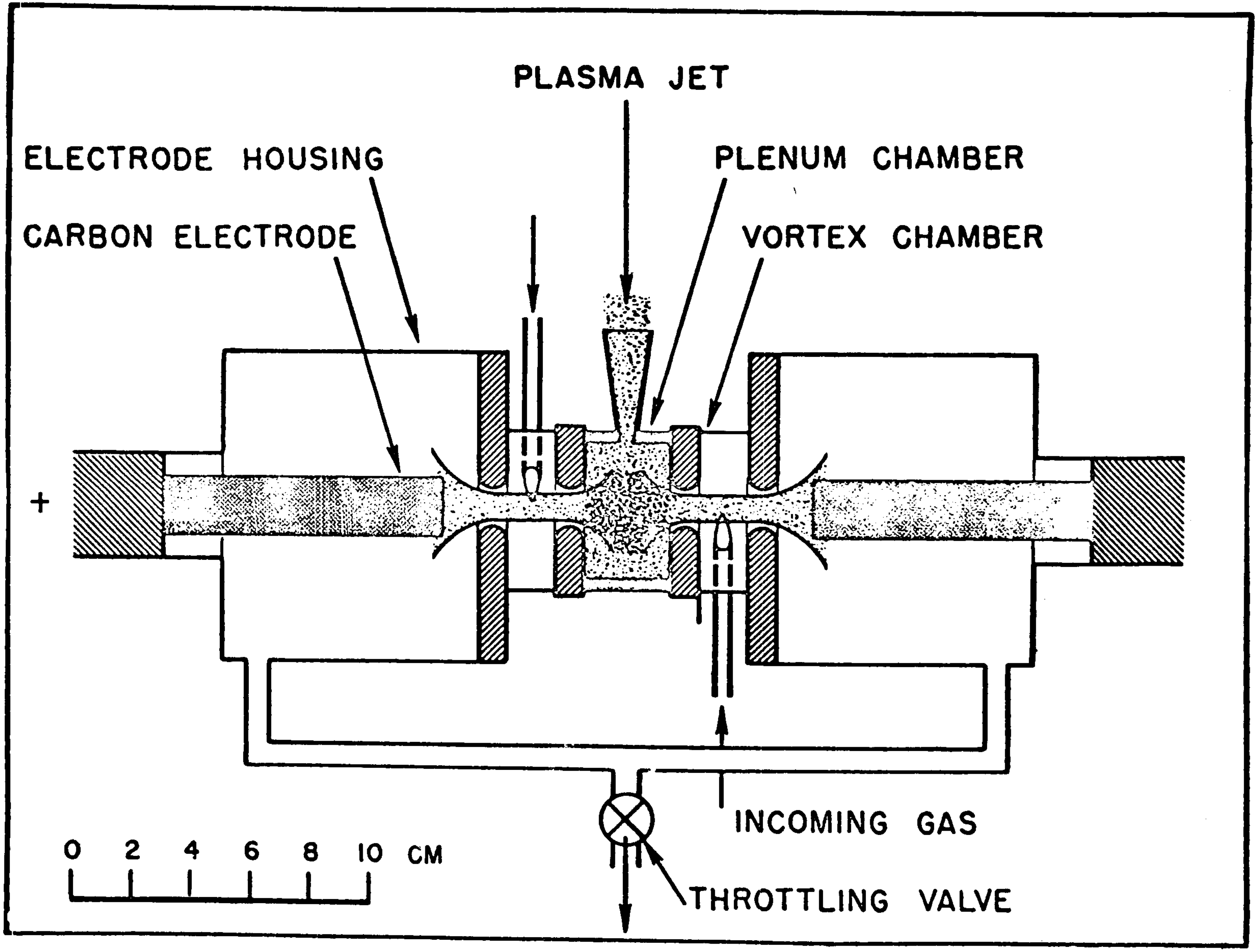

Figure VII-2. General Arrangement of the Tandem-Gerdien Plasma Jet Apparatus

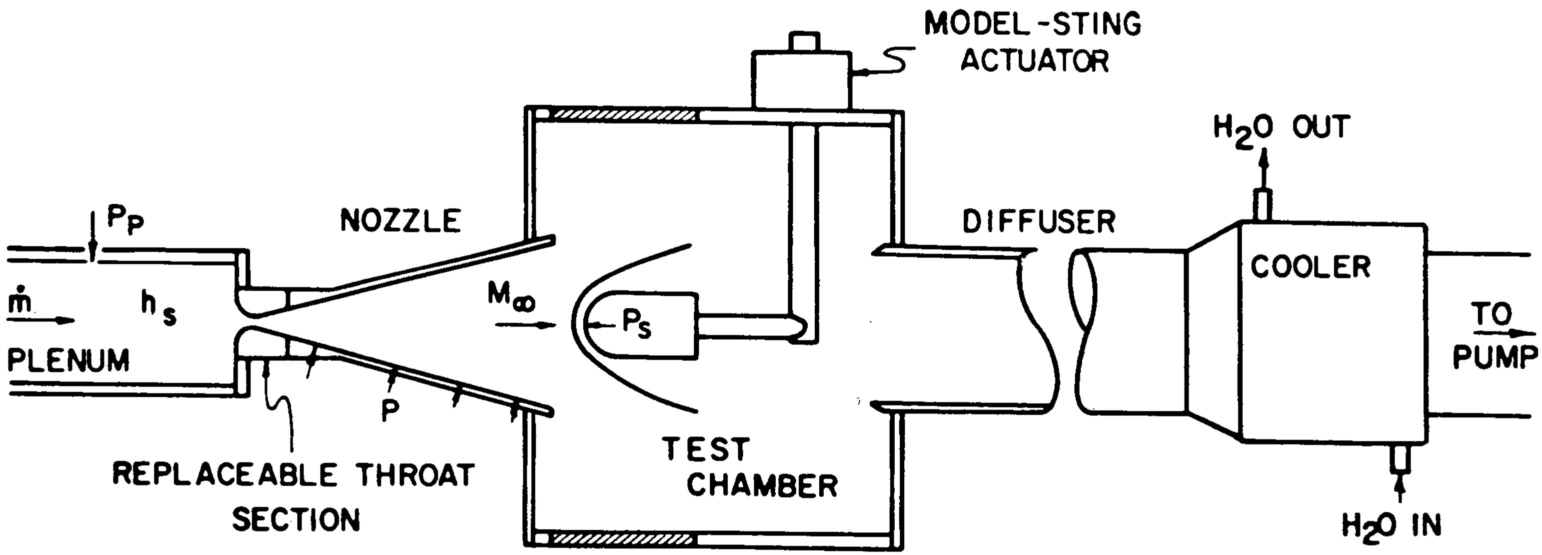

TYPICAL TEST MEASUREMENTS

MODEL

1. SURFACE T
2. SUB-SURFACE AND BACKWALL T
3. SURFACE P
4. SURFACE $\dot{q}_o$
5. ABLATION RATE-LOCAL AND TOTAL
6. FORCES - 3 COMPONENT
7. FLOW PHOTOGRAPHY

FACILITY AND CALIBRATION

1. VOLTAGE AND CURRENT
2. ELECTRODE EROSION RATE (IF APPROPRIATE)
3. AIR MASS FLOW RATE
4. P_P
5. GAS T -THROAT, PLENUM, TEST SECTION
6. h_s CALORIMETER-TEST GAS
7. NOZZLE STATIC PRESSURE - P
8. $\dot{q}_o$ PROFILES - TEST SECTION
9. P_s PROFILES - TEST SECTION
10. LUMINOSITY FLUCTUATIONS-TEST GAS

Figure VII-3. Characteristics of Supersonic Arc Wind Tunnel

b. <u>Tandem-Gerdien Free Jet (Operational since April 1962)</u>

The Tandem-Gerdien Free Jet Arc Facility is equipped with an arc heater similar to that used on the hypersonic arc tunnel. The primary difference is in the configuration of the plenum hardware. The free jet is designed to provide highly heated gas flows into ambient atmosphere. Since the gas flow does not reach a critical value, it remains subsonic, but has a high free stream velocity due to its high temperature.

Special plenum-nozzle configurations are available which permit study of radiation effects on test specimens, apart from convective heat transfer.

The diameter of the nozzle orifice limits the model size to 1/2". Models are delivered into the plasma by a pneumatically operated, water cooled sting.

c. <u>Shroud Nozzle Air Arc (Operational since 1958)</u>

A vortex-stabilized, axial-flow electric arc unit is employed to heat air (or other gas) prior to its passage through a nozzle constricted by the test specimen (Figure VII-4). With the inlet gas flow metered and regulated, the stagnation pressure is controlled by maintaining the proper annular clearance between the test specimen and the nozzle wall, even as the specimen surface recedes. Controls permit rapid insertion of the specimen into test position after the hot flow has stabilized and withdrawal after a pre-established test time.

d. <u>Supersonic Arc Tunnel (Operational since 1958)</u>

A supersonic (M = 4.8) low density wind tunnel similar in function and purpose to the hypersonic arc tunnel and utilizing the same mechanical vacuum pumping system. However, the arc heater is of the vortex-stabilized, axial-flow type, and the nozzle exit diameter is 2.06" (area ratio of 89).

In addition to the standard conical nozzle configuration, a unique rectangular nozzle is available for test of flat plate specimens in boundary layer flow (simulating glide vehicle wing type surfaces). The specimens form the walls in the downstream portion of the nozzle.

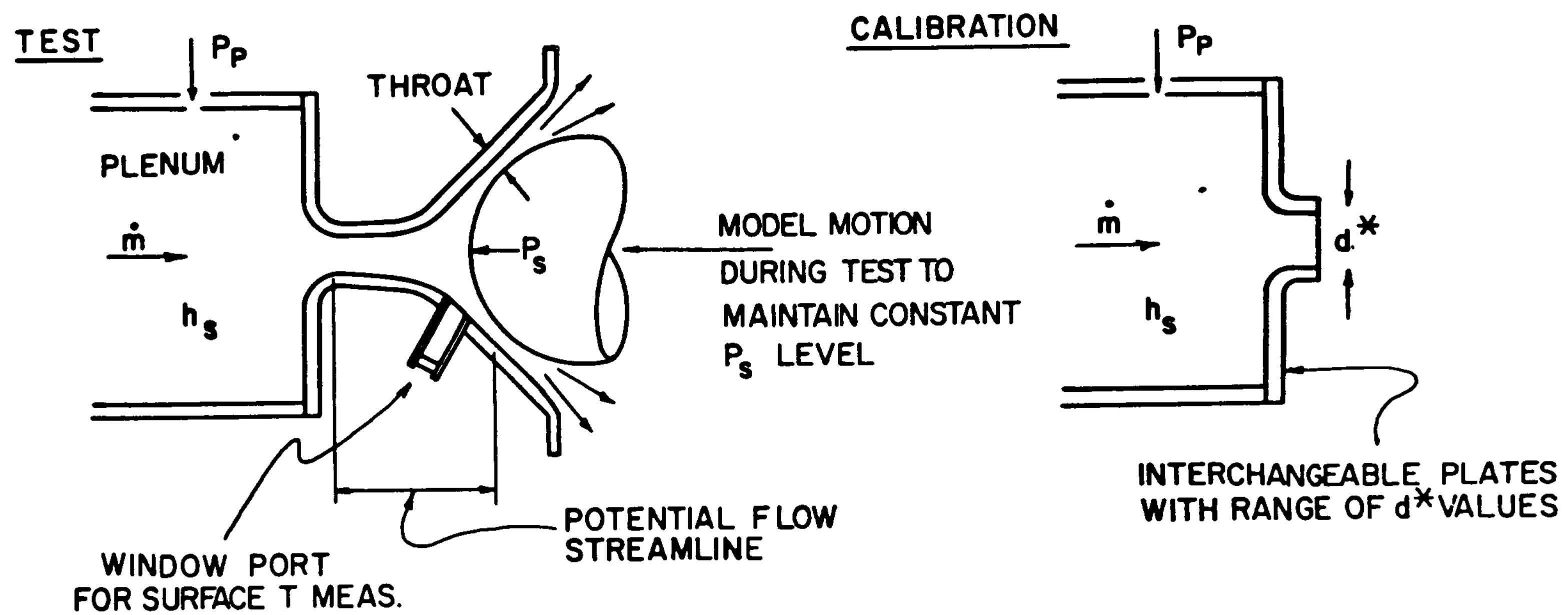

TYPICAL TEST MEASUREMENTS

MODEL

1. SURFACE TEMPERATURE
2. SUB-SURFACE AND BACKWALL TEMPERATURE
3. SURFACE PRESSURE
4. SURFACE HEAT TRANSFER RATES-NON-ABLATING
5. ABLATION RATE-LOCAL AND TOTAL

FACILTY AND CALIBRATION

1. VOLTAGE
2. CURRENT
3. ELECTRODE EROSION RATE (IF APPROPRIATE)
4. AIR MASS FLOW RATE
5. PLENUM PRESSURE
6. GAS TEMPERATURE - THROAT
7. GAS TEMPERATURE - PLENUM

Figure VII-4. Characteristics of Shroud Arc Test Facility

e. Arc-Heated Aerothermodynamic Test Facilities

Table VII-1 summarizes the performance characteristics of the facilities described in a. to d. above.

f. Arc Facilities Power Supply

All arc heated test facilities are d-c powered from a 500-kw variable ballast stabilized rectifier system.

g. Arc Facilities Instrumentation

Oscillographs and Ink Recorders, multi-channel

Spectrographs, ultraviolet through visible

Pyrometers: Photo-electric, two-color
Visual-optical
Total radiation, Golay cell

Thermopiles

Calorimeters: Model, slug
Survey Rake
Total, heat balance

Thermocuples

Mass Flow Meters

Voltmeters and Ammeters

Pressure: Transducers
Manometers
McCleod
Pirani

Force Balance, three component

Langmuir Probes

Electron Beam

TABLE VII-1

ARC-HEATED AEROTHERMODYNAMIC TEST FACILITIES

	Hypersonic Arc Tunnel	Supersonic Arc Tunnel	Tandem-Gerdien Free Jet	Shroud Nozzle Arc
Stagnation Enthalpy (Btu/lb)	4500 - 19,000	1300 - 7400	6800 - 14,500	3400 - 6800
Stagnation Pressure (psia)	15 - 25	4.3 - 14.7	16.	30 - 75
Model Stag. Press. (psia)	0.1 - 1.0	0.5 - 1.0	15.	30 - 75
Model Stag. Heating Rate (Btu/sec-ft^2)	60 - 250*	35 - 80*	380 - 2950**	300 - 3000*
Aerodynamic Shear lb/ft^2	$0.2 < \tau < 1.0$	0.5 - 2.0	$1 < \tau < 3$	$8 < \tau < 20$
Mass Flow (lb/sec)	0.0010 - 0.0020	0.0005 - 0.0026	0.003	0.005 - 0.010
Contamination Level of Heated Air (% carbon by weight)	<<0.1	<4.	<1.	<4.
Testing Time (seconds)	≤1000	≤1300	≤150	≤30
Mach Number	3 - 8	~5	<1	<1
Simulation: Velocity (ft/sec)	13,000 - 31,000	5,000 - 19,000	18,000 - 27,000	11,000 - 18,000
Altitude	200,000 - 270,000	190,000 - 230,000	145,000	80,000 - 120,000
Model Size	≤3." dia	≤1.5" dia. (or 10 sq." flat plates in rectang. nozzle, 2/test***)	≤0.5" dia.	0.67" - 1.50" dia.
Test Specimen Data:	Mass loss, dimension change, surface temperature, sub-surface temperature surface pressure, calorimeter heat transfer, surface and internal damage penetration and characteristics, photo and visual observation (except shroud nozzle arc).			

* to 1.0" dia. hemisphere

** to 0.5" dia. hemisphere

*** heat rate = 3-5 Btu/sec-ft^2

h. Arc Facilities Test Specimen Environmental Conditioner

An apparatus for exposing arc facility test specimens to vacuum conditions approximating that of near space in combination with radiant heat capable of bringing such specimens to space equilibrium temperature. Material specimens can be heated to $500^{o}F$ or any specified lower temperature in vacuo (to 10^{-6} mmHg depending upon outgassing characteristics of the material) and maintained at these conditions for long periods of time prior to being subjected to re-entry testing in one of the arc facilities. Six specimens may be conditioned simultaneously on an individual basis.

C. OTHER APPLICATIONS OF ESM SERIES THERMAL SHIELD MATERIAL

1. APOLLO COMMAND MODULE RADOME

GE-RSD submitted a proposal to NAA on 25 January 1963 for the design, fabrication, and qualification testing of the Apollo Radome. This proposed design employed the unique capabilities of the ESM material to obtain a radome fully compliant with the procurement specification and at a weight only 74 percent of the target weight. A type of non-charring material, designated ESM 1020, was specified for this application because of the requirement for antenna transmission before and after experiencing the re-entry heat flux. A preliminary sample was formulated during the proposal period and tested for thermal and transmission properties. A test specimen after exposure to a representative heat flux is shown in Figure VII-1. Note that very little crust or siliceous layer is formed on the surface by exposure to the thermal environment, as desired for this specific application. Results of the transmission testing were very close to the required performance indicating that no problems will be encountered in meeting all objectives with minor reformulation. This demonstrates the unique flexibility and the ease of tailoring ESM material to a specific design requirement.

The radome assembly consists of the ESM 1020 heat shield bonded to a fiberglass substructure with the antenna assembly (furnished by NAA) foamed into place within the fiberglass assembly. The low-density ESM 1020 (20 lb/ft^3) acts as an ablator-type heat shield and at the same time insulates the structure and internal components from excessive heat. This design was achieved at a weight of 34.6 pounds versus the weight target of approximately 47 pounds.

2. APOLLO SERVICE MODULE

Discussions have been held with both design and thermodynamic personnel at NAA concerning the use of ESM series materials on the service module. Two specific uses are contemplated:

(1) protection against the exhaust of the attitude control nozzles and

(2) main engine protection of the service module aft face.

Both of these uses are in the discussion phase only, but the results of the present NAA ESM 1002 assessment will be reviewed by Mr. P. Hogenson of NAA with service module use in mind.

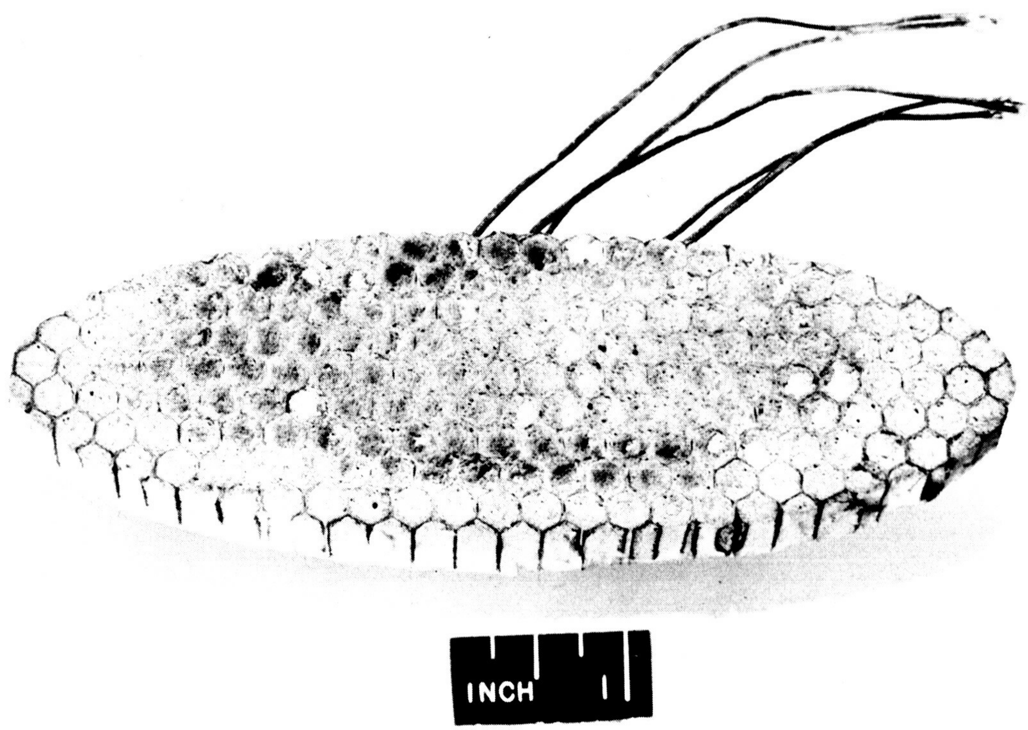

Figure VII-5. Sample of ESM 1020-type material, 43 lb/ft^3, after exposure in a hypersonic arc tunnel for 834 seconds at 6 Btu/ft^2-sec.

VIII. ADVANCED ESM CONCEPTS

General Electric has a number of programs currently underway in the synthesis of new ablation materials. After pioneering in the use of phenolic nylon as a thermal protection material for re-entry vehicles, GE developed the Century Series of ablators. More recently, the ESM 1000 Series materials have been developed, and additional work with this series is planned.

The following discussion is limited to the ESM development work, which, to date, has been concentrated on the ESM 1000 Series wherein the elastomeric filler material is contained in and supported by fiberglass honeycomb. However, many variations of this concept and other concepts are feasible and potentially are of great value in reducing manufacturing problems or for specific applications. In working with the material over an extended period from the standpoint of providing even better materials for next-generation vehicles, many of these design variations have been identified and are being studied for further development. Further study and development programs will be carried out as funding becomes available. Plans have been made for some of these and can be implemented as soon as approved. It is planned to investigate the full scope of applications of this extremely versatile material within the limits of GE-RSD capabilities.

A. UNREINFORCED FOAM

The simplest way to avoid problems associated with the honeycomb core is to eliminate the core or any other means of supporting the foam filler. Then a continuous foam blanket can be poured, and a large part of manufacturing and quality control problems and costs will be eliminated. A program has been planned to establish the performance of this type material in various environments and to obtain design data. This concept has such tremendous possibilities that it has been given high priority for development.

B. RANDOM FIBRE REINFORCED ESM

This concept, as shown in Figure VIII-1, is a compromise between the unreinforced foam and the filled matrix type such as the honeycomb-supported ESM 1000 Series. It is expected to have most of the superior manufacturing advantages of the unsupported foam while retaining most of the strength and shear resistance of the honeycomb matrix. Variations composed of different types and percentages of random fibres or of chopped cloth should be tested to establish material performance and design data.

C. CLOTH LAYERS IN FOAM

Cloth can be included in the foam in complete layers so as to obtain exact orientation and maximum strength. A sample of this type, shown in Figure VIII-2, was fabricated of fiberglass cloth and maximum density (unfoamed) filler. This sample exhibits all of the strength, toughness, and durability characteristic of a rubber tire.

D. TAPE WOUND

A concept is shown in Figure VIII-3 that is designed to give maximum strength and shear resistance. The tape is wound on a mandrel and at a slope to the shield surface so that optimum fibre orientation results. The ESM filler compound is introduced at the time of winding and may or may not be foamed afterwards. The lengthwise fibres of the tape are oriented to resist circumferential shield stresses while the crosswise fibres resist shears and radial stresses.

E. TWO LAYER MATRIX

Since the ESM has maximum insulation properties at low density while strength and shear resistance are better at high density, a two-density approach is proposed and is shown in Figure VIII-4. The high-density layer is sufficiently thick that all degradation takes place in this layer. The low-density layer provides insulation to limit structure temperature to the maximum allowable. The specific means of reinforcement to be used should be chosen for the particular design. Honeycomb, random fibres, or oriented cloth could be used for the low-density or the high-density or for both.

F. FILAMENT-WOUND LAYUP

This concept employs a criss-cross pattern filament winding of fiberglass or other suitable material to form the re-inforcing matrix into which the filler material will be foamed. An early test layup is shown in Figure VIII-5. Variations may be obtained by the size and spacing of the fibres, by variation of the filler, or by precoating the fibres with the ESM before winding. A variation of this in a flat form is shown in Figure VIII-6.

G. ORIENTED FIBRES WITH CLOTH BACKING

Figure VIII-7 depicts a means of reinforcing the ESM foam filler by a mat of stiff fibres oriented normal and woven into a cloth backing. In this concept, the fibres provide reinforcement to the foam and resist shear forces, while the cloth backing provides a continuous surface for hard bonding to structure. It is intended to thus avoid some of the manufacturing and design problems associated with the use of honeycomb as a reinforcement.

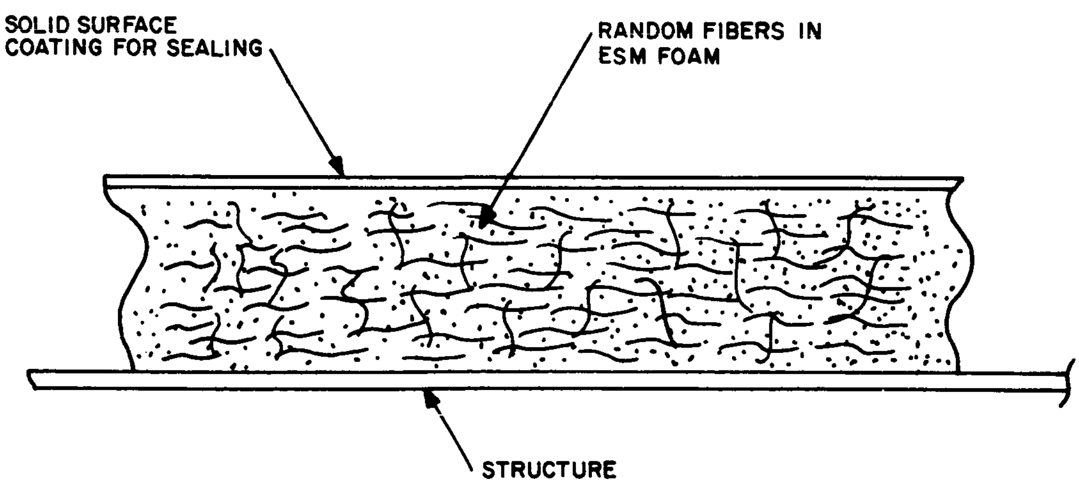

Figure VIII-1. Random Fibre Reinforced ESM.

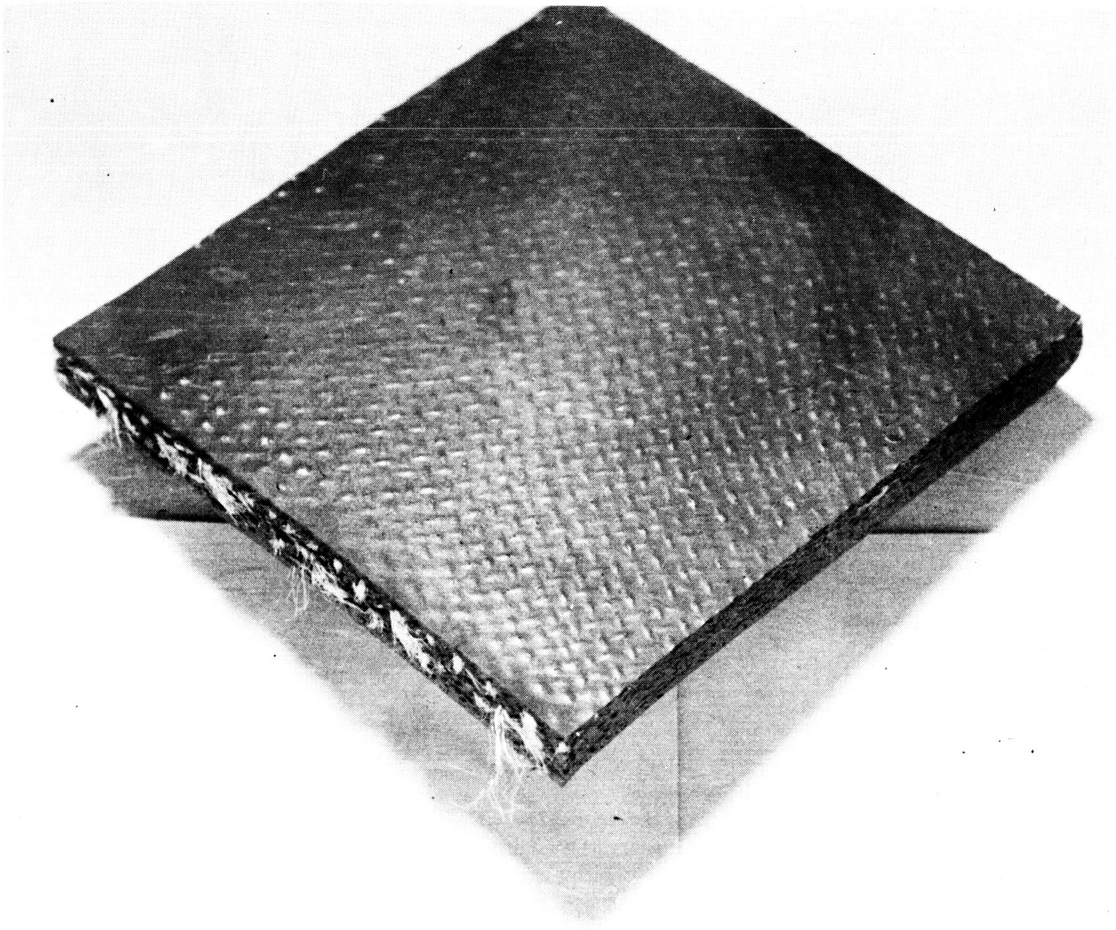

Figure VIII-2. Cloth Reinforced ESM.

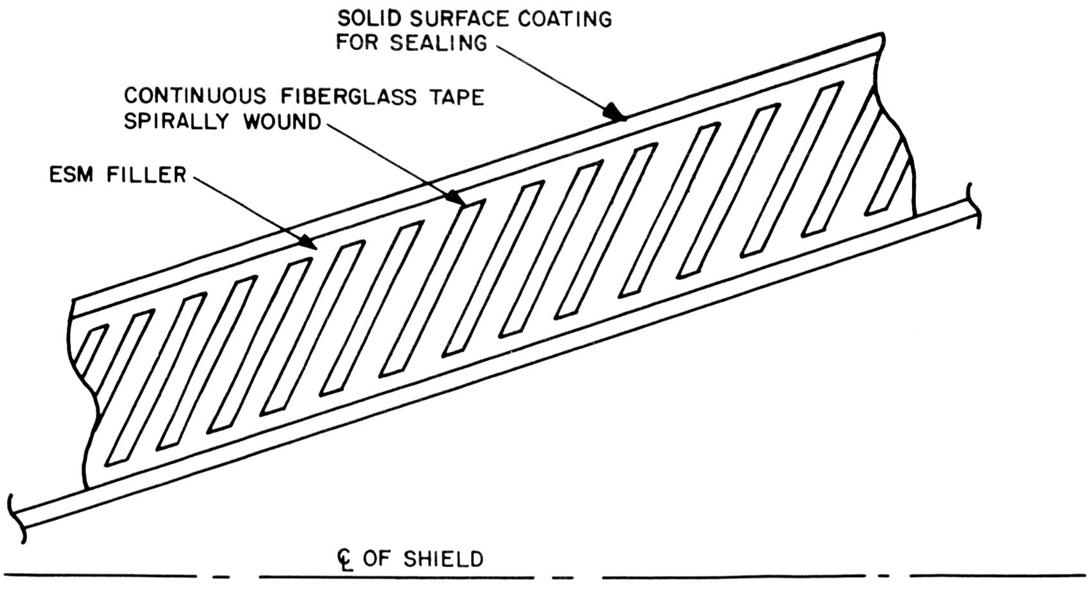

Figure VIII-3. Tape-wound ESM Shield.

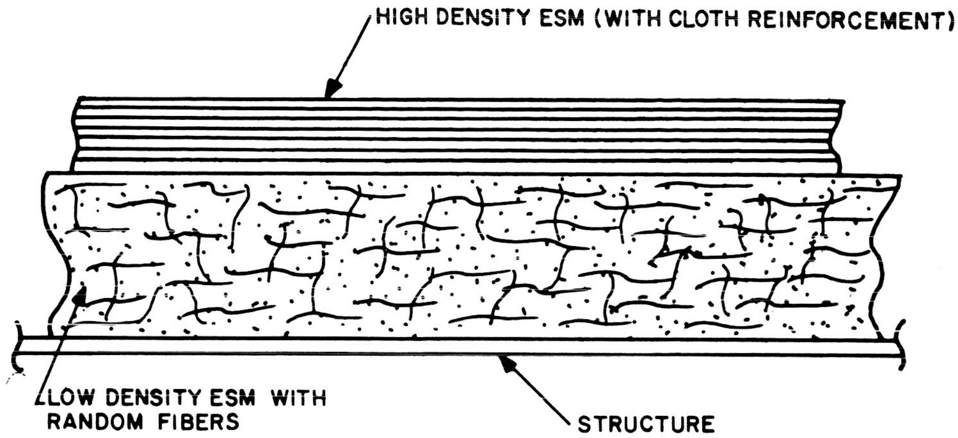

Figure VIII-4. Two Layer Matrix ESM Shield.

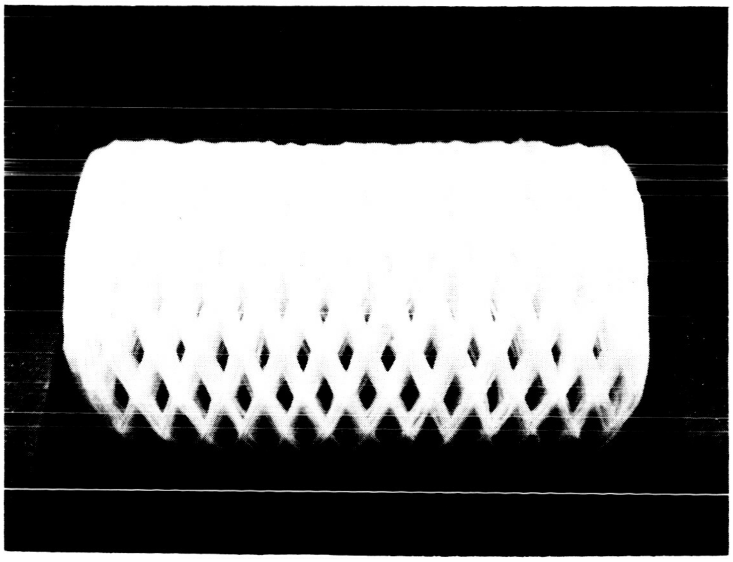

Figure VIII-5. Filament-wound Layup.

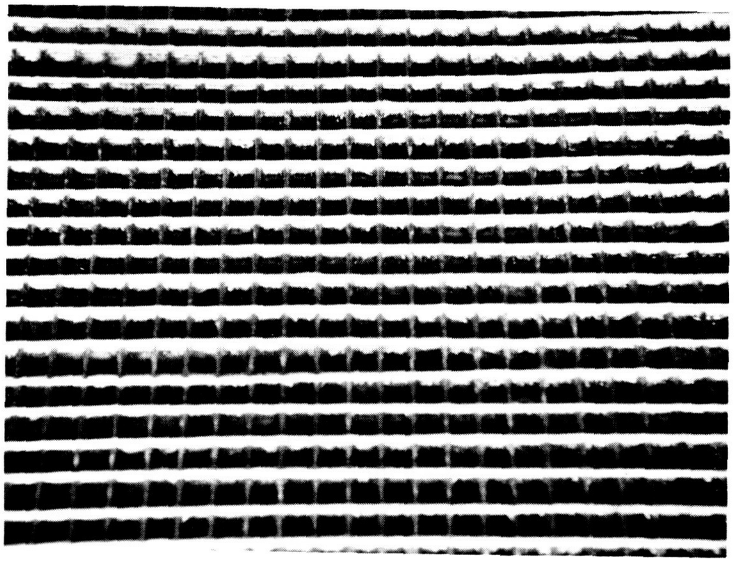

Figure VIII-6. Flat Filament Layup.

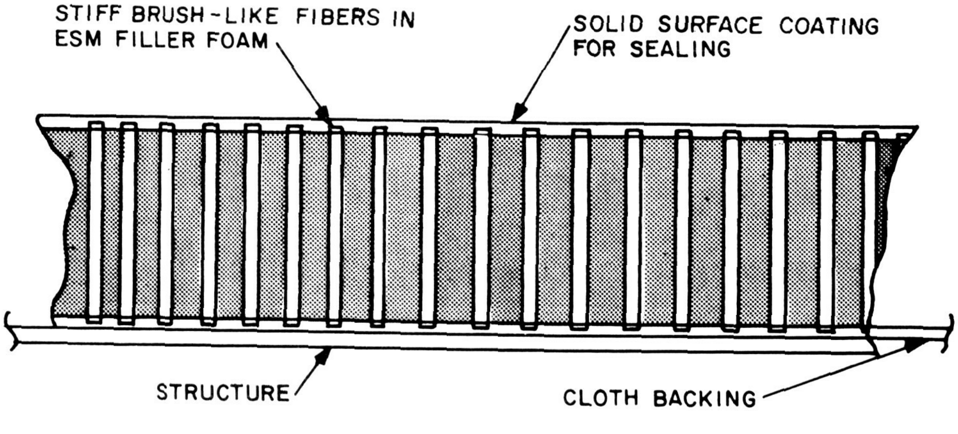

Figure VIII-7. Oriented Fibres with Cloth Backing.

IX. ESM DEVELOPMENT PLANS AND GE-FUNDED PROGRAM

For the first half of calendar year 1963, the General Electric Re-entry Systems Department has planned a required program aimed principally at extending the adaptability range of the basic ESM 1000 heat shield material. By examining the physical, density, and thermal modifications that can be achieved with slight formulation changes, it is probable that the shield material may be adapted for a broad range of re-entry conditions. It is imperative to continue to expand the knowledge in this field through the investigation of new elastomers, shield systems, and scale-up applications. Further investigations are expected to also result in new design applications for ESM. However, the first and most basic development steps are as presented in the following tasks:

(1) Development and Evaluation of High-Density Elastomer
(2) Evaluation of Unsupported Elastomer
(3) Development and Evaluation of Low-Density Elastomer
(4) Parametric Study of Elastomeric/Filler Systems
(5) Scale-up of ESM 1002

Two of these, Tasks 3 and 5, with immediate relation to the Apollo Thermal Shield, are partially funded by General Electric. All tasks could be undertaken or speeded up if additional funding can be obtained.

TASK 1 DEVELOPMENT AND EVALUATION OF HIGH DENSITY ELASTOMER IN HONEYCOMB

OBJECTIVES

(1) To define the maximum flux and shear level where ESM 1000 material will exhibit high performance capability. This will define the limits of use on re-entry vehicles.

(2) To develop the specific formulation(s) and/or shield systems that will perform best under the higher flux and shear levels.

(3) To generate sufficient properties data on the developed formulation(s) for a preliminary design.

BACKGROUND

Laboratory development activities in 1962 along with extensive ablation testing at 2500 Btu/ft^2-sec in the shroud arc and under high shear forces in Malta wedge models are presently being evaluated to meet objectives (1) and (2). This task will complete the program by generating ablation data in the medium flux range ($\sim$1400 Btu/ft^2-sec) and basic mechanical properties. The ensuing thermal and stress analysis will provide the necessary inputs for preliminary design and system trade-off studies.

Subtask 1

From the results of formulation testing at 2500 Btu/ft^2-sec, a series of samples will be fabricated and tested in the shroud arc at a medium heat flux level ($\sim$1400 Btu/ft^2-sec) representing station heating levels, other than stagnation, of typical re-entry shields.

Sample configurations and test conditions to be defined.

Data to be reported:

ΔW, ΔL, and effective heat of ablation.

Subtask 2

(1) Tensile — two formulations tested in two honeycomb directions with three replicates at -80°F, -65°F, -35°F, and R. T. = 48 samples.

(2) Coefficient of Expansion — two formulations in two honeycomb directions with two replicates tested from -250°F to +250°F = 16 samples.

(3) Compression — two formulations tested in two honeycomb directions with three replicates at R. T., 160°F, and 250°F = 36 samples.

Subtask 3

Preliminary thermal analysis to determine station-shield thicknesses for various flux levels on a specific re-entry vehicle.

Subtask 4

Preliminary stress analysis to determine mechanical safety margins for preliminary design and trade-off studies on a specific re-entry vehicle.

TASK 2 EVALUATION OF UNSUPPORTED ELASTOMERS

OBJECTIVE

To qualify formulations of unsupported ESM 1000 (not in honeycomb) and generate sufficient data for preliminary design.

BACKGROUND

Sufficient data is now being generated on ESM 1001 (a honeycomb-supported material) for preliminary design. This basic formulation might have even greater application opportunities if it were not in a honeycomb matrix. It would have a lower density, conductivity, and consequently a lower backface temperature rise. It would have a much greater strain capability for increased compatibility considerations. It would be much simpler to manufacture especially over complex shapes and surfaces. The critical qualification requirement parameter is its ability to withstand ablation-shear-pressure re-entry conditions, and its tear resistance.

Subtask 1

Ablation tests on trapezoidal specimens in the supersonic or hypersonic arc tunnel at the 3-5 Btu/ft^2-sec heating rate for applications on Apollo and similar vehicles.

Subtask 2

Ablation tests in the supersonic or hypersonic arc tunnel at the 80-120 Btu/ft^2-sec heating rate typical of the Apollo vehicle or other similar applications.

Subtask 3

Ablation tests at 900 Btu/ft^2-sec in the deep-throated shroud arc for re-entry satellite stagnation point conditions.

Subtask 4

To demonstrate resistance to shear under ablating conditions. Samples 2" x 5" x 1/2" will be bonded to half of each side of a 9° P-N wedge model. The heat flux will be approximately 400 Btu/ft^2-sec and by controlling the angle of thermal impingement the shear loads will be 1-5 lb/ft^2 on one side of the model and 50 lb/ft^2 on the other side. The P-N will be the control material.

Subtask 5

(1) Tensile — test two formulations (densities) with three replicates at -80°F, -65°F, -35°F and R. T. = 24 samples.

(2) Coefficient of Expansion — test two formulations with two replicates from -250°F to +250°F = 4 samples.

(3) Compression — Test two formulations with three replicates at R. T., 160°F and 250°F = 18 samples.

Subtask 6

Thermal Conductivity and Specific Heat — Four samples each test over the temperature range -200°F to +600°F.

Subtask 7

Laboratory investigation to define method of manufacturing and cutting large sheets to controlled densities and thicknesses.

Subtask 8

Preliminary thermal analysis to determine station-shield thicknesses for various flux levels on a typical or specific re-entry vehicle.

Subtask 9

Preliminary stress analysis to determine mechanical safety margins for preliminary design and trade-off studies on a specific re-entry vehicle.

TASK 3 DEVELOPMENT AND EVALUATION OF LOW-DENSITY ESM 1000

OBJECTIVES

To develop, qualify, and generate sufficient data on a low-density formulation (20 lb/ft^3) for preliminary design on Apollo and other low-flux re-entry vehicles.

BACKGROUND

Sufficient data is being generated on ESM 1001 and ESM 1002 for preliminary design. On major portions of re-entry vehicles such as Apollo (in low-flux areas) the insulation considerations greatly outweigh the ablation considerations. For such areas, the development and qualification of a low-density version of ESM 1000 could result in a significant weight saving due to improved insulation characteristics.

Subtask 1

Laboratory investigations to develop formulations, fabrication techniques, curing conditions, catalyst and blowing agents combinations and concentrations, etc. to produce a uniform low density material with physical integrity.

Subtask 2

Ablation tests on trapezoidal specimens in the supersonic or hypersonic arc tunnel at the 3-5 Btu/ft -sec heating rate for applications on Apollo and similar vehicles.

Subtask 3

Ablation tests in the supersonic or hypersonic arc tunnel at the 80-120 Btu/ft^2-sec heating rate typical of the Apollo vehicle or other similar applications.

Subtask 4

(1) Tensile — two formulations tested in two honeycomb directions with three replicates at -80°F, -65°F, -35°F, and R.T. = 48 samples.

(2) Coefficient of Expansion — two formulations in two honeycomb directions with two replicates tested from -250°F = 8 samples.

(3) Compression — two formulations tested in two honeycomb directions with three replicates at R.T., 160°F, and 250°F = 36 samples.

Subtask 5

Thermal Conductivity and Specific Heat — Four samples each tested over the temperature range -200°F to +600°F.

Subtask 6

Preliminary thermal analysis to determine station-shield thicknesses for various flux levels on a specific re-entry vehicle.

Subtask 7

Preliminary stress analysis to determine mechanical safety margins for preliminary design and trade-off studies on a specific re-entry vehicle.

TASK 4 PARAMETRIC STUDY OF ELASTOMER/FILLER SYSTEMS

OBJECTIVES

(1) To promote further understanding of the chemical factors and basic mechanisms affecting performance of elastomer-filler shield systems.

(2) To develop and screen new elastomer-filler combinations specifically designed for highly improved performance for thermal shields.

BACKGROUND

In the first stages of the ESM 1000 development, a few commercially available mixtures were evaluated. Various fillers and additives were incorporated into one of these resin systems to improve properties and lower the density in a controlled manner. There is little basic understanding of why this particular base resin and its filler performs well. Various basic modifications may perform better and be easier to fabricate. This task for the first six months of 1963 will not generate preliminary design data but is basic to future advances on elastomeric shield systems.

Subtask 1

Background study and analysis of chemical factors and behavior affecting performance.

Subtask 2

Laboratory studies and formulation development based on Subtask 1 and in association with resin suppliers.

Subtask 3

Screening ablation and mechanical testing of formulations from Subtask 2 under critical conditions comparable to those used for the current ESM 1000 material. Specific tests to be defined.

Subtask 4

Analysis of results and definition of formulation with sufficient potential for additional effort and data generation.

TASK 5 DEMONSTRATE AND EVALUATE SCALE-UP OF ESM 1002 IN TYPICAL VEHICLE CONFIGURATION

OBJECTIVES

(1) To define the method of fabricating thermal shields of ESM 1002 to typical vehicle configurations.

(2) To fabricate a half-scale thermal shield-structure of ESM 1002 and qualify by thermal cycling, (approximately 4' diameter x 3' high).

(3) To assure that the scaled-up shield maintains the same properties as the samples fabricated for data generation.

BACKGROUND

Although some thought and consideration has been given to the fabrication process of full-scale thermal shields of ESM 1000 material, no integrated effort has been made in this area. At this time only flat specimens of modest dimensions (up to 2' x 4' x 2") have been fabricated in the laboratory and the Plastics Shop. A demonstration of fabrication methods for cured surfaces and its qualification is necessary for any design activity, and must be completed before full-scale hardware can be manufactured.

Subtask 1

Definition of scale-up approach on half-scale, typical, conical configuration.

Subtask 2

Thermal cycle, instrumented, on shield-structure defined from Subtask 1.

Subtask 3

Selected mechanical and thermal property determinations on samples from scale-up shield. To be defined.

X. GE/ESM APOLLO SHIELD CONCEPT

A. INTRODUCTION

Throughout the previous Sections, the information at hand to support the present ability to design and fabricate a monolithic shield for the Apollo Command Module has been presented. This section will now discuss the following items:

(1) Thermal Analysis

(2) Structural Analysis

(3) Design Approaches

(4) Bond Systems Evaluation

(5) Suggested "Next-Step" Program

Based on the availability of more complete material data (compared with the last General Electric assessment of an ESM shield for Apollo in August 1962), the design approach continues to be to use the unique properties of ESM to obtain a low-weight, minimum-cost, and highly reliable thermal shield for the Apollo Command Module. The elastomeric characteristics of ESM lead to a structurally compatible shield which is highly resistant to environmental extremes and to damage attendant to normal handling and service life. Ease of repair on the ground is a simple, reliable procedure since the base material itself is used. In-flight repair of damage due to micrometeorite impact or other causes seems quite feasible.

The manufacturing problems involved in fabricating and handling a thermal shield for an Apollo-size vehicle will also be greatly alleviated by the elastomeric properties of ESM. The objectives of the proposed fabrication techniques are to provide a monolithic shield for the front surface of the Apollo and a minimum of large segments for the aft conical portion. Cutouts for access panels and antennas can be easily located and finalized after installation of the shield to the vehicle structure. Design changes can be tolerated without affecting basic shield assemblies or delivery schedules. Studies have shown at least two methods of fabrication by which it is possible to almost completely assemble the thermal shield before attachment to the structure.

B. COMMAND MODULE THERMAL ANALYSIS AND MATERIAL REQUIREMENTS

1. METHODS OF ANALYSIS

In the course of its experience in the design, fabrication, and flight testing of ablation systems, GE-RSD has developed several methods of evaluating the thermal response of thermo-plastics, thermosetting plastics, elastomeric materials, and other ablating materials when exposed to aerodynamic heating. One method employs a heat-of-ablation or degradation technique in conjunction with a one-dimensional melting conduction program or a three-dimensional heat conduction program. This technique was employed successfully on the RVX-1, RVX-2, Mk-3, Mk-6, and Discoverer Programs. While this is a valid and well-established technique, GE has continued to advance its technology by developing more comprehensive computer programs to define material ablation: the Reaction Kinetics Analog Program and the Digital Reaction Kinetics Program. These programs, which have been used on the recent Skybolt and 201 Programs, calculate material degradation from equations based on reaction kinetics theory and account for the dissipation of energy by the actual physical modes involved. In addition, they calculate the effect on material performance of the high enthalpy levels encountered in Apollo entry and relate the thickness of transient char formation to the local environmental conditions. As a result, these programs constitute an excellent method of determining material performance for all flight regimes and extrapolating known performance from one flight regime to another.

The One-Dimensional Heat Conduction Solution With Melting Surface Program employs a heat-of-ablation technique to calculate the material degradation and the associated temperature distribution in the remaining virgin material and associated back-up structure.

The Digital and Analog Reaction Kinetics Programs calculate (1) the degradation of a thermosetting plastic or silicone rubber to carbon-like char or silicone crust and gases of pyrolysis, or (2) the degradation of a subliming plastic to gases of pyrolysis with, in both cases, the associated temperature response of the surface and of the virgin plastic substrate. The dissipation of the energy resulting from aerodynamic heating is calculated for each of the following physical and chemical modes:

(1) Blocking action of mass added to the boundary layer.

(2) Energy of decomposition.

(3) Sensible heat stored in the char layer and the uncharred material.

(4) Energy absorbed by gases liberated while flowing through porous char layer.

(5) Energy radiated from surface of char layer.

The boundary conditions are the aerodynamic heating and related viscous effects, combined with the char-gas and plastic thermo-physical properties which are determined by independent analytical or experimental techniques.

The heat of degradation approach was employed to determine the material degradation reported. Since certain of thermo-physical properties of ESM materials, which are required for REKAP (an evaluation of shield degradation utilizing reaction kinetics theory), were not yet available at the time of this report, this program was not employed.* For this specific material, these properties are being determined experimentally, so that the reaction kinetics programs can be used for the future detail design. The heat of degradation of ESM material was estimated from the test data obtained by GE as discussed in the previous section. However, the effects of char layer thickness on overall material performance for an Apollo environment had been previously obtained for other similar materials, and these results were used as a guide to the performance of ESM.

For the purpose of this report, these details are omitted. As noted above, the design approach utilized was that of an effective heat of degradation in an IBM 7090

* Such as gas product analysis and char-gas conductivity.

computerized conduction solution with surface melting. This solution requires:

(1) The effective heat of degradation.

(2) Condensed phase thermal conductivity specific heat and density.

(3) Effective conduction temperature (obtained from thermogravimetric analysis).

The values of these parameters have been developed in Section III-A. They are:

(1) Heat of degradation — 8000 Btu/lb

(2) Condensed phase thermal conductivity (Figure III-14, Section III-A).
Specific heat : .38 Btu/^{o}F-lb
Density: 45 and 20 lb/ft^3

(3) Effective conduction temperature: 1200^{o}R

The Apollo spacecraft dimensions used for this evaluation are presented in Figure X-1, along with identifying stations. These correspond directly to those specified in the North American Aviation RFQ for Apollo Heat Shield Panels, Reference (1). The Aerodynamic heating environment was also taken directly from Reference (1), for the locations noted on Figure X-1. It was determined that trajectory 1 represented the most extreme condition from the standpoint of highest thermal load combined with greatest re-entry time. Although the trajectories presented in Reference (1) (and corresponding heat rates) were not shown to ground impact, an estimate of this terminal phase of the trajectory was made to size insulation requirements. Further, a backup structure equivalent to 0.040 inch of stainless steel was used to complete the insulation evaluation.

2. RESULTS

An evaluation of thickness requirements was made for 45 lb/ft^3 ESM material on the forward face (75 lb/ft^3 at the knuckle) and for both the 45 and 20 lb/ft^3 ESM material on the afterbody. Degradation at several representative locations on the command module are presented in Figure X-2. As shown in Figure III-1 of Section III-A, it does not appear that even limiting undershoot trajectories will result in significant

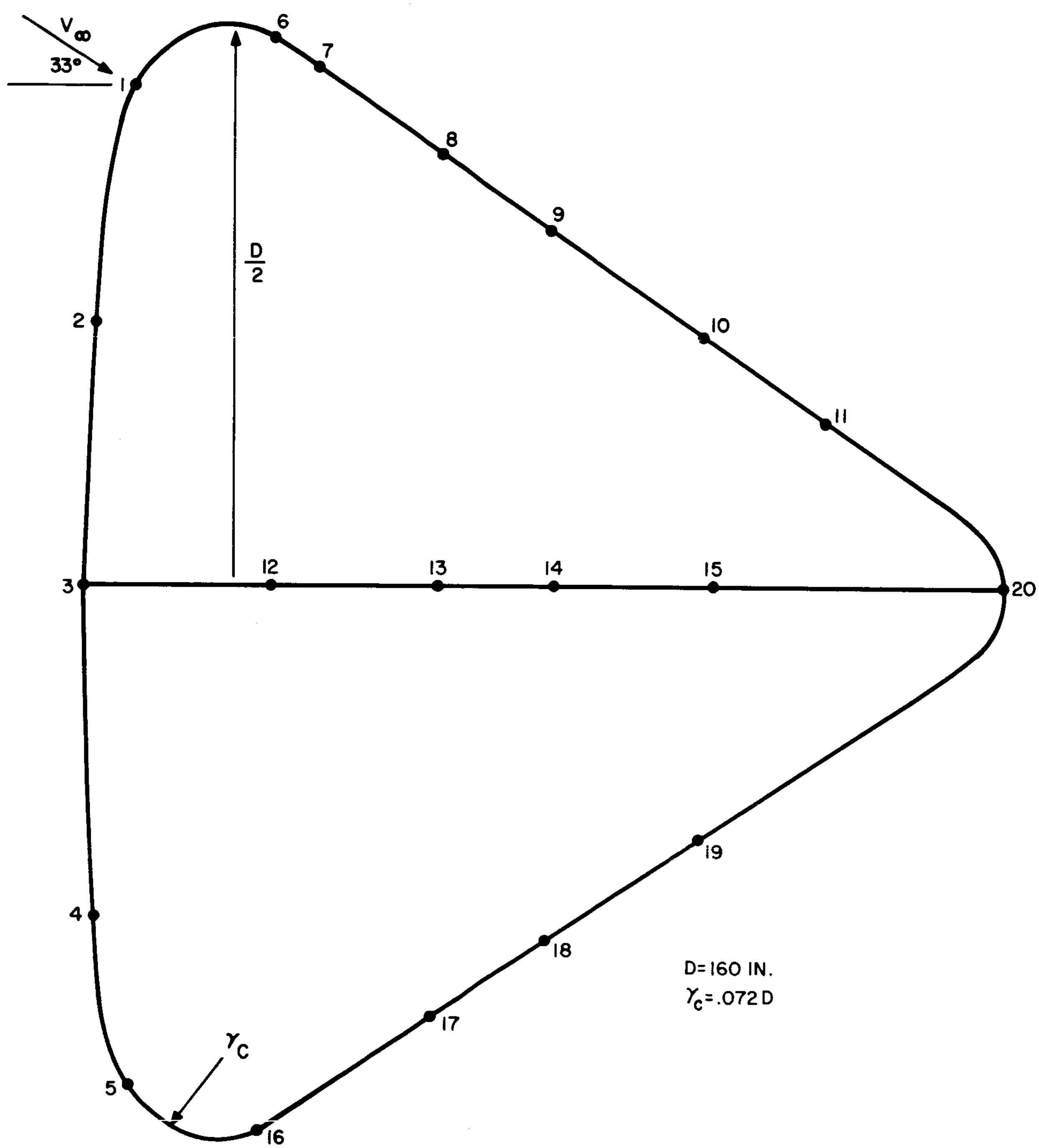

Figure X-1. Apollo Configuration and Reference Point Locations changes in the heat of degradation of the ESM material.* Temperature distributions through the ablative material at representative locations are presented in Figures X-3, X-4, and X-5, including a description of ESM 20 lb/ft^3 gradients. These results are presented for the thicknesses required to maintain the back face at 600^oF.

Table X-1 provides a summary of thickness requirements for the command module for limiting back face temperature conditions of 500^o and 600^oF respectively. Table X-2 compares degradation for the three NAA trajectories listed in Reference (1).

3. COMMAND MODULE HEAT SHIELD WEIGHT

Figure X-6 presents the variation in command module heat protection system weight with margin. Margin is defined in the figure. As shown in previous studies of re-entry system ablative heat protection system reponse, system margin based on degradation for satellite re-entry systems is approximately one-half the margin based on thermal load.

Actual margins selected should reflect sufficient test points to provide statistical evaluation of variation in thermal load and material response.

4. REFERENCE

North American Aviation, Inc., "Procurement Speciation — Apollo Command Module Heat Shield Ablative Panels." Specification MC 364-0001, 17 January 1962.

*While undershoot trajectories result in higher heating rates and shear forces than the overshoot case (trajectory[1]), the integrated thermal load is significantly lower. Consequently, decreases in the heat of degradation are compensated to a large degree by decreased in the thermal load.

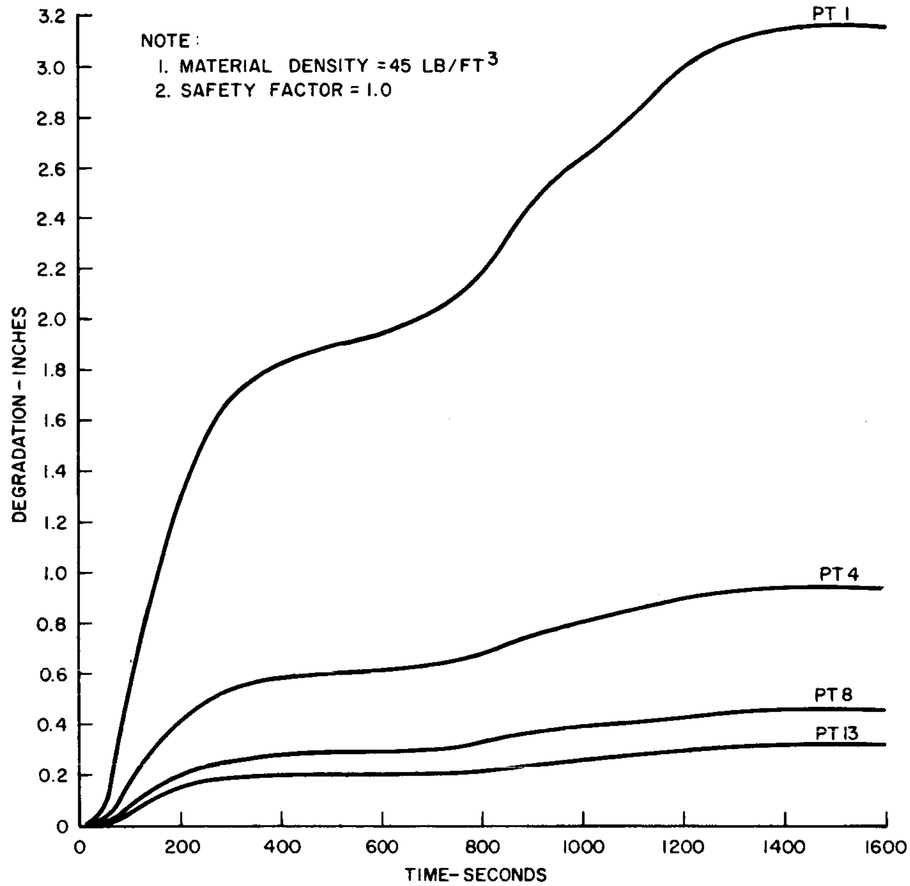

Figure X-2. Apollo Shield Nominal Degradation Histories for Trajectory 1

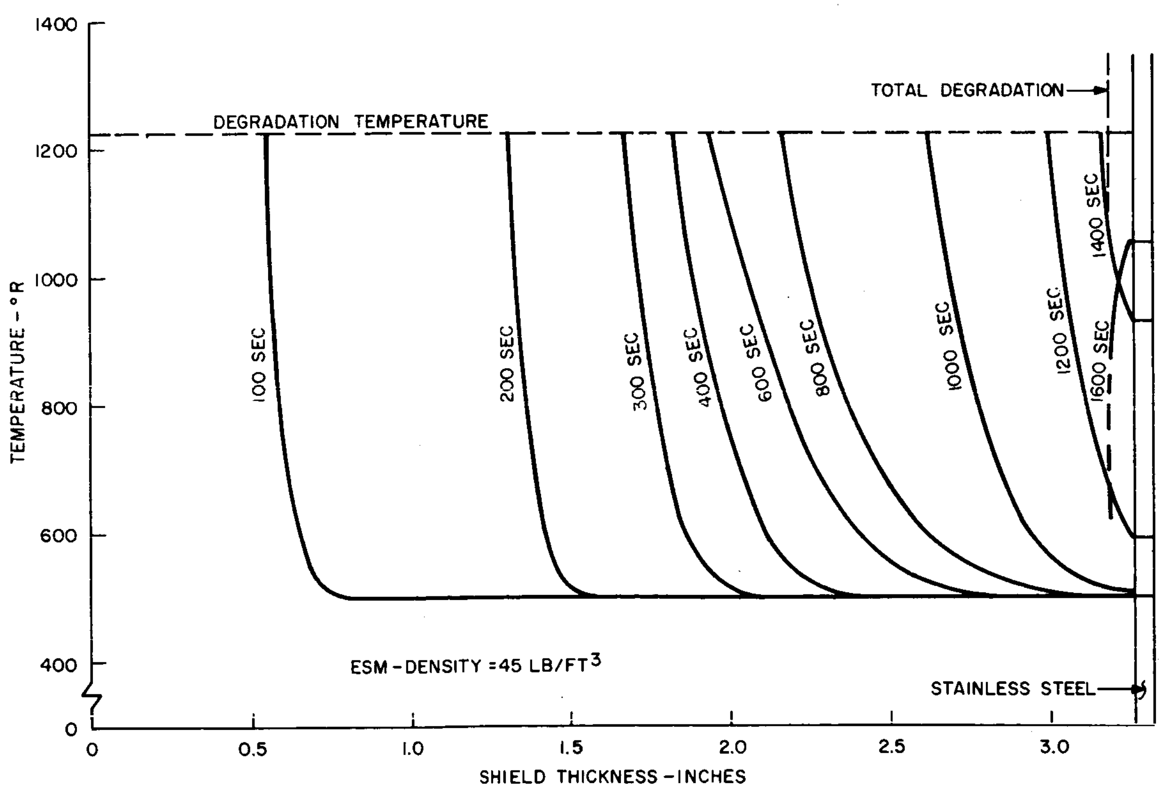

Figure X-3. Apollo Shield Temperature Profiles for Location 1

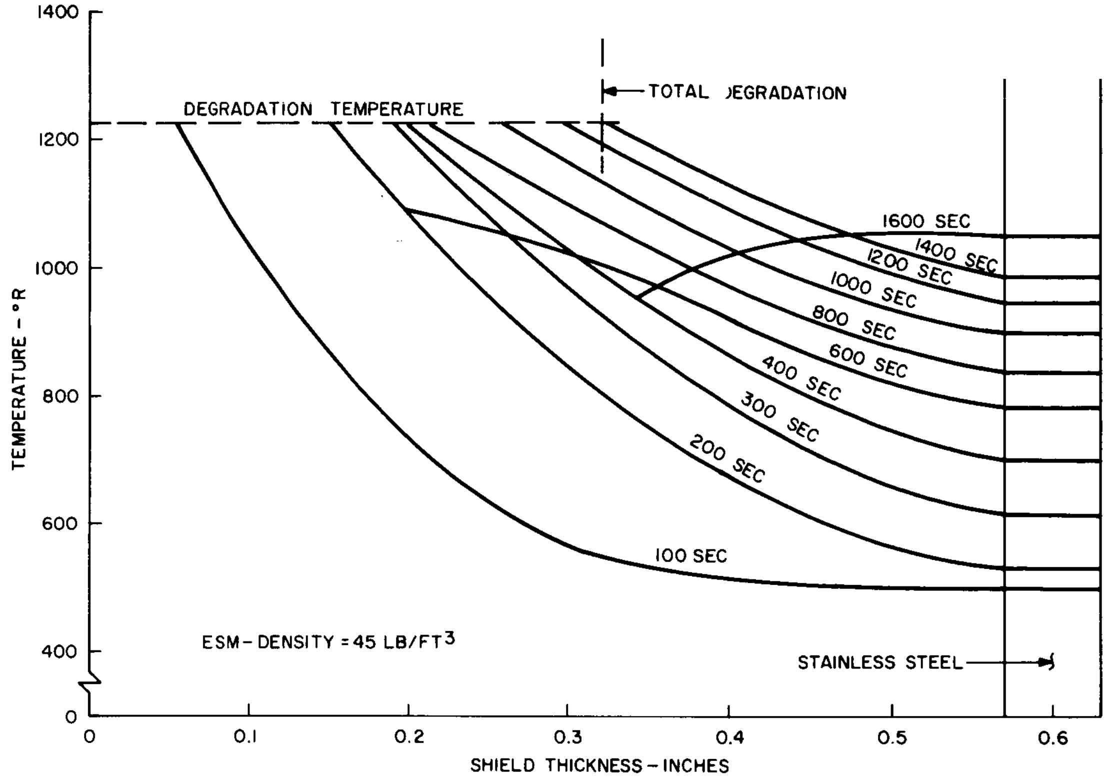

Figure X-4. Apollo Shield Temperature Profiles for Location 8

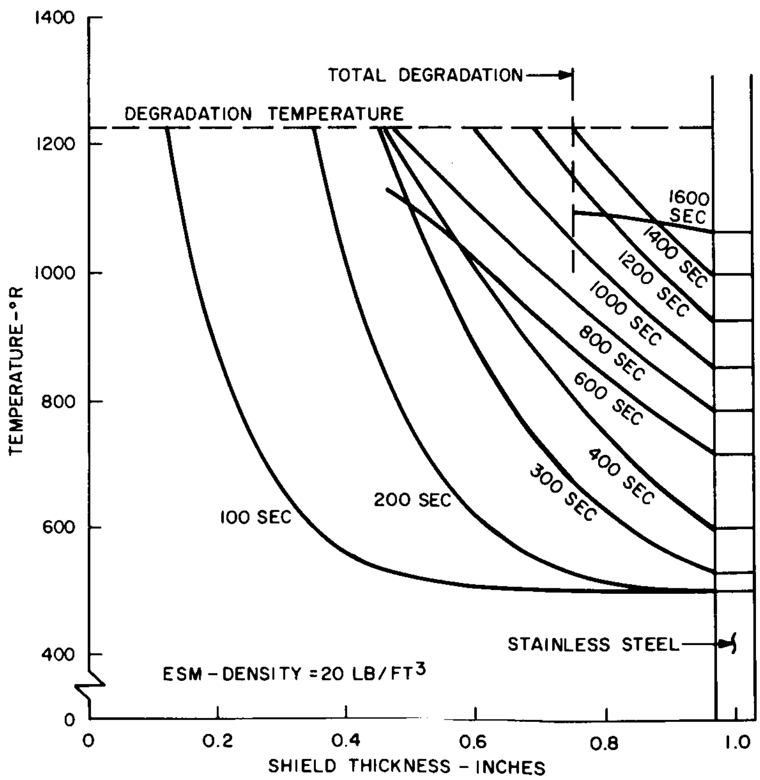

Figure X-5. Apollo Shield Temperature Profiles for Location 8

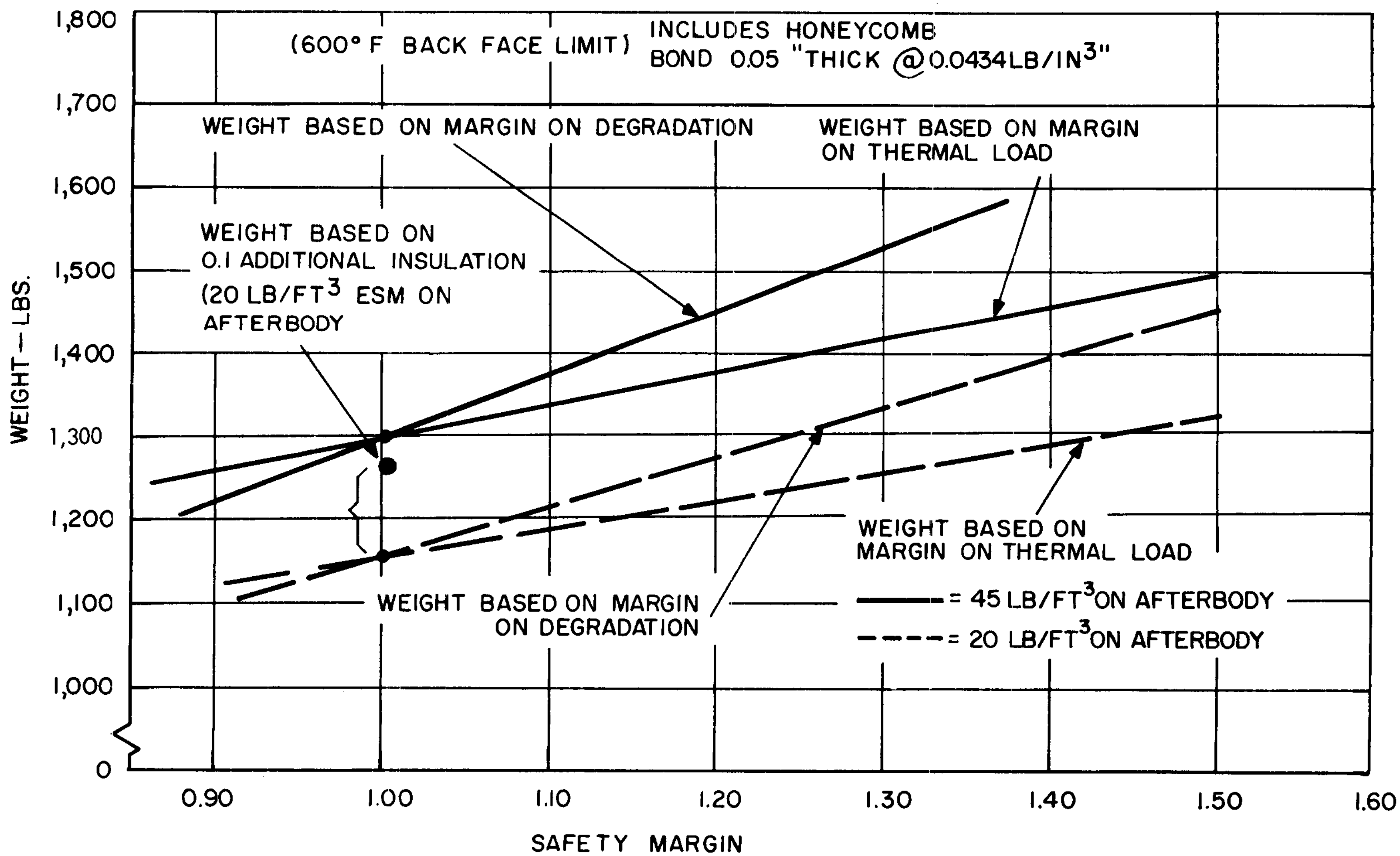

Figure X-6. Command Module Shield Weight

TABLE X-1. THICKNESS REQUIRED FOR APOLLO SHIELD, COMMAND, MODULE (NO SAFETY FACTOR)

Material: ESM — 1000 series
0.040" Stainless steel structure

ρ = 77 lb/ft^3

		Backface Temperature Limit			
		T_L = 500°F		T_L = 600°F	
Location	Deg.	Insul.	Deg. & Ins.	Insul.	Deg. & Ins.
1	1.79"	0.23"	2.02"	0.13"	1.92"

ρ = 45 lb/ft^3

		Backface Temperature Limit			
		T_L = 500°F		T_L = 600°F	
Location	Deg.	Insul.	Deg. & Ins.	Insul.	Deg. & Ins.
1	3.16"	0.18"	3.34"	0.10"	3.26"
2	0.94"	0.31"	1.25"	0.17"	1.11"
4	0.46"	0.39"	0.85"	0.24"	0.70"
8	0.32"	0.40"	0.72"	0.25"	0.57"
13	0.003"	0.387"	0.39"	0.307"	0.31"
17	0	0.17"	0.17"	0.14"	0.14"

ρ = 20 lb/ft^3

		Backface Temperature Limit			
		T_L = 500°F		T_L = 600°F	
Location	Deg.	Insul.	Deg. & Ins.	Insul.	Deg. & Ins.
8	0.75"	0.36	1.11	0.22	0.97
13	0.015"	0.355	0.44	0.295	0.37
17	0	0.27	0.27	0.23	0.23

If stainless steel is to be removed add the equivalent thermal thicknesses of ESM.

ρ_{ESM}	Δt
77	0.086"
45	0.14"
20	0.34"

These thicknesses are based on soak temperatures at impact.

TABLE X-2. COMPARISON OF APOLLO SHIELD DEGRADATION FOR SEVERAL NAA TRAJECTORIES

ρ = 45 lb/ft^3	Degradation		
Location	Trajectory 1	Trajectory 2	Trajectory 3
1	3.16	1.39"	2.15"
2	0.94		
4	0.46		
8	0.32	0.28"	0.32"
13	0.003	0.005"	0.001
17	0	0	0

C. STRUCTURAL ANALYSIS

This analysis discusses the structural feasibility of ESM 1002 as a heat shield material and summarizes the analysis done to date. Analyses were made for the Apollo configuration as depicted in Figure X-7. Consideration was given to both a flexible bond design and a design where the glass honeycomb is hard bonded to the structure. The results of the analysis indicate that the basic problems in the design will be with the internal interaction between the filler and the glass honeycomb, the glass honeycomb cell bond, and edge effects. Further, it is concluded that these effects would be minimized if the glass honeycomb were hard bonded to the structure. However, thermal cycling has been completed successfully on specimens employing soft bond. Relative reliability of the soft-bond system could be established by building hard- and soft-bond specimens of adequate size and thermal cycling them through the temperature extremes.

1. OVERALL SHIELD ANALYSIS

For the Apollo vehicle, the main frustum section was analyzed with a heat shield material of ESM 1002 bonded to the structure with the filler material.

<u>Material Properties:</u>

<u>ESM 1002</u>
<u>160°F</u>

Ribbon Direction

$\alpha = 5\,(10)^{-6}$ in/in $-^{\circ}F$

$E = 650$ psi

$\nu = 0.5$

Across Ribbon Direction

$\alpha = 220\,(10)^{-6}$ in/in $-^{\circ}F$

$E = 650$ psi

$\nu = 0.5$

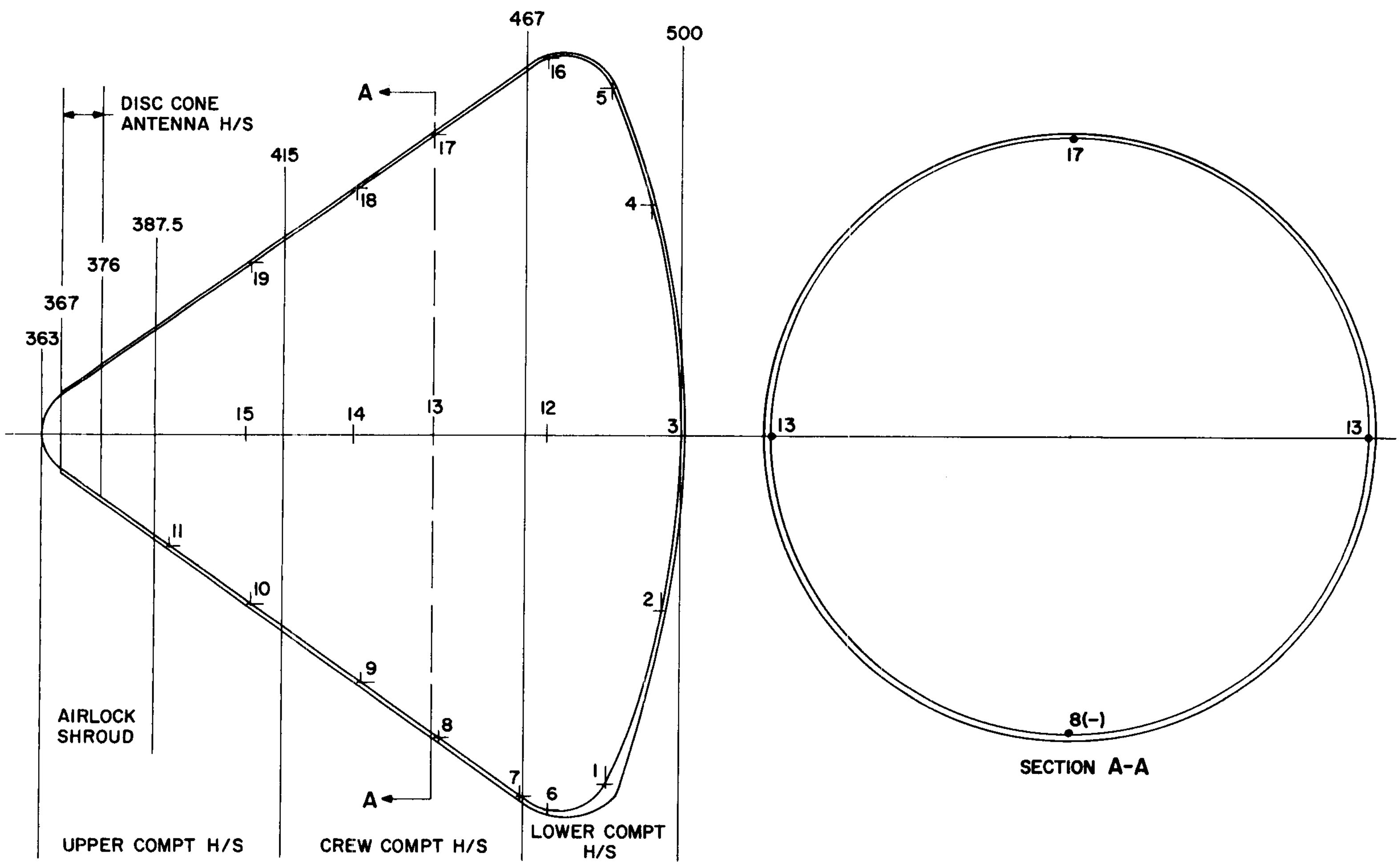

PT	1	2	3	4	5	6	7	8	9	10
THK	3.260	1.110	.910	.700	.650	1.140	1.170	.970	.910	.870
PT	11	12	13	14	15	16	17	18	19	
THK	.840	.3105	.310	.3094	.3085	.190	.190	.190	.190	

Figure X-7. Apollo Command Module Heat Shield

-100°F

Ribbon Direction

$\alpha = 9(10)^{-6}$ in/in -°F

$E = 2800$ psi

$\nu = 0.5$

Across Ribbon Direction

$\alpha = 295(10)^{-6}$ in/in -°F

$E = 2800$ psi

$\nu = 0.5$

Substructure (Rene 41) (160°F and -100°F)

$\alpha = 7.5(10)^{-6}$ in/in -°F

$E = 30(10)^6$ psi

$\nu = 0.33$

Bond Properties:

160°F

$E_b = 100$ psi

$G_b = 33.3$ psi

-100°F

$E_b = 400$ psi

$G_b = 133$ psi

The frustum was analyzed for a 160°F soak condition and a -100°F soak condition with the ribbon direction in both the meridional and circumferential direction for both of the shield thicknesses. These temperature limitations were chosen since preliminary property data was not available beyond these extremes. Wider limits can, of course, be expected to indicate more problem areas. The ends were restrained from meridional movement in one case and were free to move in another. The following combinations were analyzed:

Run	Temperature	Shield Thickness	Ribbon Direction	End Restraint
1	$-100^{o}F$	Maximum	Meridional	Yes
2	$-100^{o}F$	Maximum	Meridional	No
3	$160^{o}F$	Maximum	Meridional	Yes
4	$160^{o}F$	Maximum	Meridional	No
5	$-100^{o}F$	Maximum	Hoop	Yes
6	$-100^{o}F$	Maximum	Hoop	No
7	$160^{o}F$	Maximum	Hoop	Yes
8	$160^{o}F$	Maximum	Hoop	No
9	$-100^{o}F$	Minimum	Meridional	Yes
10	$-100^{o}F$	Minimum	Meridional	No
11	$160^{o}F$	Minimum	Meridional	Yes
12	$160^{o}F$	Minimum	Meridional	No
13	$-100^{o}F$	Minimum	Hoop	Yes
14	$-100^{o}F$	Minimum	Hoop	No
15	$160^{o}F$	Minimum	Hoop	Yes
16	$160^{o}F$	Minimum	Hoop	No

This analysis is a membrane analysis that takes into account the variation of shield thickness along the length of the vehicle and is solved on the IBM 7090 computer using a numerical integration technique. Typical results of the $160^{o}F$ runs are shown in Figures X-8 and X-9. The maximum bond and shield stresses are tabulated as follows:

Maximum Stresses
(psi)

Run	Meridional Shield Stress	Circumferential Shield Stress	Bond Shear Stress	Bond Normal Stress
1	86.0	180.0	4.1	-17.5
2	86.0	180.0	16.1	-15.0
3	- 6.2	- 14.6	0.3	1.4
4	- 6.2	- 14.6	3.8	1.3
5	185.0	86.0	5.7	- 9.0
6	183.0	86.0	16.2	- 6.0
7	- 15.0	- 6.3	0.5	0.7
8	- 14.8	- 6.2	7.9	0.5

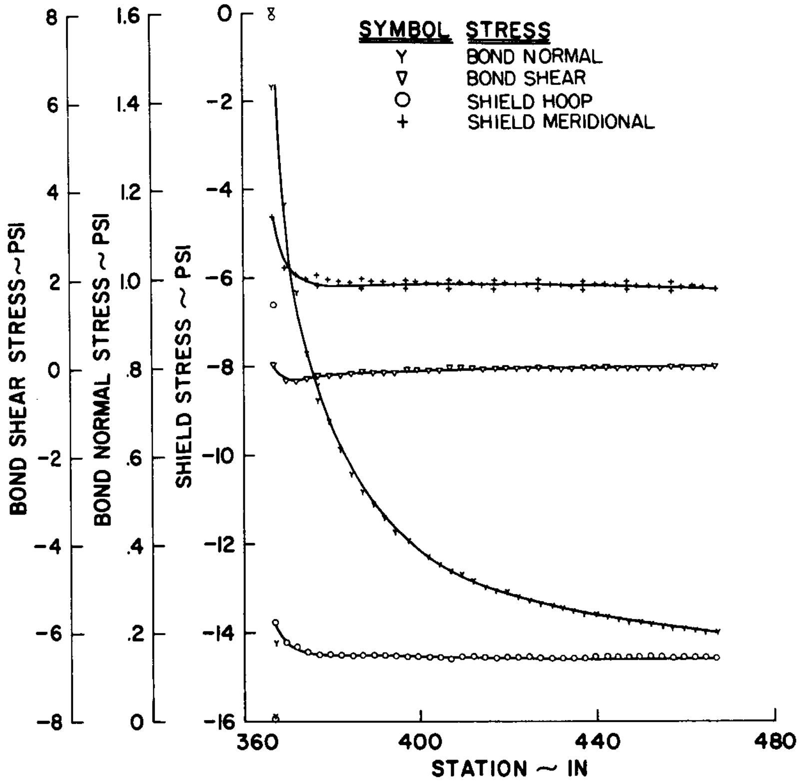

Figure X-8. Stress vs Station. Maximum Shield Thickness ("P" Direction). T = 160°F, Restrained Edge, Run 3.

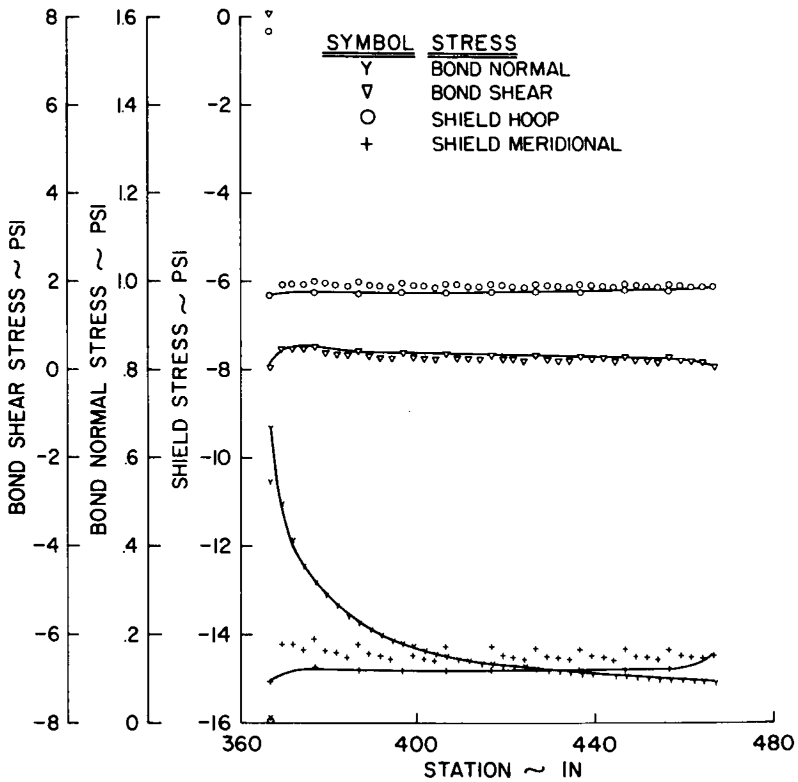

Figure X-9. Stress vs Station. Maximum Shield Thickness ("T" Direction). T = 160°F, Restrained Edge, Run 7.

Maximum Stresses
(psi) (Continued)

Run	Meridional Shield Stress	Circumferential Shield Stress	Bond Shear Stress	Bond Normal Stress
9	87.0	181.3	2.0	- 7.0
10	86.0	181.3	16.2	- 5.5
11	- 6.2	- 14.6	0.1	0.6
12	- 6.2	- 14.6	0.2	0.5
13	185.0	86.0	2.4	- 3.3
14	183.0	86.0	16.2	- 2.3
15	- 15.0	- 6.7	0.2	0.3
16	- 14.8	- 6.3	5.2	0.2

The point of interest here is the low bond stresses that are obtained in the flexible bond. Run No. 7 indicates that with the ribbon in the hoop direction, with end restraint and maximum shield thickness, we have less than one psi tension and shear in the bond at 160°F. Without an end restraint, Run No. 4, the ribbon in the meridional direction will give the minimum shear stress at the free ends of four psi at 160°F. When compared with other shield systems on a flexible bond this is phenomenal.

It should be pointed out that this analysis was performed using preliminary property data and the values used at low temperature are conservative. The shield stresses shown are the average elastic stresses due to the thermal incompatibility with the substructure and in no way reflect the total stress in the honeycomb and the filler. The stresses shown would be greatly reduced if the substructure were fiberglass rather than steel.

These results can be considered to be quantitative, in view of the assumptions made and the material properties used. The shield material in question is inelastic and orthotropic in nature. Use of the available uniaxial test data and the assumed Poisson's Ratio is, of course, incorrect for such a material.

Nevertheless, the analysis does indicate that when considering ESM 1002 as a continuous shield material bonded with a flexible bond, overall stress levels are low. However, the internal stresses in the shield are higher and this is where the design problems are to be found. Some of these problems may be:

(1) Adhesion of filler to the phenolic glass honeycomb.

(2) Adhesion of filler to the substructure.

(3) Adhesion of the phenolic glass honeycomb cells.

(4) The interaction between filler and phenolic glass cell.

Many of the aforementioned problems can be tested by thermal cycling the composite material to the extreme environments. In some cases it would be advantageous to thermal cycle the composite material before bonding to the substructure.

2. ANALYSIS OF HONEYCOMB CELL INTERNAL STRESSES

A detailed analysis was performed to determine the internal stresses in the phenolic glass honeycomb and the filler. This was an analysis using a hard bond and the individual properties of the phenolic glass honeycomb and the filler material.

These equations were derived for the condition away from the edge of the frustum and set up such that there was strain and force compatibility. This is a membrane solution. Two solutions are obtained from this analysis: (1) on the stresses in the composite shield at temperature before it is made compatible with the substructure and (2) the final stresses in the honeycomb, the bond, and the substructure at temperature.

The properties used in this analysis were:

<u>$160^{o}F$</u>

$$\alpha_{Filler} = 1000 \; 10^{-6} \text{ in/in -}^{o}F$$

$$E_{Filler} = 117 \text{ psi}$$

$$\nu = 0.4$$

$-100^{o}F$

$$\alpha_{Filler} = 1000\ 10^{-6}\ in/in\ \text{-}^{o}F$$

$$E_{Filler} = 2000\ psi$$

$$\nu = 0.4$$

Phenolic Glass Honeycomb:

1/4" hex-cell 0.010" ribbon thickness

$$\alpha_g = 6\,(10)^{-6}\ in/in\ \text{-}^{o}F$$

$$\nu_g = 0.25$$

$$E_g = 3\,(10)^{6}\ psi$$

Substructure

$$E_m = 30\,(10)^{6}\ psi$$

$$\nu_m = 0.3$$

$$\alpha_m = 7.5\,(10)^{-6}\ in/in\ \text{-}^{o}F$$

$$\text{Shield thickness} = 1.0\ in.$$

$$\text{Radius} = 45''$$

The above properties were assumed and are intentionally high. The results of this analysis are shown below:

Stresses With Hard Bond

Soak Temp.	Filler Stress (ESM 1002)		Glass Hexcel Stress	
	Hexcel Bonded to Metal	Shield Not Bonded to Metal	Hexcel Bonded to Metal	Shield Not Bonded to Metal
$160^{o}F$	- 18 psi	- 18 psi	404 psi	661 psi
$-100^{o}F$	+562 psi	540 psi	-992 psi	-20,532 psi

From these results, there are indications of possible trouble in tensile strength of the filler material at $-100^{o}F$, tensile strength of the adhesive holding the laminated honeycomb together at $-100^{o}F$, and the possibility of failing the honeycomb by a peeling action at 160^{O}F. At -100^{O}F the filler material and the honeycomb adhesive must be able to withstand 562 psi tension. There could be the possibility of local tensile failures of the filler or in the adhesion of the filler to the glass honeycomb. This local separation is not expected to be detrimental to the system. Local separations relieve the thermal loads and this type of failure would not propagate.

The second mode of failure could be that the adhesive holding the honeycomb together might fail due to a biaxial tensile load of 562 psi at -100^{O}F. The best way to test for this type of failure is to build a sample specimen of sufficient size to eliminate the edge effects and reduce the temperature to -100^{O}F.

The third mode of failure could be due to peeling failure of the honeycomb adhesive at 160^{O}F.

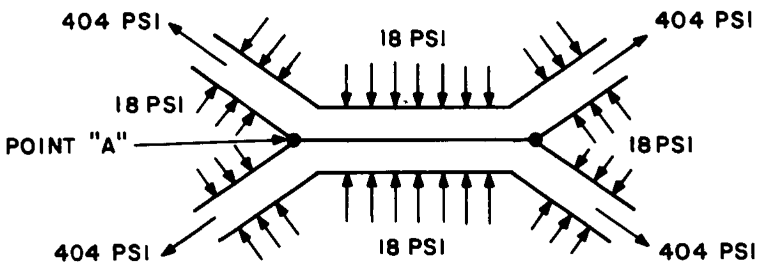

Peeling action would tend to fail the honeycomb adhesive at Point "A". Therefore, the indications are that the adhesive may fail at point "A" when at 160 and then when going to the -100^{O}F condition, the 562 psi tension could cause the remainder of this adhesive to fail to give a complete separation of the honeycomb. Again, the best way to test for this type of failure is to build specimens and cycle them to see if it occurs.

It should be noted that the peeling loads at $160^{o}F$ will be reduced from 661 psi tensile stress to the glass honeycomb to 404 psi tension if the glass honeycomb is bonded to the metal substructure with a rigid adhesive. With a flexible bond system, this glass stress will be between 661 and 404 psi. For reliability, it appears that the use of a rigid bond would be advantageous.

At a free edge there is a special problem due to the fact that the loads on the glass honeycomb are not symmetrical.

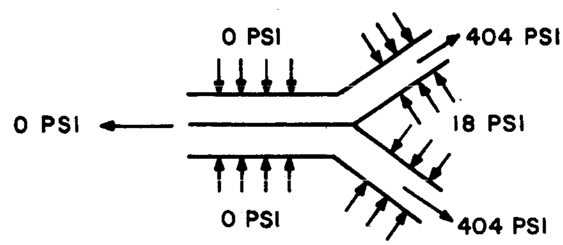

This condition may cause separation of the honeycomb cell at the edge that will relieve the load in the next cell and cause an unsymmetric load in the next cell. This would tend to cause propagation of this failure. Again because of this mechanism, it is recommended that the glass honeycomb core be bonded to the metal substructure with a rigid bond to prevent this type of propagation and increase the reliability of the system.

D. BOND SYSTEM EVALUATION

Having completed the material screening program, and assuming the ESM 1002 material is still under consideration, the next logical step would be to perform a preliminary design assessment and finalization of design and fabrication approach. There are two basic approaches: (1) bonding pre-foamed ESM 1002 to the structure with a high temperature elastomeric bond, and (2) hard-bonding the honeycomb to the structure (see Figure X-10).

1. ELASTOMERIC BOND

It is planned to preform or buy preformed honeycomb segments to the approximate radius and to a pattern and size of a quarter segment of a conical section. After proper priming etc, the honeycomb would be placed in a simple sheet female mold or holding fixture onto the evenly distributed resin system. After foaming, the excess material over the honeycomb surface would be removed and the shield system post-cured for stabilization. After proper surface preparation of both the shield and

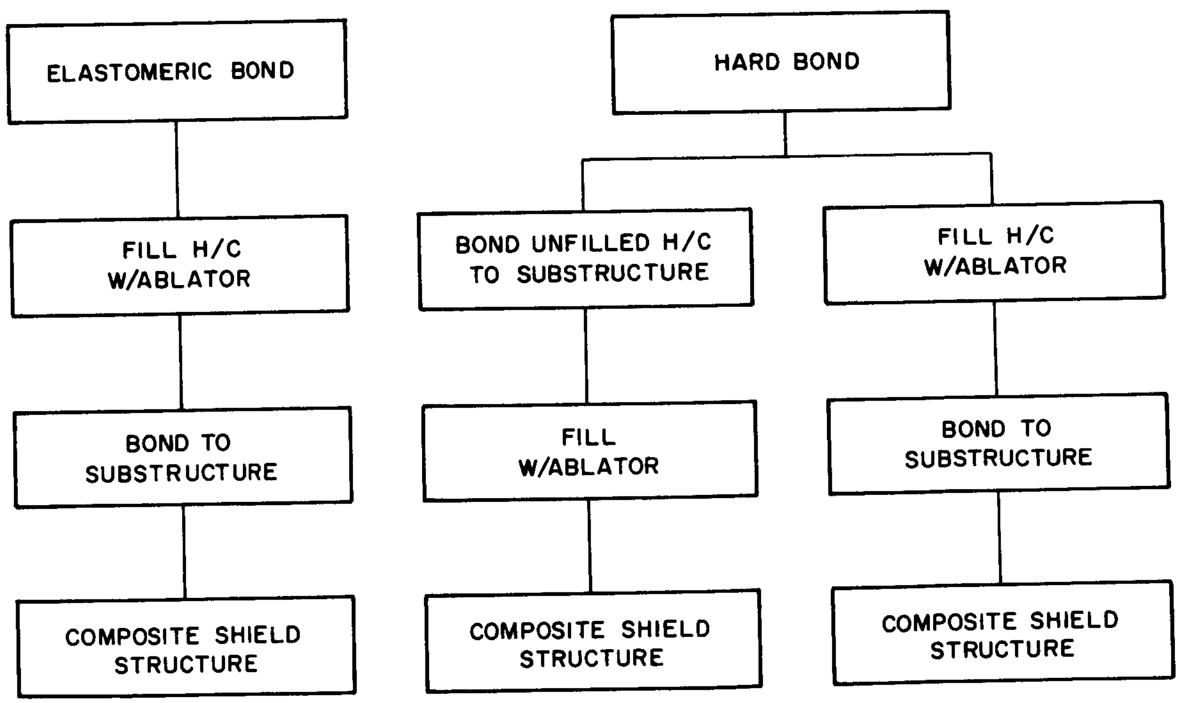

Figure X-10. Possible Choices for Bonding Elastomeric Thermal Shield to Substructure.

structure, the segment would then be bonded to the substructure with the elastomeric bond material. The shield segments may be joined in at least two ways, dependent upon the recommendations of stress and the results of current thermal cycle tests of segments bonded to rigid, restricted molds.

In one case, the edges of the shield segments would not be filled in the foaming process. When these segments were bonded to the structure they would be joined by press-interlocking the segment edges to the adjacent segments. Consequently, these narrow interlocking strips would be locally filled and foamed in place.

However, if analysis indicated otherwise, the fully filled segments would be tailored to butt-fit the adjacent segment or to a controlled gap that then could be filled with the unfoamed shield material which would serve as an ablative, compressible gap sealant. These segment sections and gaps would be oriented so that they were not parallel to the flow during re-entry. If necessary, the segment edges, ends, and the strips surrounding cut-outs would be hard-bonded to the structure. The formulations and density can be controlled over the vehicle surface, of course, to achieve an optimized material designed for the specific re-entry conditions encountered over the various body stations. In addition, the density of the foam in a specific area can (1) be kept uniform through its thickness by allowing the foam to move in both directions through the honeycomb cell openings or (2) by anchoring the honeycomb to the female mold surface and allowing only one degree of freedom in the foaming process. The resultant foam will decrease in density (and increase in insulation properties) towards the surface ultimately bonded to the structure. Further, an overlay of heavily filled, non-foamed material may be metered onto the shield surface to increase the ablation performance while maintaining beneath the better insulation properties of the lower density foam. These and other variations may be made to achieve a specifically tailored shield system of the lowest possible weight.

In addition to controlling density of the base material in the honeycomb matrix, the foaming and low-temperature cure effect other advantages. This base material is difficult to bond under the best conditions since plastic materials contract during cure. However, by foaming, a restricted pressure is exerted against the cell walls which greatly increases adhesion and eliminates the shrinkage effect. By foaming and curing at low temperatures (R.T. to 140°F), the foam is at a non-stressed condition at a relatively low temperature (to further decrease the tendency for the material to pull away from the cell walls at very low temperatures). This is an attractive advantage when coupled with the extremely low glass transition temperature of the elastomeric filler material.

2. HARD BOND

The alternate method of hard bonding the honeycomb to the structure with a rigid adhesive, with or without glass scrim cloth reinforcement, also has two basic approaches: (1) the honeycomb bonded to the structure and then filled and foamed and (2) the filled ESM 1002 bonded to the structure. In both cases, the honeycomb would be preformed to shape.

The honeycomb could be bonded to the structure rather simply with commercial film adhesives etc., with interlocking joints or with controlled gaps. After suitable priming, etc., a process would have to be devised to fill the honeycomb cells with the elastomeric material. This might be rather difficult for the following reasons. After mixing, the elastomeric materials have a good but definite pot life at room temperature. The honeycomb cells have to be filled uniformly from the top surface without air entrapment at the base of the cell. The honeycomb surface is convex and the shield would have to be filled and foamed in segments so that after filling, the material would not flow out of the cells on rotation. In addition, the foam would decrease in density from the structure to the surface, which is opposite to that desired. This process could conceivably work, however, by developing a machine that would fill the honeycomb sections connected to an automatic metering and mixing device to which the filling nozzle would be attached.

The entire vehicle frustum could be on a rotating table and, as a section was filled by the moveable nozzle, would be foamed and cured sufficiently by portable local heat sources for frustum rotation. Although more complex, this approach could be used, if necessary, to meet design requirements.

In the second approach, the material would be foamed in the honeycomb in the simple female mold, as with the elastomeric bond system, with these variations. A means would be defined to permit hard bonding to structure after core filling such that adequate bond strength will be obtained. The following concepts have been studied briefly and should be evaluated to fulfill this requirement.

(1) The simplest approach is to machine the bonding surface after filling the honeycomb with foam. This is an operation of contouring the inner surface of the filled honeycomb to exactly match the structure and will be required in most cases either before or after foaming. By performing this after foaming, the edges of the honeycomb cells will be exposed and can then be hard bonded to structure. This bond should develop a large percentage of the strength obtained by bonding the core to structure before filling, but tests must be run to establish design values and repeatability.

(2) One means of circumventing the filling problems is to preform fillets on the core by dipping in bond and hardening on a very smooth surface such as glass. Then when the core is filled, foaming can still take place and be checked through both ends of the cells. After removing the excess foam on the filletted side of the core and complete inspection, it can then be hard bonded to the structure and should develop full-bond strength by virtue of the preformed fillets. Another means of obtaining the same results is to dip the core (bond surface only) in a soluble material that can be dissolved after foaming in the filler, so that a hard bond to the structure can still be used.

(3) This concept uses an unfilled fiberglass cloth as a medium to preform fillets on the honeycomb core. The core is bonded to the fiberglass cloth with a hard bond. Then the core is filled with the elastomeric compound which is foamed into place. The loose weave of the cloth permits air to escape from the cells and allows inspection after foaming (as shown in Figure X-11). The completed assembly is then hard bonded to structures with the fiberglass cloth carrying the load between the core and structure, thereby effecting a continuous hard bond. These concepts must be evaluated to establish design data before a final selection can be made.

To permit orderly evaluation of the bonding systems and to allow valid system tradeoffs, the Table X-3 has been constructed listing the advantages and disadvantages of each approach. It is seen from the table that Method 3 combines the advantages of the first two methods with no attendant disadvantages but with certain unknowns as, for example, the resistance of the hard bonded shield to micrometeorites.

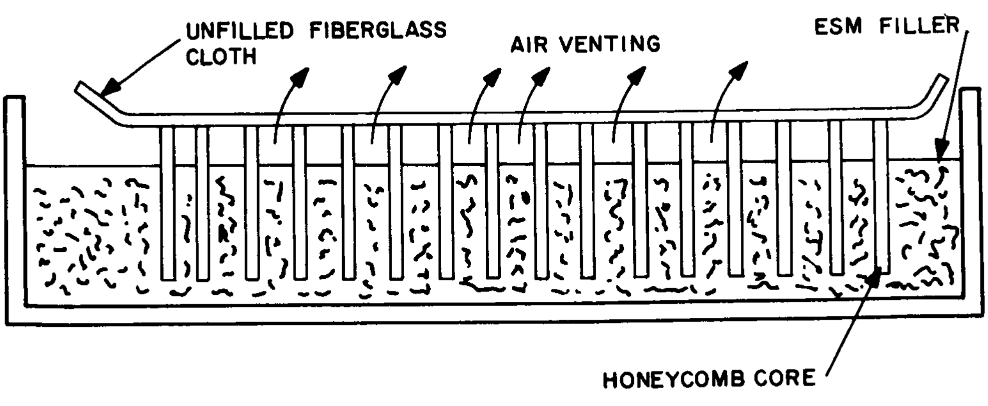

Figure X-11. Prebonding of Unfilled Glass Cloth

TABLE X-3

METHOD	ADVANTAGES	DISADVANTAGES
1. Fill H/C with ablative material and soft bond to substructure with elastomeric.	1. Fabrication ease. 2. Best retention for micro-meteorites. 3. Reliability (Both sides of H/C open).	1. Edge problem.
2. Hard bond unfilled H/C to substructure and fill with ablative material.	1. No edge problem. 2. Provides best design choice from stress view-point. 3. Minimizes structure-shield interface.	1. Quality assurance (reli-ability) of shield after filling difficult. 2. Fabrication difficulties with air entrapment. 3. Micrometeorite resistance not evaluated.
3. Fill H/C with ablative material and hard bond to substructure.	1. Fabrication ease. 2. Provides best design choice from stress stand-point. 3. Simpler interface. 4. Would eliminate need for NAA to ship structure out of house for shield instal-lation. 5. Reliability (both sides of H/C open).	1. Micrometeorite resistance not evaluated.

E. DESIGN APPROACH

The shield design presented herein has not been detailed because of lack of definition of the exact configuration, hatches, and antennas of the Apollo Command Module. This next step can be quickly accomplished if further information becomes available. The design has thus far been kept general since a firm selection of fabrication and bonding techniques has not been made. Two basically different approaches have been studied based on the use of (1) a hard (phenolic resin) bond or (2) a soft (elastomeric material) bond. These were described in more detail previously under "Bond System Evaluation". For both the hard- and soft-bond systems, it is planned that it would be possible to assemble the thermal shield into the following major assemblies before attachment to the substructure:

(1) Forward face shield including most of knuckle.

(2) Two or more large assemblies for the aft conical sections and upper portion of knuckle.

(3) Small units to be separately attached to removable doors or panels.

The heat shield would be designed and fabricated of the ESM 1000 Series material, a specific formulation which has been furnished to NAA for evaluation. Other advanced concepts are described in Section VIII, but no tests have been made so that no design data is available on these. The present ESM 1000 material (silicon-base material in phenolic-fiberglass honeycomb) would be used since much data has been generated and design can begin immediately. The only modifications to this material would be minor changes such as those required to obtain a lower density (20 lb/ft^3) which would be used on the conical section because the insulation requirements are overriding. In addition, certain changes to alleviate manufacturing problems would be evaluated such as the use of a larger-cell size honeycomb. This is certain to be easier and cheaper to fabricate and would lead to lower densities since the core is lighter. In addition, since the cell size restricts foaming action, larger cells would lead to relief of foaming problems and also permit lower foam densities. In order to evaluate this concept, samples with larger cells must be built and tested thermally to evaluate performance.

However, all further material refinement can be done during the development and evaluation program and can run concurrently with design and analysis.

For application of the large assemblies to structure, the appropriate hard or soft bond would be used. Means of obtaining the hard bond to structure after filling the honeycomb cells are also discussed under section "Bond System Evaluation." The joints remaining between the assemblies would then be filled with an ESM sealer compound applied by a pressure feed technique similar to the channel groove sealing procedure used on integral fuel tanks.

Cutouts in the shield assemblies, where required for hatches or sensors, can be omitted or built undersize and trimmed to exact substructure fit after installation. The simple techniques for cutting and trimming the ESM shield are of great importance in avoiding manufacturing problems at this assembly stage. Repair techniques are also available to preclude any schedule interruption in case of design changes or assembly errors. The trimmed shield edges would be sealed with an ESM compound similar to RTV-60 to prevent absorption of moisture or other deleterious environmental effects.

Shields over removable hatches or sensors can be attached to their individual supports. Then to seal the joint to the main heat shield, a simple ESM material extrusion can be used. This permits complete sealing within the heat shield thickness by a material compatible with the thermal shield and flexible over a very wide temperature range.

Manufacturing techniques are available within the GE-RSD Plastics Shop where the ESM 1002 test samples for NAA evaluation were fabricated and where the thermal shield would be fabricated and assembled. A detailed manufacturing plan can be completed upon final design definition and bond selection.

F. SUGGESTED PROGRAM

The structural incompatibility of conventional plastic ablative heat protection systems with the load-carrying substrate under extreme temperature environments has presented major problems on large-scale re-entry systems. These problems are not readily apparent from small-scale test pieces, but appear in dramatic fashion on large-scale (full-scale) ICBM and re-entry system tests. Consequently, intense General Electric effort has been directed toward compatible ablative shield-structure systems, such as that which the ESM material concept offers, to eliminate fabrication and reliability problems associated with more conventional systems.

This final section of this study, a Suggested Program, has been prepared to provide all possible cooperation to both NASA and North American. It is hoped that these suggestions may be helpful for further planning for an alternate Apollo thermal shield. Of course, the planning presented is influenced by the concepts that GE would consider applicable to the ESM material.

A suggested program would be to fabricate test specimens of the composite shield and structure for each of the three methods discussed. These specimens should be relatively large (30" x 40") and of the proper thicknesses and cycled through the environmental extremes to observe their behavior, as indicated in Figure X-12. The goal of this program is, of course, to select the fabrication and bonding methods which offer the best trade-off with material performance.

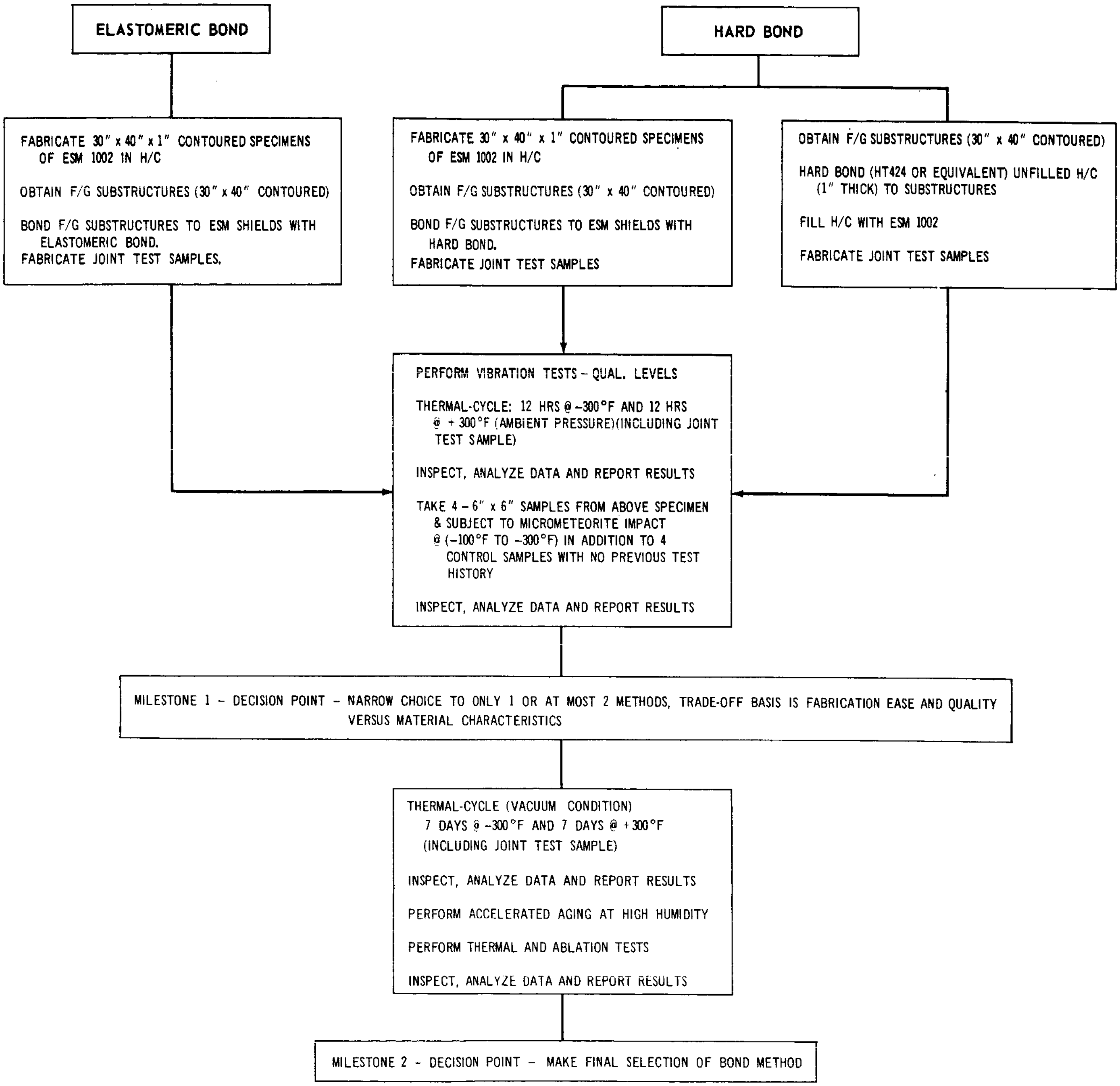

Figure X-12. Suggested Evaluation Program for Bond Evaluation

In addition investigations and tests should be performed in the following areas:

(1) Shield repair - both ground and in-flight

(2) Sensor, window, and hatch Installations.

(3) Joint technique tests

(4) Sealants

(5) Emissivity coating - development, application, and qualification

The following material property data will be required of the bond method which is finally selected:

(1) Physical

(a) Tensile - isothermal and transient

(b) Compression - including determination of glass transition temperature

(c) Shear - of shield-bond system

(d) Tear resistance

(e) Stress relaxation

(f) Fatigue

(g) Impact

(h) Bi-axial

(2) Thermal

(a) Coefficient of expansion

(b) Thermal conductivity

(c) Specific heat

(d) T.G.A.

It is estimated that the suggested program up to Milestone 2 could be performed in a three-month period. It is recommended that concurrently with these tests that a preliminary design phase should be initiated to allow a rapid detailed design phase and fabrication of a full-scale Apollo thermal shield to follow.